UNIVERSITEIT•STELLENBOSCH•UNIVERSITY
jou kennisvennoot • your knowledge partner

Design of a Self Regulated and Protected Electrification Transformer

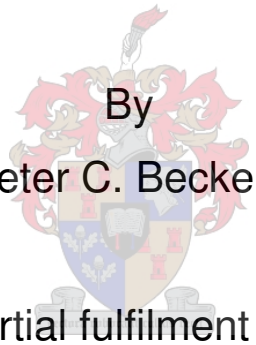

By
Peter C. Beckers

Thesis presented in partial fulfilment of the requirements for the degree of Master of Science (Engineering) at the University of Stellenbosch

Supervisor: Dr H.J. Beukes

March 2007

Declaration

I, the undersigned, hereby declare that the work contained in this thesis is my own original work and that I have not previously in its entirety or in part submitted it at any university for a degree.

Signature: _____

Date: _____

Abstract

Electrification of rural areas is one of the biggest challenges faced by ESKOM and methods are required to extend medium voltage distribution lines to these often remote areas. As loads increase due to line-extension, in-fills and energy theft, maintenance cost and life expectancy of distribution and power transformers becomes more critical. The thesis addresses these two aspects with the development of a self regulated and protected electrification transformer that makes use of current, voltage and ambient temperature measurements to regulate voltage and protect hardware from overloading. The design of the hardware that allows the system to run at 200% load without decreasing the lifetime of the transformer is examined. Temperature estimation techniques are used to estimate the temperatures in the 16 kVA, 22 kV to 230 V, distribution transformer to run above nameplate ratings without causing damage. The control of the system is implemented on TMS320F2812 digital signal processor from TI that is DSP/BIOS compatible. The control software is implemented using DSP/BIOS, which allows real-time scheduling and monitoring of procedures. Furthermore a distribution transformer was fitted with temperature sensors and heat run tests were performed. The results of the temperature tests were used to verify the estimation techniques and to determine constants used for temperature estimation.

Opsomming

Die verskaffing van elektrisiteit in landelike gebiede is een van die grootste uitdagings vir ESKOM. Metodes word dus benodig om medium spanning lyne te verleng om hierdie afgeleë plekke te bereik. Laste wat styg as gevolg van lyn verlenging, uitbreiding en diefstal veroorsaak dat daar al hoe meer klem gelê word op instandhouding en leeftyd verlenging van distribusie transformators. Hierdie tesis bespreek die ontwerp van `n self regulerende en beskermde distribusie transformator wat van stroom, spannings en temperatuur lesings gebruik maak om spanning te reguleer en om die hardeware te beskerm teen oor belasting. Die hardeware ontwerp van die transformator wat toelaat dat die transformator by 200% las kan funksioneer, sonder ingekorte leeftyd, word bespreek. Temperatuur skatting metodes word gebruik om die temperature binne die 16 kVA, 22 kV na 230 V distribusie transformator af te skat terwyl dit onbeskadig bo die standaard vermoë funksioneer. Die beheer van die sisteem word op `n TMS320F2812 verwerker van Texas Instruments implementeer wat DSP/BIOS verenigbaar is. Die sagteware word geïmplementeer met DSP/BIOS en laat intydse skedulering en monitering van die program toe. Vêrder is `n distribusie transformator met temperatuur sensors toegerus om hitte toetse op gedoen. Die uitkomste van die hitte toetse is gebruik om die temperatuur skattings metodes te bevestig en om sekere konstantes te bepaal.

Table of contents

Pectora roborant cultus recti

List of figures

List of tables

Pectora roborant cultus recti

Acknowledgements

I would like to thank the following persons:

Dr H.J. Beukes, my supervisor for his support and guidance and for giving me the opportunity to attain a degree.

My parents, for their financial and moral support and for raising me the way they did.

All the members from the power electronics group for their help and support, especially Jaco. Furthermore I would also like to thank everybody at the workshop for always being prepared to help.

Finally I would also like to thank my girlfriend, Birgit, for always trying to cheer me up and support me when I lacked motivation.

Pectora roborant cultus recti

List of abbreviations

ADC – Analogue to Digital Converter

AC – Alternating Current

BIOS – Binary Input Output System

CCS – Code Composer Studio™

CPU – Central Processing Unit

CT – Current Transformer

CVT – Constant Voltage Transformer

DC – Direct Current

DSP – Digital Signal Processor

EMIF – External Memory Interface

EOC – End of Conversion

EVA – Event Manager A

EVR – Electronic Voltage Regulator

I/O – Input or Output

IDE – Integrated Developers Environment

IEC – International Electrotechnical Commission

IEEE – Institute for Electrical and Electronic Engineering

IGBT – Insulated Gate Bipolar Transistor

ISR – Interrupt Service Routine

LED – Light Emitting Diode

LSB – Least Significant Bit

MIPS – Million Instructions per Second

MOV – Metal oxide varistors

MOSFET – Metal-Oxide-Semiconductor Field-Effect Transistor

MSB – Most Significant Bit

ONAN – Oil Natural Air Natural

PC – Personal Computer

PWM – Pulse Width Modulation

PIE – Peripheral Interrupt Expansion

RAM – Random Access Memory

RMS – Root Mean Square

RST – Reset

RTC – Real Time Clock

SARAM – Single Access Random Access Memory

SCI – Serial Communication Interface

SOC – Start of Conversion

SPI – Serial Peripheral Interface

SRAPET – Self Regulated and Protected Electrification Transformer

VT – Voltage Transformer

1. Introduction

Eskom, the main electricity provider in South Africa, has the aim of supplying electricity to all South Africans by 2015 [1]. To fulfil this aim, cost efficient methods have to be used and developed to electrify rural and urban areas as cheaply as possible. One of the biggest problems, however, is reaching these rural areas as they are often far away from existing power grids and are very sparsely populated. The extension of high voltage (HV) power lines is therefore too expensive and alternative methods, that supply energy to these areas at a minimum cost, must be considered. Research has shown that the extension of medium voltage (MV) lines, by allowing higher voltage drops on the line, is a cost effective solution to the problem. The low voltages, caused by the lengthening of the line can be adjusted to the acceptable limits by means of converter based voltage regulators or step changing transformer regulators.

The Self Regulated and Protected Electrification Transformer (SRAPET) is primarily aimed at load management, voltage regulation and temperature regulation, by shutting off the load, changing the winding ratio of the transformer and indicating the status of the system. SRAPETs will be situated at the end of long medium voltage lines where low voltages are caused by load growth that is caused by in-fills, maturing loads, theft and MV line extension. The purpose of the SRAPET is to minimise maintenance time for staff, provide overload protection and to increase the lifetime of the distribution transformers that are used for the electrification of rural areas.

The transformer discussed in this thesis is a 16 kVA, 22 kV to 230 V, distribution transformer with taps situated on the 230 V side. The controller measures the output voltage, input voltage, output current, ambient temperature and thyristor heat sink temperature to implement the control of the system as seen in Figure 1-1. It makes use of the current measurement as well as the ambient temperature measurement to estimate the transformer's internal temperatures that are used to

implement temperature protection of the transformer. An enclosure with the thyristors, the controller and the measurement equipment is fitted underneath the transformer, on a pole, to implement the control of the system. This provides an easy solution for upgrading and monitoring of distribution transformers that are already in operation. The advantage of separating the thyristors from the transformer is that the heat generated by the transformer does not influence the cooling of the thyristors and vice versa.

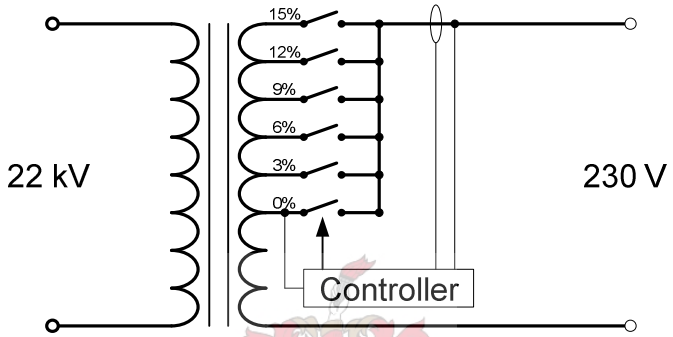

Figure 1-1: Electronic step voltage regulator for 230 V distribution network

All the voltage and current measurements are taken on the low voltage (LV) side of the transformer to simplify the implementation. This eliminates the need for expensive voltage measurement transformers. The input voltage is therefore measured at the nominal tap of the transformer, in front of the thyristor switches and is used as the input voltage for selection of the correct tap setting. Furthermore, the system also measures the over currents up to the maximum fault current by making use of two current transformers (CTs).

Provision for data logging and communication, with external devices, is provided. The system is fitted with 2 MB of flash memory that can be used to store data for gathering information or for data that is used for system initialisation. The stored data can be sent to a host by means of an on-board Bluetooth module or a RS232 serial communication interface. The hardware for the communication is provided and can therefore be implemented in software to perform data logging and data

storage. This has the advantage that the load profiles for transformers at different locations can be obtained to determine if a certain device is over loaded constantly and can thus be replaced by a bigger one. It could also be used to detect energy theft.

The development of the SRAPET was based on the electronic voltage regulator (EVR) discussed [22]. The main difference however is that the control was implemented differently. The EVR makes use of a TMS320F2403A processor with a clock speed of 40 MHz. This is considerably slower than the TMS320F2812 processor, with a clock speed of 150 MHz, used for the SRAPET and has the advantage that a data logging module and transformer temperature estimation techniques can be implemented on the same processor. Furthermore the F2812 digital signal processor (DSP) is DSP/BIOS compatible that enables real-time processing to be employed, which was not possible on the F2403 DSP.

1.1 Structure of report

Chapter 2 presents the need for voltage regulation and different techniques that can be used to improve the voltage regulation of MV and LV lines. It looks at different voltage regulators that can be used to extend the length of MV lines by boosting the LV voltage levels. Some existing solutions are also described that cover transistor based regulators as well as transformer based step changing solutions. Comparisons between insulated gate bipolar transistors (IGBT) and thyristors are also made to give an indication of the advantages and disadvantages of the applications they are intended for.

In chapter 3 dynamic thermal modelling of transformers is explained. The derivation of the thermal estimation techniques by using the analogy between electrical circuits and thermal circuits is discussed. Models as proposed by the Institute for Electrical and Electronic Engineering (IEEE) and the International Electrotechnical Commission (IEC) are presented and are used to estimate the

top oil temperature of the transformer as well as the hotspot temperature. The differential method proposed by the IEC is also discussed and is the method that is used to implement the estimation technique on the processor. An explanation of the implementation of the differential equation, by use of difference equations, on a processor is given.

The voltage regulation and temperature estimation are applied in the hardware design and the implementation of the controller software and is discussed in chapter 4. The maximum fault current is calculated and thyristors are chosen so that the system can function as required. In addition the design of the measurement circuitry, the communication circuitry and the thyristor driver circuitry is discussed. The implementation of the controller software using the DSP/BIOS real-time kernel form TI is also discussed. The operation of the DSP/BIOS kernel is explained to highlight its advantages, compared too commonly used embedded processor implementation software.

The voltage regulation of the SRAPET as well as the temperature estimation techniques used for over temperature protection were tested and are discussed in chapter 5. The estimation techniques are compared to measurements and the voltage regulation is tested to determine if the system functions as required. Heat run test were done on a transformer to obtain temperature measurements that are used to verify values given by the IEC standards and to determine values needed for the estimation techniques.

Chapter 6 contains conclusions drawn from the development of the SRAPET. It also has recommendations on what can be improved or changed to advance the functionality and reliability of the device. Suggestions for future development that are not in the scope of this thesis are given.

2. Voltage Regulation

In South Africa a lot of people in rural areas are still living without electricity in there homes. ESKOM is trying to change this and has undertaken efforts to electrify these, often remote, areas. The problem however is that these rural areas are often very sparsely populated and are situated far away from existing power grids, making it very difficult to supply cheap electricity [1].

When supplying these communities with electricity it has to be decided whether existing grids should be extended by means of HV lines or MV lines. These decisions are influenced by the following factors:

- Distance
- Terrain
- Climate
- Future growth
- Reserve capacity
- Cost
- Load size

MV and LV networks generally provide a bigger possibility for saving, in terms of network extension capital cost, than HV networks [1]. It is therefore necessary to develop cost effective technologies that support these long and lightly loaded networks to create networks that are flexible by means of upgrades in order to utilise them effectively [2] [3] [4].

Table 2-1 gives the definitions for EHV, HV, MV and LV ranges as used in South Africa, where U_n is the nominal line-to-line voltage levels [6].

Classification	Range
Extra high voltage (EHV)	220 kV< U_n ≤ 400 kV
High voltage (HV)	44 kV < U_n ≤ 220 kV

Medium voltage (MV)	1 kV < U_n ≤ 44 kV
Low voltage (LV)	U_n ≤ 1 kV

Table 2-1: South African voltage level definitions

2.1 Line technologies

The specific focus to date, to make rural electrification more affordable, has been on alternative MV line technologies and the effective use of LV single- and dual-phase systems. The line technologies that are currently used by ESKOM to support this cost drive, as they provide a greater scope for savings than HV systems, are single wire earth return (SWER) networks, phase-phase MV networks, dual phase LV networks and single phase LV networks [1]. The main cost advantages of these line technologies are that longer span lengths can be achieved, less line hardware is required and transformers are cheaper [1]. The supply technologies together with the LV distribution alternatives are given in Figure 2-1, Figure 2-2 and Figure 2-3. For three phase LV systems 50 kVA or 100 kVA transformers are used, whereas dual phase and single phase systems use 32 kVA and 16 kVA transformers respectively [1] [9].

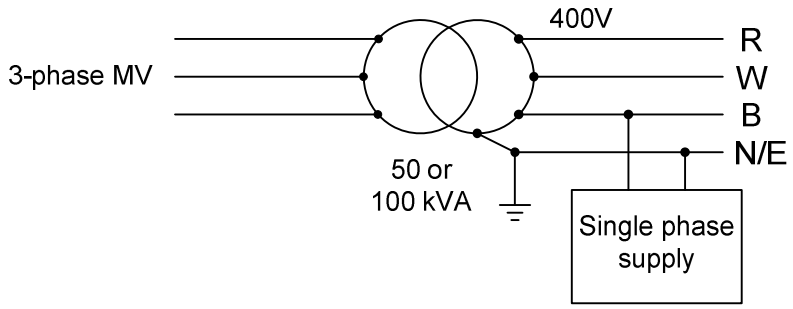

Figure 2-1: Typical LV three phase system

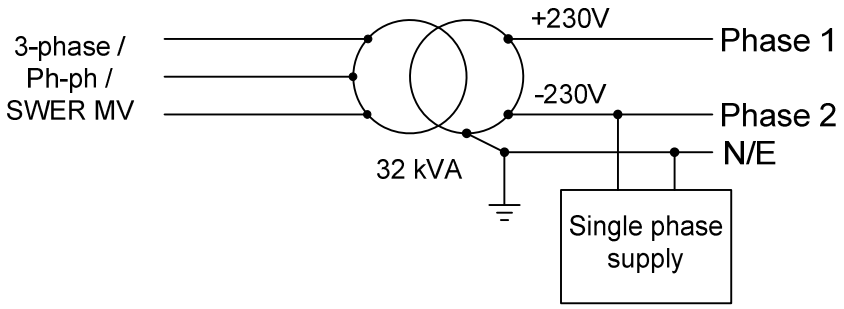

Figure 2-2: Typical LV dual phase system

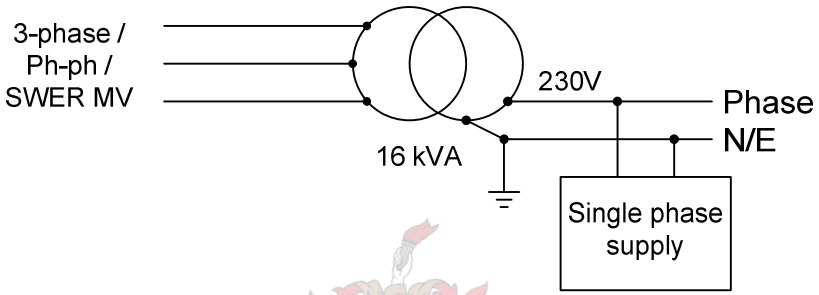

Figure 2-3: Typical LV single phase system

It is standard practice to maintain voltage levels of ±5%, of the nominal system voltage, for systems with voltages larger than 500 V and ±10% for systems with voltages smaller than 500 V [5]. By allowing the voltage of the LV system to drop lower than the recommended 10%, the MV lines can be extended considerably. Table 2-2 illustrates an example of how the distance (*d*) of a MV SWER network can be increased by allowing the voltage drop over the MV line to increase. Where, $d_{10\%}$ is the maximum distance of the line, for a 10% voltage drop, with a point load of 1 MVA at the end of the line ($d_{20\%}$ is 20% voltage drop etc.).

	$d_{10\%}$ [km]	$d_{20\%}$ [km]	$d_{30\%}$ [km]	$d_{40\%}$ [km]
bantam	10.9	19.4	25.5	29.1
magpi	19.5	34.7	45.5	52.0
squirrel	38.1	67.8	88.9	101.7
fox	44.9	79.8	104.7	119.7
mink	65.4	116.3	152.6	174.4

hare	80.4	143.0	187.7	214.5

Table 2-2: Load-reach capabilities of SWER networks for a 1 MVA point load

Automatic voltage stabilisers can be used to regulate the voltage at the MV/LV distribution transformer or on the LV line. They can be installed at different positions in the system to achieve this. The devices that are installed on the LV line can be installed at the distribution box or at the connection box of the costumer. Voltage stabiliser technologies that were considered are listed below [8] [10]-[12] [14]:

- Electro-mechanical (Motorised variac)
- Constant voltage transformers (Ferro-resonant transformers)
- Electronic step regulators (Tap changers)
- Saturable reactors
- Electronic voltage regulators
- Electronically controlled auto-transformers

The technologies that were considered were evaluated against the following aspects to determine the ideal voltage stabiliser technology for the intended application. The importance of these aspects were categorised as shown below, where reliability represents the most important characteristic of the device and ease of installation, the least important.

- Reliability
- Maintenance
- Peak over current capability
- Construction cost
- Efficiency
- Response time
- Ease of installation

Thyristors and IGBTs, of similar rating, were then compared to provide some insight into which switching device would be better suited for the intended voltage stabiliser application.

In the context of this thesis it will be assumed that all transformers are step down distribution transformers as the main problem is the regulation of LV voltages in rural areas, meaning that the focus is on the improvement of LV system and the extension of MV lines.

2.2 Continuous Voltage Regulators

2.2.1 Converter-based voltage regulators

Converter-based voltage regulators make use of IGBT switching and pulse width modulation (PWM) to adjust the output voltage to the required levels. They can be placed at the output of the distribution transformers, at the distribution boxes or at the costumer connection box, depending on which connection is the most feasible and practical. This section will discuss some types of switching converters that are used for voltage regulation.

Pectora roborant cultus recti

A commonly used power electronic converter for voltage regulation consists of back-to-back alternating current (AC) to direct current (DC) converters. The first converter converts the sending end AC voltage (V_S) to DC and the second converter then converts it back to AC (V_R), as shown in Figure 2-4. The converters make use of a half-bridge or full-bridge configurations that must each be able to transfer the rated power of the load. This means that two converters, with a power rating equal to or bigger than the rated power of the line, have to be used [13], which makes the system more expensive. For DC to AC switching converters that have a typical efficiency of 97%, the system seen in Figure 2-4 would be 94% efficient.

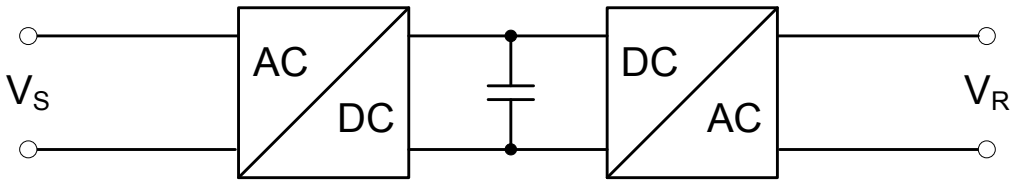

Figure 2-4: AC-to-AC converter using two back-to-back switching converters

Another converter configuration that is used and similar to the one mentioned above is the one shown in Figure 2-5. It makes use of a diode bridge rectifier and a DC-to-AC converter. In this case only one switching converter is used, which significantly reduces cost. The problem with this configuration is that it is not very practical to use in motor drive applications. If the motor brakes, the power flows back into the system but is blocked by the diode bridge (unidirectional power flow) [13]. In the case of the two back-to-back AC-to-DC converters, this is not a problem as power can flow in both directions (bidirectional power flow). In both converters electrolytic capacitors are used as the dc link for filtering and absorbing fluctuations. Their limited lifetime, however, makes the system unreliable and maintenance dependent. The diode bridge rectifier will have an efficiency of 98% and the DC to AC converter will have an efficiency of 97% yielding an efficiency of about 95%.

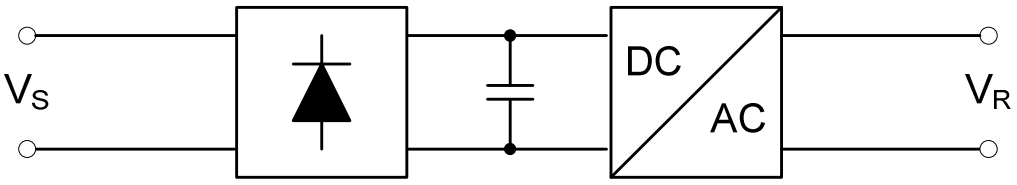

Figure 2-5: AC-to-AC converter using rectifier and switching converter

A transistor-based AC-to-AC converter that was also considered is shown in Figure 2-6 [9] [13]. The AC input voltage is directly converted to AC voltage required at the output by chopping and filtering the input voltage. There are a few topologies that can be used which each have their own distinct advantages [9].

They make use of IGBTs that are controlled by PWM and therefore allow accurate continuous control with a fast response times. Unlike AC-to-AC converters that make use of back-to-back DC-to-AC converters, the AC-to-AC converter shown below cannot implement phase and frequency control. Because the current through the converter is continuous only the magnitude of the output voltage can be controlled and not the phase. In AC-to-AC converters with back-to-back DC-to-AC converters the phase and the frequency of the input and the output are independent of each other. The efficiency of the AC-to-AC converter is typically about 94%, due to losses in the series connected IGBTs, as seen in [9]. AC-to-AC converters are less reliable than devices that make use of thyristors, as they make use of IGBTs, which cannot handle such large peak currents [7].

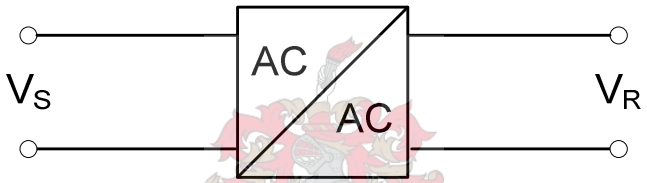

Figure 2-6: AC-to-AC converter

The main advantages of AC-to-AC converters are [14]:

- High stabilisation accuracy
- Very fast response (typically 10 ms)
- Wide input voltage variation without need for tap changers
- Insensitive to input frequency variation
- Small size and weight

The main disadvantages of AC-to-AC converters are [14]:

- Not as reliable as thyristor controlled devices
- Electrolytic capacitors used for DC-to-AC converters also introduce reliability issues
- More expensive than similarly rated devices
- Less efficient than solid-state step changers

- Considerably lower peak over current capabilities due to use of IGBTs

2.2.2 Saturable reactor regulator

The saturable reactor topology that is given in Figure 2-7 is another method used for voltage regulation. It does not make use of taps but only makes use of a saturable compensation transformer to increase or decrease the output voltage. It operates by generating a magnetically controlled moving tap that is produced by a twin saturable-core reactors assembly. A DC current is applied to the reactors, which are placed so that they increase the voltage for both the negative and the positive half-cycle of the 50 Hz voltage. By controlling the DC voltage supplied to the saturable reactors accurately the output voltage can be controlled continuously. The saturation, of the inductors, however introduces distortion which has to be filtered out and makes the system less efficient. This topology is simple and therefore easy to implement. It also has a good line transient rejection, but it has a slow response time of about 10 to 20 cycles, due to the inductance of the transductors [8] [14] [10]. Due to the saturation of the inductor large magnetic fields are generated that could influence the electronics and introduce reliability issues. The efficiency of a saturable reactor, also known as magnetic amplifier, is about 90% which is not very good when compared to other voltage regulation solutions [16].

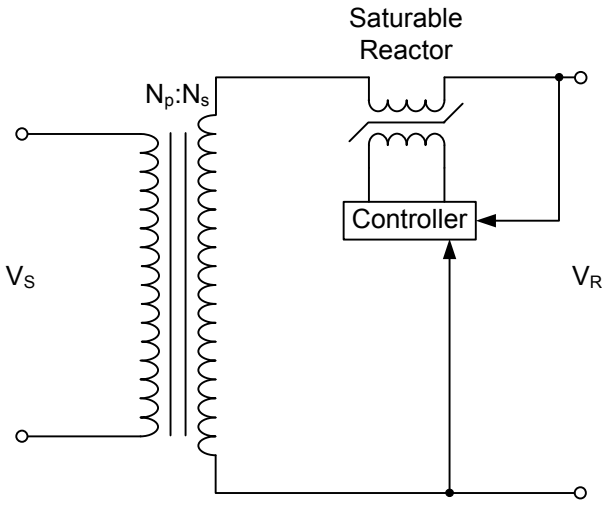

Figure 2-7: Voltage regulator with saturable compensation transformer

The main advantages of saturable reactors are [14]:

- No-moving parts
- Smooth continuous control

The main disadvantages of saturable reactors are [14]:

- Large size and weight
- Very slow response time
- Large magnetic fields can be generated
- Output voltage range is power factor dependent
- High internal impedance can effect some high current loads
- Output waveform distortion is dependent on supply frequency
- Output accuracy is dependent on input frequency and power factor

2.2.3 Motorised voltage regulator

Motorised variable transformers, as seen in Figure 2-8, are well known voltage regulators. They make use of an electronically controlled motor that uses a slider, on the secondary winding of the transformer, which varies the voltage on the compensation transformer. In the topology of Figure 2-8 it is clear that voltage can only be added to the system as the voltage of the compensation transformer

cannot be out of phase. This problem can however be solved by making some adjustments to the configuration below by for example adding a switch that changes the polarity of the taps.

Although this configuration can handle large surge currents it is not practical for the application considered in this particular thesis, as the response time of the system is extremely slow. Furthermore it is very difficult to implement a regulator like this in existing distribution transformers. Another problem of the regulator would be maintenance, as there are a lot of moving parts. The moving parts also increase the chance of failure which makes the mechanism unreliable. Due to the slow response time of the system, transient suppression is a problem.

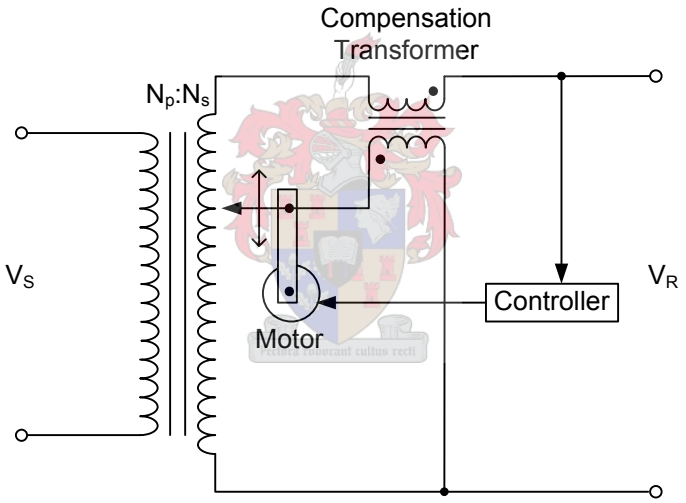

Figure 2-8: Voltage regulator using a motorised variac

The main advantages of motorised variacs are:

- Continuous control
- Accurate output voltage control
- Insensitive to load factor and input frequency

The main disadvantages of motorised variacs are:

- Very slow response time
- Large size and weight

- Expensive
- High maintenance (many moving parts)
- Unreliable

2.2.4 Constant voltage or Ferro-resonant transformer

The circuit diagram for a constant voltage transformer (CVT) is shown in Figure 2-9. It consists of one primary winding, three secondary windings and a shunt capacitor. The magnetic reluctance of the shunts is very high compared to the magnetic reluctance of compensation winding. The leakage inductance produced by the magnetically shunted secondary and neutralising winding, together with the shunt capacitor, create a resonant circuit. The flux in the transformer core increases as the input voltage increases until the inductive reactance of the secondary winding is equal to the capacitive reactance of the shunt capacitor, thereby keeping the output voltage high even if the input voltage is low. The neutralising winding is used to reduce the output distortion and does so considerably [8] [11] [14].

CVTs are ideally suited for relatively low power applications and constant loads which is not the purpose these voltage regulators are intended for. For variable loads the output voltage is more difficult to regulate because the circuit is adjusted for a certain load [17]. Furthermore CVTs are very large, because four windings instead of two are required which makes the system expensive.

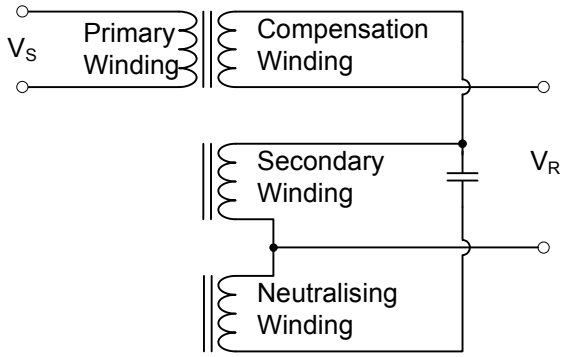

Figure 2-9: Constant voltage or ferro-resonant transformer

The main advantages of CVTs are [14]:

- Exceptionally wide input range for low loads
- Output currents will be automatically limited in the case of an overload

The main disadvantages of CVTs are [14]:

- The current limiting characteristics makes it difficult to be used with loads that require a large start-up current
- Because the CVT relies on resonance it is extremely sensitive to input frequency
- Modest stabilisation accuracy (±3%)
- Produces very high magnetic fields around the transformer, due to saturation
- Large size and weight compared to similarly rated devices
- CVTs are only about 95% efficient [15]
- Not suited for non-constant loads and is thus not suited for the purpose the regulator is intended for

2.2.5 Primary tapped transformers with pulse width modulation

Another tap changing transformer topology that is used for voltage regulation is given in Figure 2-10. In this configuration the taps are situated on the primary side of the transformer. Three pairs of IGBTs are used for switching. Depending on which pair of IGBTs is on, the winding ratio of the transformer is changed to adjust the output voltage [18].

By switching at a high frequency between the taps of the transformer the output voltage of the system can be kept constant for changes in load as well as changes in the power grid. Because of the high frequency switching between the taps the continuous control of the output voltage can be achieved. The required voltage rating of the IGBTs is also acceptable as the configuration is setup so that the entire bus voltage does not need to be blocked by the IGBTs.

A protective device, called a crowbar, is used to make sure a conduction path for the current is always present. The device makes use of an impedance which is current and voltage dependent. The main purpose of the crowbar is [19]:

- To protect the IGBTs when the transformer is switched on
- Carry the inrush current of the transformer at switch on
- Carry the over current or short circuit current should one occur

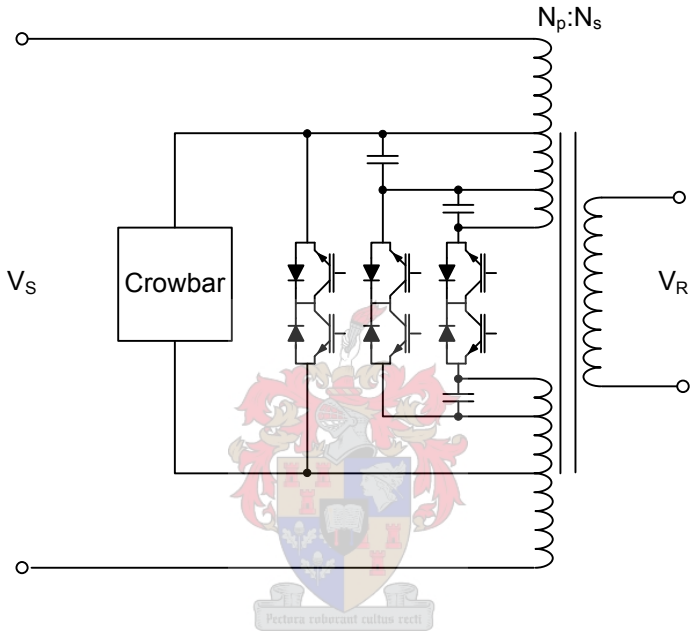

Figure 2-10: Primary side tap changer with crowbar

The system described above and the use of the crowbar has the advantage that the IGBTs used for switching, is designed to manage the tap voltage and the nominal currents only. However, for the application that this system is intended for, namely extension of MV lines this system is not practical as it entails fitting distribution transformers that are currently used with taps on the MV side.

2.3 Step voltage regulators

2.3.1 Tap changer with injection transformer

Figure 2-11 shows a tap changer transformer, which was adapted to increase or decrease the output voltage by means of an injection or compensation transformer. The total secondary windings of the transformer are connected to the load. The voltage on the compensation transformer is then added or subtracted from the output voltage. The compensation transformers voltage is adjusted by switching the taps of the transformer. Depending on whether a switch below or above the centre tap is switched on, the voltage of the compensation transformer will be out of phase or in phase with the output voltage. When it is above the centre tap voltage is added while it is subtracted when the switch is below the centre tap [20].

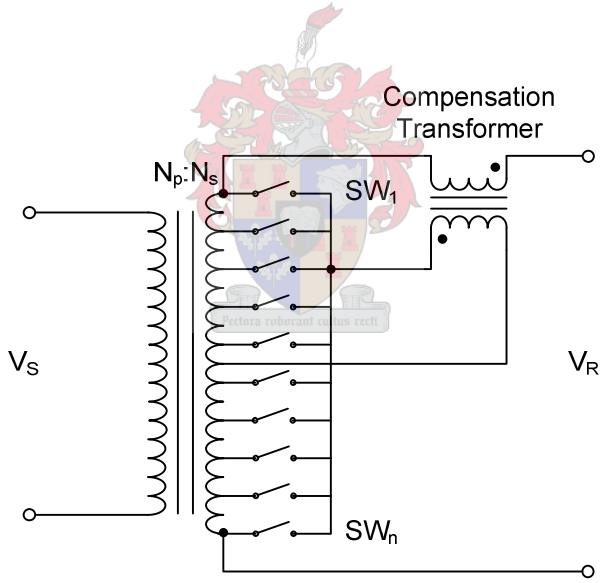

Figure 2-11: Tap changer with compensation transformer

As only the power added or subtracted to the output flows through the compensation transformer the power ratings required by the switching devices are quite low. This has the advantage that IGBTs can be used as switching devices. This enables the system to react quickly as IGBTs can be force commutated and therefore allow faster response times. The response time of this system is

therefore good if solid state switching is used. Problems with this topology are that a compensation transformer needs to be added to existing system and that conventional tap changing distribution transformers cannot easily be adapted to the configuration that is used. The taps can also be moved to the primary side as discussed in the next section.

2.3.2 Tap changer with compensation transformer on primary side

A tap changing voltage regulator, with the taps situated on the primary side of the transformer and a compensation transformer is given in Figure 2-10. The compensation transformer is used as a dip compensator or as a power conditioner. The response time of the system is very fast. It however has the problem that all the control is implemented on the primary side of the system. This means that for the purpose of this project, the primary side voltage would be 22 kV and would require semiconductor devices with extremely high voltage ratings. The topology is therefore not a practical solution for the intended application [21].

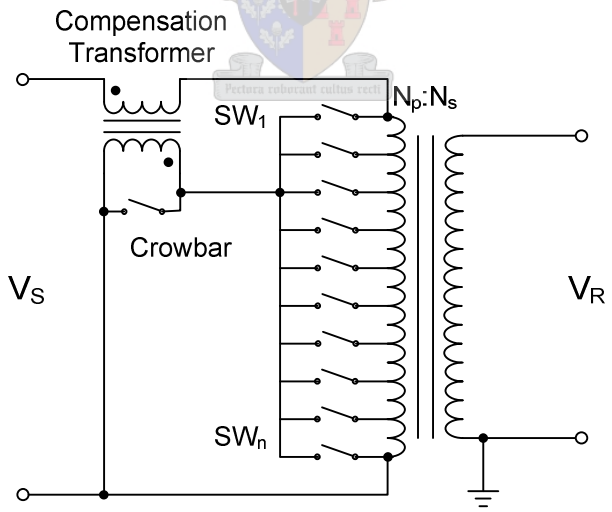

Figure 2-12: Tap changer with compensation transformer on primary side

2.3.3 Electronic controlled auto-transformer

Another in-line voltage regulator that makes use of thyristor switches and an auto-transformer is shown in Figure 2-13 [12] [22]. The taps of the transformer can be positioned at the primary or the secondary side. It is however more advantageous to put them at the input as they can then control the switching on, of the regulator, thereby controlling the inrush current to the auto-transformer. Taps on the secondary side of the auto-transformer will therefore not be further discussed. The controller measures the input voltage for one 50 Hz cycle before switching and therefore has a minimum response time of 20 ms. The main advantage of the thyristor based regulator is the robustness of the regulator and the simplicity of the design. The advantages and disadvantages of thyristor and IGBTs as switching devices will be discussed later in this chapter.

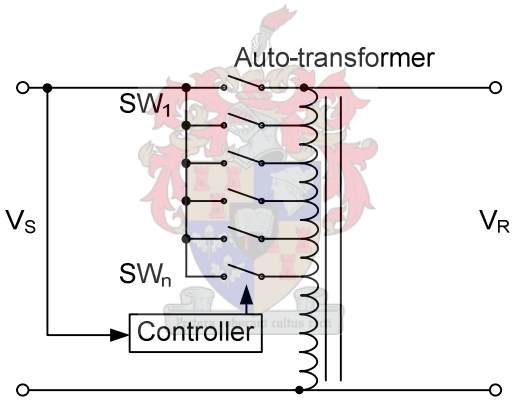

Figure 2-13: Electrically controlled auto-transformer

The main advantages of electronically controlled auto-transformer are [22]:

- Fast response (typically 20-30 ms)
- Relatively inexpensive
- Very reliable (thyristor switches)
- Insensitive to input frequency variation
- Small size and weight
- Low maintenance

The main disadvantages of electronically controlled auto-transformer are [22]:

- Discrete voltage steps (not very accurate)
- Small input range (depends on the number of taps)

2.3.4 Solid state tap changer

Tap changing transformers are traditionally used as voltage regulators. They have additional windings added to the secondary side that can be used to buck or boost the output voltage as required. They can however only adjust the voltage in discrete steps. These steps are fixed and cannot be changed and therefore make the system inflexible. A control system, that measures the voltage, is used to decide on an appropriate tap setting. Tap switching was traditionally done using mechanical switches but was then replaced by electronic switches. Electronic switches allow faster switching time and significantly simplify the control of the tap changer. The most common switching devices that are considered for these applications are thyristors and IGBTs and are compared in the next section. Electromechanical switches are not considered as they require maintenance and are unreliable compared to the semiconductor switches. Furthermore it is not possible to achieve exact switching of electromechanical switches, which complicates the control of the system.

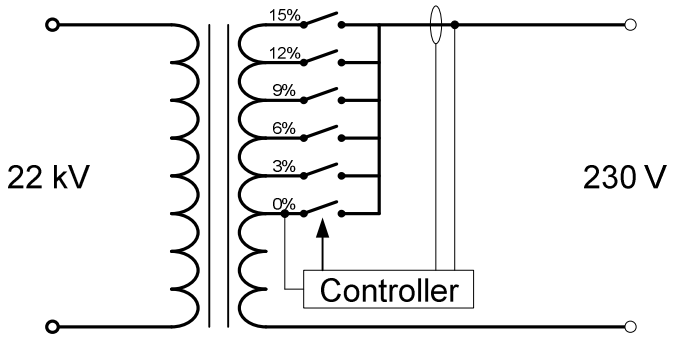

Figure 2-14: Solid-state tap changer

The main advantages of a tap changer are:

- High efficiency (99%)

- Insensitive to input frequency
- Small size and weight
- Insensitive to load changes
- Fast response time (typically 20-30 ms)
- Relatively low cost

The main disadvantages of the tap changer are:

- Discrete voltage step (not very accurate)
- Output voltage tolerance is normally not smaller than 3%, else is becomes to expensive

Considering the pros and the cons of all the devices discussed above, the tap changing transformer is the option that is best suited for the application the devices are considered for. Because reliability, maintenance, cost and peak current capability are the main concern, the controlled tap changing regulator is the preferred alternative. Other considerations are that these devices have to be installed in the existing system and must therefore make use of existing equipment.

Having decided on the type of voltage regulators to use, the next point of discussion is the switching device. IGBTs and thyristors are the most commonly used switching devices and are compared and discussed in the next section.

2.4 Thyristor and IGBT comparison

The previous sections discussed some voltage regulation solutions considered for improving the voltage quality of MV and LV systems. After analysing some of the solutions it was concluded that the step voltage regulator was best suited for the intended application of the voltage regulators. Another point for discussion though is the use of the semiconductor switches that are to be used for the switching of the taps of the step regulator transformer. The semiconductor switches that are

discussed are IGBTs and thyristors. Electromechanical switches were not considered due to reliability, maintenance and switching complications.

Figure 2-15 illustrates the configuration of a thyristor and an IGBT module as they will be used for switching between the taps of a tap changing regulator. Modules with similar ratings are compared to provide some insight to which would be better suited for the switching application. Table 2-3 shows some of the characteristics of a “SKKT 162 / 12 E” thyristor module and an “SKM 200 GB 123 D” IGBT module containing two diodes.

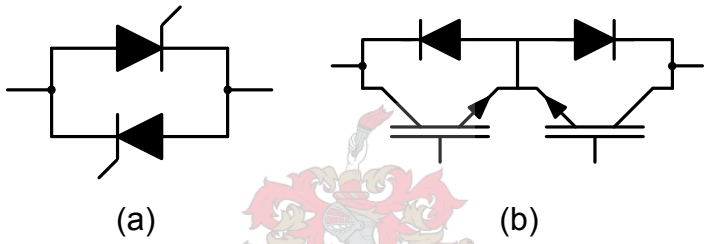

Figure 2-15: (a) Thyristor module (b) IGBT module with diodes

Pectora roborant cultus recti

	SKKT 162 / 12E	SKM 200 GB 123 D
Maximum blocking voltage	1200 V	1200 V
Maximum current	250 A*	200 A**
Max. power losses due switching	145 W***	550 W ***
Maximum junction temperature	125 ℃	150 ℃
Peak current	5000 A	1450 A
Price (Sep 2006)	R346	R664

Table 2-3: Thyristor and IGBT comparison

Note:

** Maximum RMS on-state current*

*** Maximum continuous collector current*

**** Represent the losses of one module at 140 A load current (200% load).*

By comparing the characteristics of the thyristor module and the IGBT module in the table above it can be seen that the thyristor module, which is considerably cheaper than the IGBT module, is also better suited for this application. The blocking voltage of the IGBT is the only feature that can compare with the voltage of the thyristor. The losses, of the IGBT module, are more than three time more than those of the thyristor modules. That is partly because of the series diodes that have to be added to the IGBT module.

The bigger losses of the IGBTs would also require a bigger heat sink or a cooling fan. Cooling fans are however not considered as they use moving parts which require maintenance. The failure of a cooling fan could also cause the system to fail and therefore introduce reliability issues. The maximum peak voltage of the thyristor is also considerably higher than that of the IGBT. Considering the advantages and disadvantages of the thyristors compared to IGBTs it was thus decided to make use of thyristor modules as switching devices for the step voltage regulator.

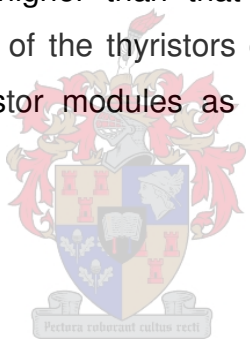

2.5 Summary

Several different voltage regulation devices and their intended purposes were examined in this chapter. Their main advantages as well as disadvantages were discussed. The different line technologies together with the intended purpose of the regulation devices were also specified. The main purpose of the regulation devices considered is the extension of MV and LV lines, for the electrification of rural areas. It therefore becomes clear that electronic step regulators together with in-line voltage regulators would be the best option to extend these networks. As switching devices thyristors seem to present the best possible solution.

3. Dynamic Transformer Temperature Estimation

3.1 Introduction

To determine the thermal capability of a transformer, the hotspot temperature of the transformer has to be known. The hotspot temperature refers to the hottest spot in the windings of a transformer and determines the rate of loss of life of the transformer as a whole. Winding insulation is the most temperature sensitive component of a transformer and is therefore the main contributor to transformer ageing. The kVA rating of a transformer is thus the rating at which the output current, at rated voltage, produces an average winding temperature rise of 65℃ above ambient. Above this voltage insulation degradation increases drastically and therefore significantly reduces the life time of the transformer.

To be able to run the transformer above nameplate ratings it is necessary to dynamically predict the hotspot temperature. If the hotspot temperature is known, the transformer can operate above 100% load for as long as the hotspot temperature of the windings is within the acceptable limit. A thermal diagram of the temperatures inside a transformer tank is illustrated Figure 3-1 [23] [24].

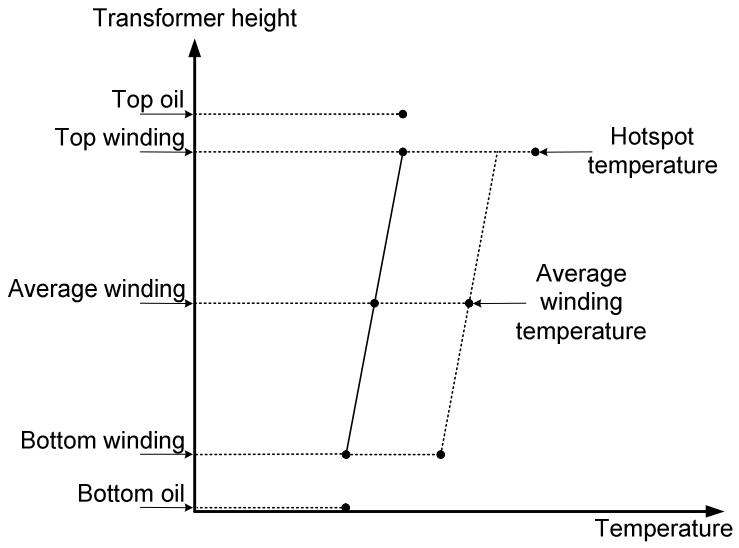

Figure 3-1: Thermal diagram of transformer tank temperatures

3.2 The thermal-electrical analogy

To predict the temperatures of the oil and the hottest spot in a transformer, the thermal-electrical analogy is used to construct a model. The analogy between electrical and thermal circuits is defined in the table below and the corresponding laws governing capacitance and resistance are also given in equation 3.1 and 3.2 [25] [26] [27] [24].

Thermal		Electrical	
Generated heat	q	Current	i
Temperature	θ	Voltage	v
Resistance	R_{th}	Resistance	R_{el}
Capacitance	C_{th}	Capacitance	C_{el}

Table 3-1: Thermal-electrical analogy

$$v = R_{el} \cdot i \Rightarrow \theta = R_{th} \cdot q \tag{3.1}$$

$$i = C_{el} \cdot \frac{dv}{dt} \Rightarrow q = C_{th} \cdot \frac{d\theta}{dt} \tag{3.2}$$

For the heat transfer case the thermal resistance through a plate, like for instance the wall of a transformer, is only linear if the rate of flow of the cooling fluid is constant. In other words, if the flow of the cooling fluid is by natural convection as with distribution transformers, the thermal resistance becomes nonlinear. To take this into account the nonlinearity exponent is introduced and equation 3.1 changes to equation 3.3.

$$q = \frac{\theta^{1/n}}{R_{th,R}} \tag{3.3}$$

Where, $R_{th,R}$ is the thermal resistance at known values of q and θ

For a constant rate of flow of the cooling fluid, the nonlinearity exponent is equal to one and equation 3.3 is linear. This is not true for distribution transformers

because the oil and air cooling is natural and the convection will therefore be greater as the temperature difference across the wall increases [27]. The recommended value for *m* and *n* in distribution transformers is *0.8* [26] [23] [24]. Where *m* is the nonlinearity exponent for oil as the cooling fluid and *n* is the nonlinearity exponent for air as the cooling fluid.

The thermal capacitance of a specific material, like for instance oil, is calculated by multiplying the specific heat capacity by the weight of the material. By using the thermal-electrical analogy and the definition of the nonlinear thermal resistance, methods for predicting the hottest spot temperature in the winding and the top oil temperature can be obtained.

The top-oil-to-air and winding-to-oil models are illustrated in Figure 3-2 and Figure 3-3 respectively. Iron and copper losses are modelled as ideal heat sources and the ambient temperature is modelled as an ideal temperature source. Equation 3.4 and 3.5 give the differential equations that describe the heat transfer from the windings of the transformer to the air surrounding the transformer.

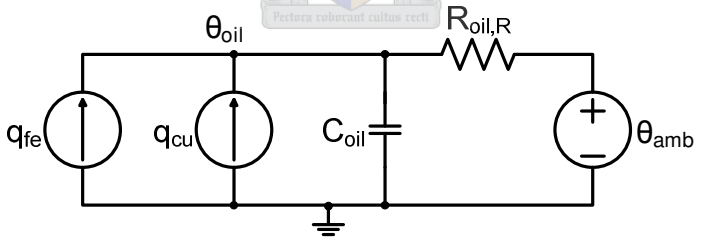

Figure 3-2: Oil-to-air heat transfer model

$$q_{fe} + q_{cu} = C_{oil} \cdot \frac{d\theta_{oil}}{dt} + \frac{1}{R_{oil,R}}(\theta_{oil} - \theta_{amb})^{1/n} \tag{3.4}$$

Where,

q_{fe} are the iron losses

q_{cu} are the copper losses

C_{oil} is the thermal capacitance of the oil

$R_{oil,R}$ is the load to no-load loss ratio at rated load

θ_{oil} is the oil temperature

θ_{amb} is the ambient temperature

$\frac{d\theta_{oil}}{dt}$ is the rate of change of oil temperature

The input values of oil-to-air model are the total heat losses at a certain output current and the ambient temperature. The oil temperature is the output of the oil-to-air model but is used as an input signal for winding-to-oil model. According to Swift in [27] it is not the total copper losses that generate the heat, but only, about 0.1% of the total copper losses. It is however valid to use the total loss figure and adjust the thermal resistance and capacitance instead.

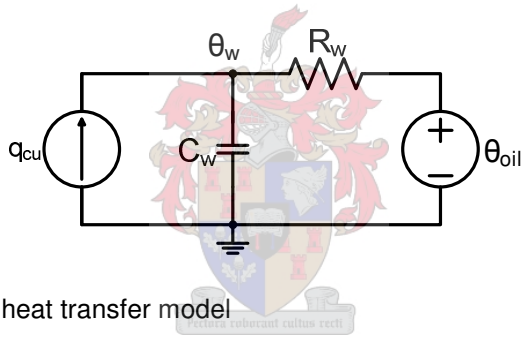

Figure 3-3: Winding-to-oil heat transfer model

$$q_{cu} = C_w \cdot \frac{d\theta_w}{dt} + (\theta_w - \theta_{oil})^{1/m} \quad (3.5)$$

Where,

C_w is the thermal capacitance of the winding

θ_w is the hotspot temperature

$\frac{d\theta_w}{dt}$ is the rate of change in winding temperature

The method for establishing the thermal model that is described above is generally accepted and used by the IEEE as well as the IEC [26] [23] [24]. Although the methods for creating the thermal models are the same, the

recommended implementations differ slightly. In the section below the transient response for a step input as well as a difference equation solution of the differential equations, as recommended by the IEC, will be discussed.

3.3 IEEE exponential method

The equations given below outline the method recommended by the IEEE to predict the top oil and the hotspot temperatures for oil immersed power transformers. The hotspot temperature is determined by adding the top oil over ambient temperature gradient and the hotspot over top oil temperature gradient, to the ambient air temperature surrounding the transformer, as seen in equation 3.6. The exponential form of equation 3.7 and 3.9 is obtained by finding the step response of the RC circuit described in section 3.2. It should also be noted that the IEEE method's oil time constant changes dynamically and should therefore be calculated for different load steps by using equation 3.11, 3.12 and 3.13.

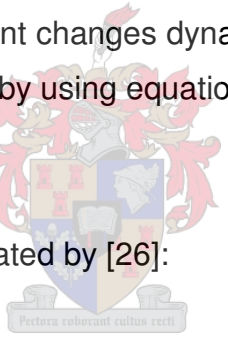

The hotspot temperature is calculated by [26]:

$$\theta_{hs} = \theta_{amb} + \Delta\theta_{oil} + \Delta\theta_{hs} \tag{3.6}$$

Where,

θ_{hs} is the hotspot temperature

θ_{amb} is the ambient temperature

$\Delta\theta_{oil}$ is the top oil over ambient temperature gradient

$\Delta\theta_{hs}$ is the hotspot over top oil temperature gradient

For a load step, the top oil over ambient temperature gradient is given by [26]:

$$\Delta\theta_{oil} = \left(\Delta\theta_{oil,U} - \Delta\theta_{oil,I}\right)\left(1 - e^{-t/\tau_{oil}}\right) + \Delta\theta_{oil,I} \tag{3.7}$$

Where,

$\Delta\theta_{oil,U}$ is the final/ultimate top oil over ambient temperature gradient

$\Delta\theta_{oil,I}$ is the initial top oil over ambient temperature gradient

τ_{oil} is the oil-to-ambient time constant

The final or steady state top oil temperature gradient is given by [26]:

$$\Delta\theta_{oil,U} = \Delta\theta_{oil,R}\left(\frac{K^2R+1}{R+1}\right)^n \quad (3.8)$$

Where,

$\Delta\theta_{oil,R}$ is the top oil over ambient temperature gradient at rated load

K is the per unit current i.e. output current divided by rated current

R is the ratio of load losses to no-load losses

For a load step, the hotspot over top oil temperature gradient is given by [26]:

$$\Delta\theta_{hs} = \left(\Delta\theta_{hs,U} - \Delta\theta_{hs,I}\right)\left(1 - e^{-t/\tau_W}\right) + \Delta\theta_{hs,I} \quad (3.9)$$

Where,

$\Delta\theta_{hs,U}$ is the final/ultimate hotspot over top oil temperature gradient

$\Delta\theta_{hs,I}$ is the initial hotspot over top oil temperature gradient

τ_W is the winding-to-oil time constant

The final or steady state hotspot over top oil temperature gradient is given by [26]:

$$\Delta\theta_{hs,U} = \Delta\theta_{hs,R} \times K^{2m} \quad (3.10)$$

Where,

$\Delta\theta_{hs,R}$ is the hotspot over top oil temperature gradient at rated load

The heat capacity of a transformer is given by [26]:

$$C = 0.132 \times W_{CC} + 0.088 \times W_{TF} + 0.351 \times VO \quad (3.11)$$

Where,

C is the heat capacity of the oil, windings, fittings and core

W_{CC} is the weight of the coils and core in kg

W_{TF} is the weight of the transformer tank and fittings in kg

VO is the volume of oil in litres

The top oil time constant at rated load is given by [26]:

$$\tau_{oil,R} = C \times \frac{\Delta\theta_{oil,R}}{P_{T,R}} \tag{3.12}$$

Where,

$\tau_{oil,R}$ is the oil-to-air time constant at rated load

$P_{T,R}$ is the total power loss at rated load

And finally, the load varying time constant is calculated as follows [26]:

$$\tau_{oil} = \tau_{oil,R} \times \frac{\Delta\theta_{oil,U}/\Delta\theta_{oil,R} - \Delta\theta_{oil,I}/\Delta\theta_{oil,R}}{\left(\Delta\theta_{oil,U}/\Delta\theta_{oil,R}\right)^{1/n} - \left(\Delta\theta_{oil,I}/\Delta\theta_{oil,R}\right)^{1/n}} \tag{3.13}$$

3.4 IEC exponential method

The IEC exponential method is similar to the IEEE method. It uses different equations for increasing and decreasing load factors. Equation 3.14 is used for an increase in load and equation 3.15 is used for a decrease in load. The top oil time constant, the winding time constant, the top oil over ambient temperature gradient and the average winding over top oil temperature gradient are determined by temperature rise tests on the transformer. The oil time constant is determined by using equation 3.11, 3.12 and 3.13. Table 3-2 contains the recommended thermal characteristics for the equations, as given in the IEC standard in [24], for oil natural and air natural (ONAN) cooled distribution transformers. It also contains the suggested nonlinearity constants for the exponential functions.

The hotspot temperature for an increase in load factor is given by:

$$\theta_{hs} = \theta_{amb} + \Delta\theta_{oil,I} + \left\{\Delta\theta_{oil,U} - \Delta\theta_{hs,I}\right\} \times f_1(t) + \Delta\theta_{hs,I} + \left\{\Delta\theta_{hs,R}K^{2m} - \Delta\theta_{hs,I}\right\} \times f_2(t) \tag{3.14}$$

The hotspot temperature for a decrease in load factor is given by:

$$\theta_{hs} = \theta_{amb} + \Delta\theta_{oil,U} + \left\{\Delta\theta_{oil,I} - \Delta\theta_{oil,U}\right\} \times f_3(t) + \Delta\theta_{hs,R}K^{2m} \tag{3.15}$$

Where,

$$f_1(t) = (1 - e^{(-t)/(k_{11} \times \tau_{oil})}) \tag{3.16}$$

$$f_2(t) = k_{21} \times (1 - e^{(-t)/(k_{22} \times t_W)}) - (k_{21} - 1) \times (1 - e^{(-t)/(t_{oil}/k_{22})}) \quad (3.17)$$

$$f_3(t) = e^{(-t)/(k_{11} \times \tau_{oil})} \quad (3.18)$$

and,

k_{11}, k_{21}, k_{22} are transformer specific constants

Constant	Value
Constant k_{11}	1
Constant k_{21}	1
Constant k_{22}	2
Oil nonlinearity exponent n	0.8
Winding nonlinearity exponent m	0.8

Table 3-2: Thermal characteristics for distribution transformers as suggested by the IEC

3.5 Differential equation method

Equation 3.19 to 3.23 show the heat transfer equations obtained from the combination of the oil-to-air and the winding-to-oil models in section 3.2. By making the infinitely small time change *dt* a discrete finite time step *Dt*, these continuous equations can be implemented in a digital processor by converting them to the difference equations 3.24 to 3.31. Although there are more accurate numerical solutions to the differential equations, such as the trapezoidal or Runga-Kutta methods, the increase in accuracy is not warranted due to the inaccuracy of the measured input data [24].

The differential equations describing the heat transfer from the top oil of the transformer to the air surrounding it, as well as the equation for calculating the hotspot temperature over top oil temperature gradient follows:

$$\left[\frac{1 + K^2 R}{1 + R}\right]^n \times (\Delta\theta_{oil,R}) = k_{11}\tau_{oil} \times \frac{d\theta_{oil}}{dt} + [\theta_{oil} - \theta_{amb}] \quad (3.19)$$

$$k_{21} \times K^{2m} \times (\Delta\theta_{hs,R}) = k_{22} \times \tau_W \times \frac{d\Delta\theta_{hs1}}{dt} + \Delta\theta_{hs1} \quad (3.20)$$

$$(k_{21} - 1) \times K^{2m} \times (\Delta\theta_{hs,R}) = (\tau_{oil} / k_{22}) \times \frac{d\Delta\theta_{hs2}}{dt} - \Delta\theta_{hs2} \quad (3.21)$$

The hotspot temperature is then calculated as follows:

$$\Delta\theta_{hs} = \Delta\theta_{hs1} - \Delta\theta_{hs2} \quad (3.22)$$

Where $\Delta\theta_{hs1}$ represents the rise in hotspot temperature generated by the windings and $\Delta\theta_{hs2}$ represents the cooling of the hotspot temperature as a result of the flow of heat from the windings to the oil. The rise of the hotspot temperature over top oil temperature ($\Delta\theta_{hs}$) is then used to calculate the hotspot temperature as shown in equation 3.23.

$$\theta_{hs} = \theta_{amb} + \Delta\theta_{oil} + \Delta\theta_{hs} \quad (3.23)$$

The difference equations for calculating the top oil gradient as well as the hotspot gradient are given below. Time step *Dt* must be smaller than half the smallest time constant in the system, which in this particular case 4 minutes. Therefore *Dt* should be smaller than 2 minutes. Besides the ambient temperature and the load factor the previous top oil and hotspot temperatures are also used as inputs to calculate the current top oil and hotspot temperatures.

$$D\theta_{oil} = \frac{Dt}{k_{11}\tau_{oil}} \left[\left[\frac{1 + K^2 R}{1 + R} \right]^n \times (\Delta\theta_{oil,R}) - [\theta_{oil} - \theta_{amb}] \right] \quad (3.24)$$

$$D\Delta\theta_{hs1} = \frac{Dt}{k_{22}\tau_W} \times \left[k_{21} \times \Delta\theta_{hs,R} K^{2m} - \Delta\theta_{hs1} \right] \quad (3.25)$$

$$D\Delta\theta_{hs2} = \frac{Dt}{(1/k_{22})\tau_{oil}} \times \left[(k_{21} - 1) \times \Delta\theta_{hs,R} K^{2m} - \Delta\theta_{hs2} \right] \quad (3.26)$$

In equations 3.27 to 3.31 the top oil and hotspot gradients, for a given time step, are added to the estimates of the previous time step. These equations together with equations 3.23 to 3.26 are implemented on a processor to estimate the hotspot temperature of a transformer.

$$\theta_{oil}(n) = \theta_{oil}(n-1) + D\theta_{oil}(n) \quad (3.27)$$

$$\Delta\theta_{hs1}(n) = \Delta\theta_{hs1}(n-1) + D\Delta\theta_{hs1}(n) \quad (3.28)$$

$$\Delta\theta_{hs2}(n) = \Delta\theta_{hs2}(n-1) + D\Delta\theta_{hs2}(n) \quad (3.29)$$

$$\Delta\theta_{hs}(n) = \Delta\theta_{hs1}(n) - \Delta\theta_{hs2}(n) \quad (3.30)$$

$$\theta_{hs}(n) = \Delta\theta_{oil}(n) - \Delta\theta_{hs}(n) \quad (3.31)$$

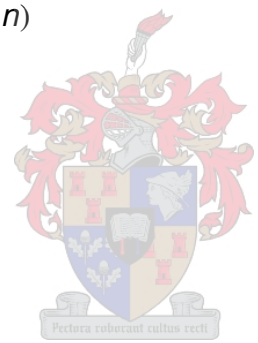

3.6 Conclusion

The formulation of the heat equations as exponential function is not ideally suited for temperature estimation for arbitrarily changing load factors but is better used for simplified scenarios [24]. It can be used for temperature tests and heat transfer parameter determination, where the load factor is kept constant for longer periods. For field implementation the differential method is much better suited because the load factor and the ambient temperature change arbitrarily. It is also easier to implement the differential equation solution in a processor as the differential equations are solved using difference equations. A three tap distribution transformer was fitted with temperature sensors and the measurements are compared to the values obtained from the methods described above. The results

of the measurements will be discussed in a later section. The heat run tests performed on the transformer will also be discussed in the chapter 5.

4. System Design and Synthesis

4.1 Introduction

The system discussed in this chapter is implemented on a 16 kVA, 22 kV to 230 V, distribution transformer. It has 6 taps on the 230 V side, from 0% to 15% and uses current sensing, voltage sensing, ambient and heat sink temperature measurements as control inputs. The temperature tests were originally done on a 3 tap transformer and the system was later implemented in a 6 tap transformer and tested. All temperature tests were done on the 3 tap 16 kVA, 22 kV to 240 V, distribution transformer. To confirm the temperature prediction methods the transformer was fitted with temperature sensors and tested at different loads. The measurements were sent to a PC via the serial port and are discussed in a later chapter.

The system is required to run at 200% load continuously and is limited by the winding hotspot and thyristor temperature. Another requirement is that the thyristors switches must be able to sustain over currents for long enough to allow the circuit breakers of the 230 V pole-top service connection boxes that supply the customers, time to trip. For the system as it functions in the field it is also assumed that the load power is constant and not the load impedance. That means, for an increase in transformer output voltage the load current decreases. Furthermore the chapter also discusses the implementation of the transformer controller on a TMS320F2812 processor from TI. Real-time processing is established by using Code Composer Studios DSP/BIOS kernel that is also discussed in this chapter.

It needs to be clearly stated that two transformers were used in the design of the SRAPET. A standard 16 kVA, 22 kV to 240 V, 3 tap transformer was used to measure the temperatures inside the transformer and compare them to the estimated values obtained by different thermal temperature estimation methods. A

second 16 kVA, 22 kV to 230 V, transformer was then used to implement the temperature estimation techniques as well as the voltage regulation and protection. The voltage regulation was also employed in the 3 tap transformer and the system was later adjusted for the 6 tap transformer. The main purpose of the 3 tap transformer was to verify the temperature estimation techniques. The software development however discusses the methods that were used in the 6 tap SRAPET.

4.1.1 Specifications

The ratings of the transformer and the SRAPET, as well as the measured load and no-load losses are listed in Table 4-1 below. Although the IEC standard [24] specifies the load to no-load loss ratio as 5 for distribution transformers, it was measured to be closer to for 4.

Transformer	**Specification**
Power	16 000 VA
Primary Voltage	22 000 V
Secondary Voltage	230 V
Primary Current	0.73 A
Secondary Current	69.6 A
Taps	0 - 21% (in steps of 3%)
Impedance	3.9%
Load losses	352 W
No-Load losses	85 W
SRAPET	**Specification**
Maximum fault current	1800 A
Continuous operating current	140 A
Voltage regulation	4%
Input voltage	± 15% of rated voltage
Output voltage	+15% -3% of rated voltage
Other features:	
Over current detection & protection, over voltage protection,	
Lightning protection and over temperature protection	

Table 4-1: Transformer and SRAPET specifications

4.1.2 System overview

A general overview of the system is given in Figure 4-1. A TMS320F2812 digital signal processor, from TI, is used for controlling the system. The DSP is used in conjunction with an eZdsp™ Development Board from Spectrum Digital which is connected to other devices/boards via jumpers. Communication with, and programming of the DSP is done via the parallel port or the J-TAG interface. The Code Composer Studio™ (CCS) interface is used for programming and debugging the C code on the DSP.

On-chip peripherals relevant to the controller are the analogue to digital converter (ADC), serial communication interface (SCI), serial peripheral interface (SPI), external memory interface (EMIF) and the Event Managers A and B (EVA and EVB) which make provision for twelve PWM outputs. The DSP is a 32 bit fixed point device equipped with 128 kW on board flash memory and 18 kW single access random access memory (SARAM), which can perform 150 mega instructions per second (MIPS) for a clock speed of 150 MHz.

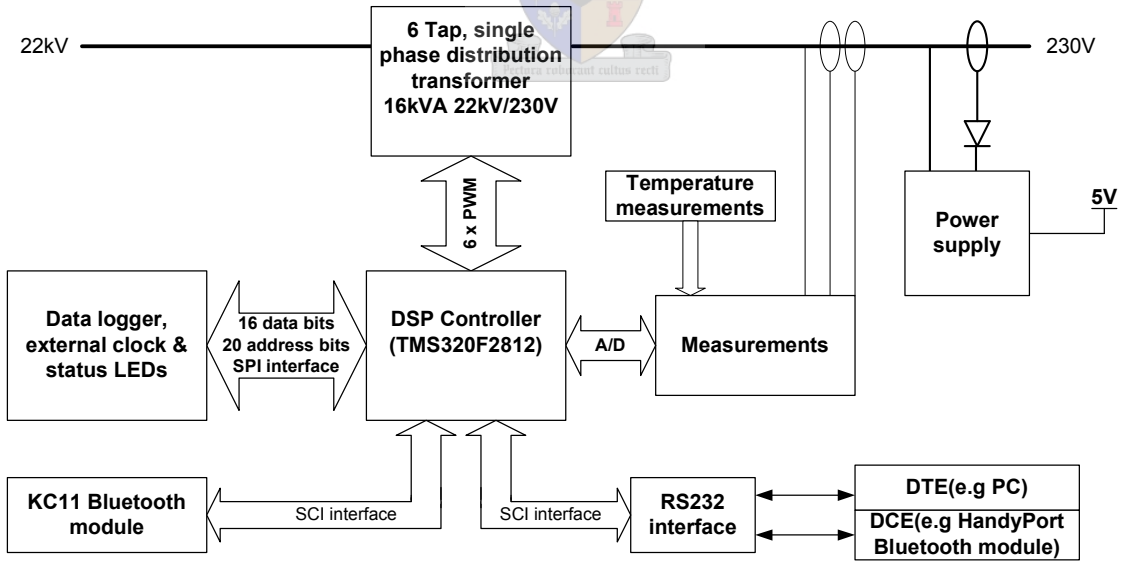

Figure 4-1: System overview

A measurement board is used for taking voltage, current and temperature readings. It converts the given voltages, currents and temperatures into voltages between 0 V and 3 V which are then read into the ADC of the processor. For the top oil and winding temperature measurements thermistors were used. In the final implementation of the controller linear thermocouples were later used to measure the ambient temperature. Two different measurement boards were used as the final implementation of the controller does not measure the temperatures inside the transformer.

The serial communication interface is used for asynchronous communication with external devices, such as a PC, a Bluetooth interface or a modem. For synchronous communication with the real time clock the serial peripheral interface is used.

2 MW of external memory, which is located on the communication board, can be accessed via the 19 address bits of the external interface. The extra address bit, that is required to access the full range of the memory, is provided by an IO pin and is switched on manually if necessary.

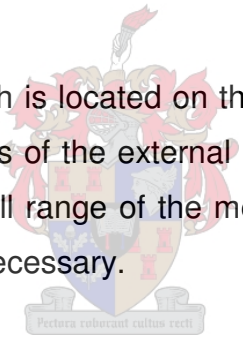

5 Volt is supplied to all boards by a power supply which functions from the 230 V output of the system. Each board is fitted with a 3.3 V voltage regulator to supply the external boards with the required voltage. The eZdsp™ development board only uses 5 V supply and also makes use of an onboard voltage regulator to provide 3.3 V and 1.9 V to the processor.

4.2 Tap selection design

4.2.1 Calculating the fault current

To calculate the maximum short circuit fault current of the system, the short line model, for transmission lines shorter than 100 km is used [31]. The transformer impedance is referred to the high voltage, primary side, of the transformer as

shown in Figure 4-2 and the maximum fault current is then calculated, for the primary and secondary side, using equation 4.1 to 4.4.

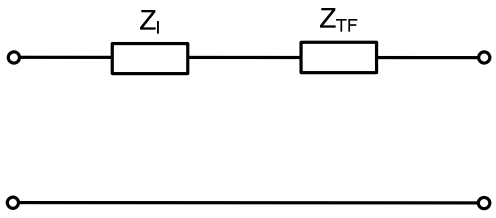

Figure 4-2: Simplified circuit of line and transformer referred to 22 kV side

$$Z_b = \frac{V_b^{\,2}}{S_b} = \frac{(22\times10^3)^2}{16\times10^3} = 30.25\ k\Omega \tag{4.1}$$

$$Z_{TF} = Z_b \times Z_{pu} = 30.25\ k\Omega \times 3.9\% = 1.18\ k\Omega \tag{4.2}$$

$$I_{fp} = \frac{V_b}{Z_l + Z_{TF}} \tag{4.3}$$

$$I_{fs} = I_{fp} \times \frac{V_{rp}}{V_{rs}} \tag{4.4}$$

Where,

Z_b is the base impedance

V_b is the base voltage

S_b is the base power

Z_{TF} is transformer impedance

Z_{pu} is the per unit impedance

I_{fp} is the primary side fault current

I_{fs} is the secondary side fault current

Z_l is the transmission line impedance

V_{rp} is the rated primary side voltage

V_{rs} is the rated secondary side voltage

A transformer impedance of 3.9% is used to calculate the maximum fault current, because this is the value which was measured by the load and no-load tests on

the transformer. In Table 4-2 the fault current for different conductor types and transmission line models for a 30 km medium voltage lines, is shown. To calculate the absolute maximum fault current, the line impedance can be ignored and Z_l in equation 4.3 is made zero, as the line impedance is much smaller than the transformer impedance. This is also relevant because the length of the transmission line may differ in length and could be quite short. The secondary side fault current is thus calculated by using equation 4.3 and 4.4 as shown below.

$$I_{fp} = \frac{22000}{1180} = 18.6\ A \Rightarrow I_{fs} = 18.6 \times \frac{22000}{230} = 1.78\ kA$$

		R [Ω/km]	X [Ω]	I_{fs} [A]	I_{fp} [A]	Z_l [Ω]
bantam		3.969	0.361	1552	16.93	119.6
magpi		2.231	0.111	1618	17.65	67.0
squirrel		1.132	0.156	1661	18.12	34.3
fox		0.860	0.450	1668	18.20	29.1
mink		0.500	0.440	1681	18.34	20.0
hare		0.362	0.403	1686	18.39	16.3
OLP Model:						
squirrel	A-frame	1.626	0.506	1638	17.87	51.1
	Staggered	1.626	0.476	1639	17.88	50.8
fox	A-frame	0.930	0.489	1665	18.16	31.5
mink	A-frame	0.544	0.472	1679	18.31	21.6
hare	A-frame	0.320	0.456	1686	18.39	16.7

Table 4-2: Fault currents for different conductor types and transmission line models of a 30 km line

4.2.2 Thyristor selection

Switching between the different taps of the transformer is done by modules containing two back-to-back thyristors. One for forward conduction and one for reverse conduction of the current, as shown in Figure 4-3. Thyristors were chosen

as switching devices, because they are more robust and have better high power ratings than other switching devices of the same cost as explained in section 2.4.

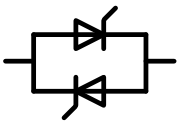

Figure 4-3: SEMIKRON back-to-back thyristor module used for tap switching

Although stud mount thyristors are, generally, cheaper than thyristor modules, modules are used as they have built-in isolation (isolated case). Because stud mount thyristors' metal casing are at a live potential the heat sinks on which they are mounted would need to be electrically insulated. This has the obvious disadvantage that each thyristor would have to be mounted on a separate insulated heat sink for cooling, thus making the required heat sink very large. Using modules with isolated base plates, as shown in Figure 4-4, allows all the modules to be mounted on one heat sink. Another advantage of modules is that all modules can be mounted on one heat sink, which has the required thermal resistance to cool one module (not the added thermal resistance to cool all six thyristor modules). This can be done because only one module will be used at a time, as only one tap of the transformer should be on at a certain time.

Figure 4-4: SKKT SEMIPACK 2 thyristor modules from SEMIKRON with isolated base plate

The thyristors should be of such a rating that they can handle fault currents and continuous over currents of up to 200% of the rated load. Selection of thyristors is thus determined by their rated root mean square (RMS) current capabilities, short circuit current capacity, maximum reverse blocking voltage and maximum rate of voltage rise. The transient thermal impedance is also very important in this particular case because the system must be able to conduct over currents and short circuit currents long enough for the circuit breakers, installed in the service connection boxes on the 230 V line to trip. This is necessary to provide protection coordination and costumers are disconnected if a fault occurs behind a 50 A breaker, as seen in Figure 4-5. The transient impedance of the thyristors is therefore also evaluated and maximum over current situations are compared to the circuit breaker curve of the connection box.

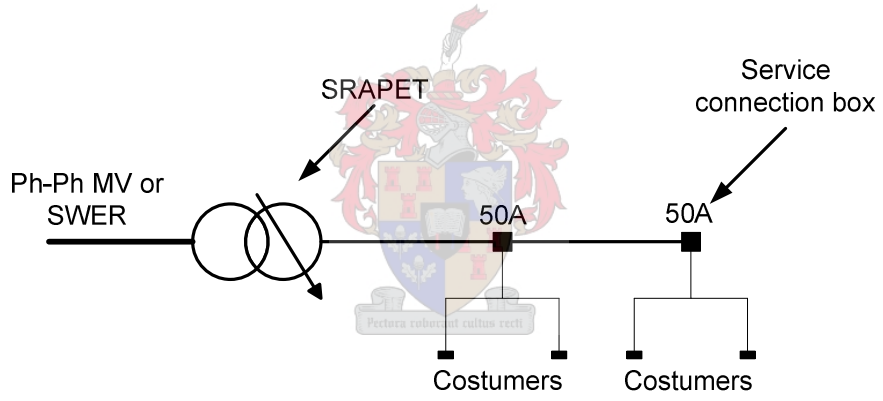

Figure 4-5: MV line and LV line with SRAPET and service connection boxes

Table 4-3 gives some of the available thyristor modules from SEMIKRON that were considered. The table shows the maximum rate of voltage rise (*dv/dt*), rated RMS current for the correct choice of heat sink (I_{TRMS}), maximum short circuit current capacity (I_{TSM}), direct maximum on state voltage (V_T), maximum junction temperature (θ_j), maximum reverse blocking voltage (V_{PRM}) and the power dissipation of the module at 200% load current (*q*).

	dv/dt [V/µs]	I_{TRMS} [A]	V_T [V]	I_{TSM} [A]	Θ_j [°C]	V_{PRM} [V]	q [W]
SKKT106/12E	1000	180	1.65	1900	125	1200	160
SKKT122/12E	1000	195	1.55	3200	125	1200	155
SKKT132/12E	1000	220	1.85	4000	125	1200	170
SKKT162/12E	1000	250	1.45	5000	125	1200	145
SKKT213/12E	1000	370	1.50	7500	130	1200	150
SKKT250/18E	1000	420	1.30	8000	130	1800	125

Table 4-3: SEMIKRON thyristors considered for tap switching

The transient thermal impedance, which is given in the datasheets, is used to estimate the thermal behaviour of the thyristor for short period over currents. Assuming that the thyristor modules absorb all the heat generated by the fault currents for the first 20 seconds, the allowable over currents are plotted against time to be compared to the tripping time of a Curve 1, 50 A, circuit breaker. From Figure 4-7 the correct thyristor module can then be chosen. The power dissipated by the thyristor modules is calculated by multiplying the on-state voltage of the thyristor with the current flowing through it. The on-state voltage for different currents is obtained Table 4-3. The required thermal impedance is then calculated, for different load currents, using an ambient temperature of 50 °C, a junction temperature 125 °C or 130 °C and the power dissipation, as shown in equation 4.5 and Figure 4-6. By using the calculated thermal impedance, the times these over currents can be sustained are then obtained from the graph supplied in the datasheets.

$$Z_{js} = \frac{\theta_j - \theta_{amb}}{q} \tag{4.5}$$

Where,

Z_{js} is the thermal impedance from junction to sink

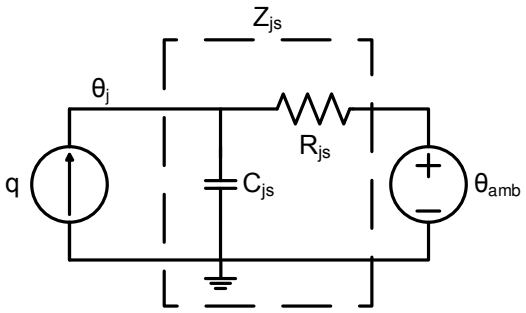

Figure 4-6: Thermal impedance network of thyristor module

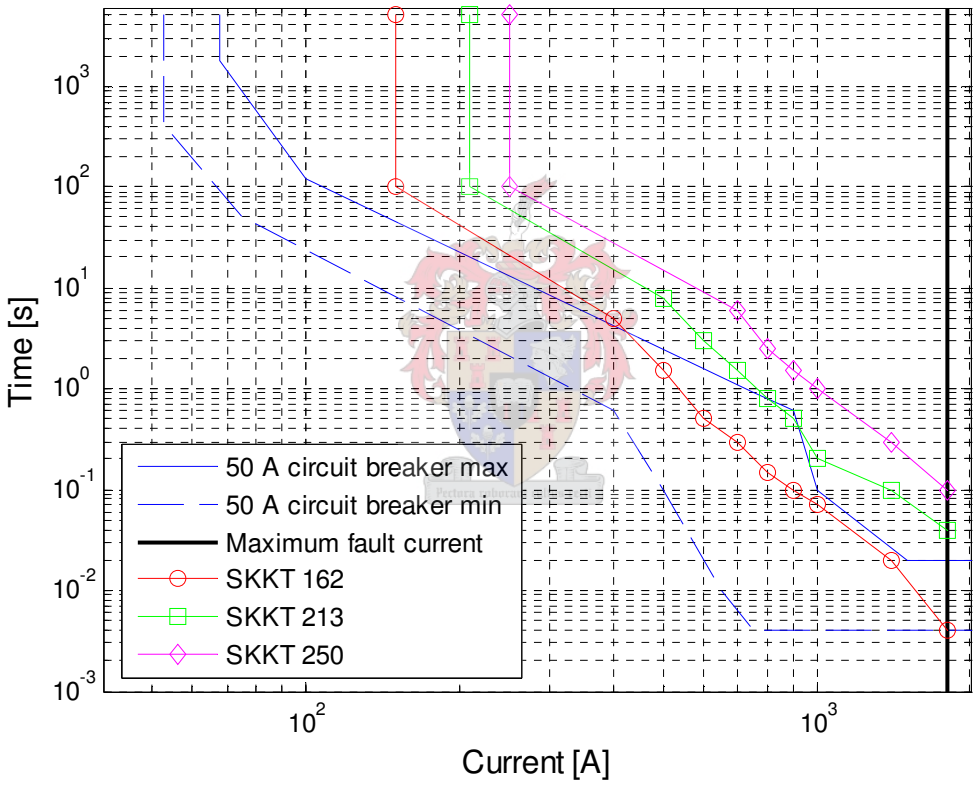

Figure 4-7: Thyristor over current capabilities compared to Curve 1 circuit breaker

By using Table 4-3 and Figure 4-7 it was thus decided to use five SKKT 162 and one SKKT 250 module. The SKKT 250 module is used for switching the nominal tap and is switched on in the case the output current exceeds 400 A. The SKKT 162 modules are used for switching taps 1 to 5 (3% to 15%). This has the advantage that only one of the more expensive SKKT 250 modules is used,

without sacrificing the over current capabilities of the system. The SKKT 213 module was not considered due to availability problems. The SKKT 250 cost roughly twice as much as the SKKT 162.

4.2.3 Heat sink design

The heat sink design is based on the thermal characteristics of the SKKT 162 thyristor module as that is the smaller of the two thyristor modules that are used. Figure 4-8 is used to model the heat flow from the junction of the thyristor module to the heat sink. The power dissipation (q) due to conduction losses is given as 145 W at 200% load current. The required heat sink thermal resistance can thus be calculated using equation 4.6. For a maximum ambient temperature of 50 ℃, a maximum junction temperature of 125 ℃, thermal resistance from junction to case of 0.09 ℃/W and a thermal resistance from case to heat sink of 0.05 ℃/W.

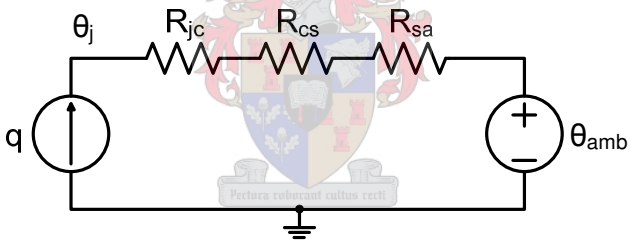

Figure 4-8: Steady state thermal circuit for thyristor module

The required heat sink thermal resistance is determined by using equation 4.6.

$$R_{sa} = \frac{(\theta_j - \theta_{amb})}{q} - R_{jc} - R_{js}$$
$$= \frac{(125-50)}{145} - 0.09 - 0.05 \qquad (4.6)$$
$$= 0.377 \ ^\circ C/W$$

Where,

θ_j is the junction temperature

θ_{amb} is the ambient temperature

q is the power dissipation per module at a given current

R_{jc} is the junction to case thermal resistance per module

R_{cs} is case to heat sink thermal resistance per module

R_{sa} is heat sink to ambient thermal resistance

A SEU16 aluminium heat sink from SEMIKRON with a length of 300 mm and a thermal resistance of 0.34 ℃/W, for natural cooling, was chosen. This also provides enough space for all six thyristor modules to be fitted onto the heat sink.

4.3 Communication

The communication board consists of three main components namely serial asynchronous communication with external devices, synchronous communication with the Real Time Clock (RTC) and an external flash memory used for logging data. The board also contains LEDs which indicate the status of the controller and the current tap setting. There are four status LEDs, indicating current errors, voltage errors, temperature errors and normal operation. They are driven by a 74LCX541 line driver which is able to supply sufficient current to the LEDs and the thyristor drivers. It also serves as a buffer between the thyristor driver circuit and the processor.

4.3.1 Asynchronous serial communication

The asynchronous communication interface consists of a RS232 that can be used in conjunction with a HandyPort-Serial Bluetooth module, a KC11 Class 1 Bluetooth module or a serial cable to establish communication with a PC.

The HandyPort-Serial Bluetooth module can be plugged into a D_Sub 9 pin Male connector to establish communication between the host and the controller, via the RS232. The same module is also fitted onto the host and is thereby able to set up

communication between the 2 devices. Some of the modules features are given below:

- Baud Rate: Up to 115.2 kbps (Recommend above 2.4 kbps)
- Supports: 1.2/2.4/4.8/9.6/19.2/38.4/57.6/115.2 kbps
- Range: Up to 100 m
- Connection: Point-to-Point
- Signal: DCD, TxD, RxD, GND, CTS/DSR, DTR, RTS
- RS-232 Interface: D_SUB 9 Pin Female
- Standard: Bluetooth Specification Version 1.1

The KC11 Class 1 Bluetooth module is a surface mount device which is smaller and cheaper than the HandyPort-Serial device. The KC11 Class 1 module is therefore the preferred module. Some of the features are given below,

- Baud Rate: Up to 723.2 kbps
- Supports: all Bluetooth data rates from 57.5 to 723.2 kbps
- Range: Up to 200 m
- Connection: Point-to-Point or Point-to-Multipoint
- RS-232 Interface: Surface mount
- Standard: Bluetooth Specification Version 1.2
- Other: USB2.0 compatible/SPI interface/ Central processing unit (CPU), radio, antenna & firmware on module

For the temperature tests that were done on the transformer, data was sent to the PC from the controller via a serial cable. When implementing the device in the field, Bluetooth modules will be used because it is safer and easier to operate. The Bluetooth modules are currently not used and are added to the system to implement a data logger to the system in a later version. The logger will make use of the external memory and the selected Bluetooth module to implement the data logger.

4.3.2 Synchronous serial communication

Synchronous serial communication is used to send data between the Real Time Clock and the controller. It makes use of a Receive, Send, Clock and Enable pin to communicate and uses a Lithium Coin Battery as backup power when the system is off. The enable pin of the RTC is connected to a general IO pin of the processor and can therefore be set high or low as desired. Some of the RTC features are listed below,

- Counts seconds, minutes, hours, date of month, month, day of week and year with leap year (an eighth register is used as control register)
- Serial I/O for minimum pin count
- Full operation for 2.0 V to 5.5 V
- Uses less than 300 nA at 2.0 V
- 24 hour clock or 12 hour clock with AM/PM indicator

The registers of the clock can be read individually or can be extracted using the burst mode command. In burst mode, all eight clock registers are sent to the processor successively. When burst mode is disabled the registers can be read independently. To set the clock, burst mode can also be used to set all eight registers at once.

4.4 Tap switching

The thyristor driver circuit used for switching the transformer between its different taps is shown in Figure 4-9. A metal-oxide-semiconductor field-effect transistor (MOSFET) is switched by the PWM signal which is received from the processor via a line driver. Pulse transformers are connected to the MOSFET signal and isolate the switching circuitry from the thyristors. The PWM signal, seen in Figure 4-10, is set to a third of the switching period prevent the pulse transformers from saturating. Further, a diode is added to the primary side of the pulse transformer so that the transformer is demagnetized when the MOSFET is off. Equations 4.7 and 4.8 are used to determine the values of the different components. A minimum

current of 150 mA and 200 mA is required to switch on the SKKT 162 and SKKT 250 modules respectively. The winding ratio of the pulse transformers is 1:1.

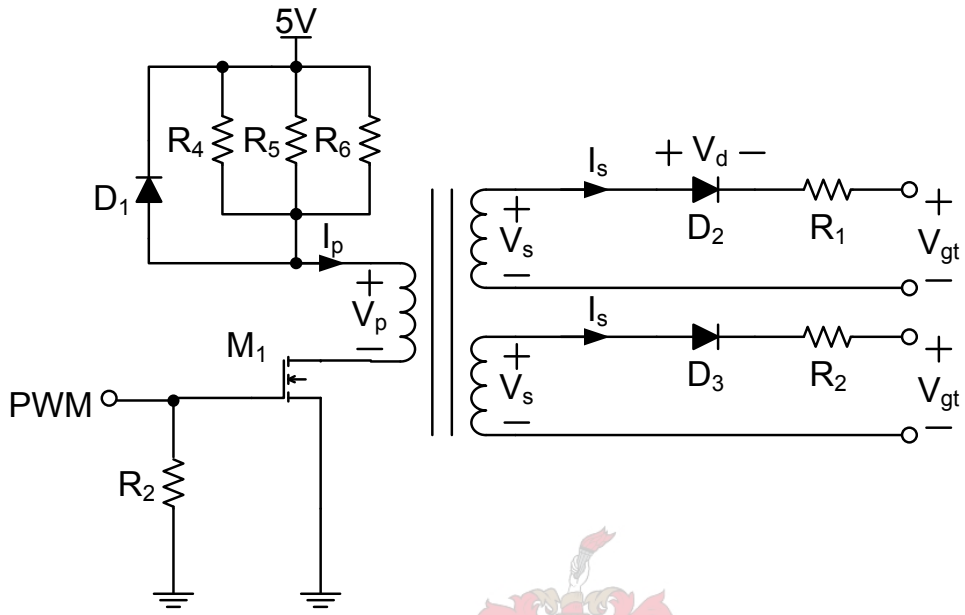

Figure 4-9: Thyristor driver circuit

$$R_1 = R_2 = \frac{V_s - V_d - V_{GT}}{I_s} = \frac{5 - 0.8 - 1.2}{0.2} < 15\ \Omega \tag{4.7}$$

Where,

V_S is the secondary side voltage of the pulse transformer

V_d is the diode on-state voltage

V_{GT} is the thyristor gate voltage

I_s is the secondary current

$$R_{tot} = \frac{V_p - I_p \cdot R_{on}}{I_p} = \frac{5 - 0.2 \cdot 4}{0.2} < 16\ \Omega \tag{4.8}$$

Where,

V_p is the primary side voltage of the pulse transformer

R_{on} is the on resistance of the MOSFET

I_p is the primary side current

R_{tot} is total resistance of R_4, R_5 and R_6

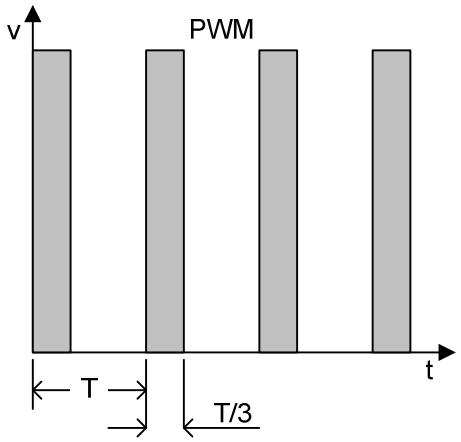

Figure 4-10: Thyristor switching pulse train supplied to thyristors

4.5 Pulse suppression

The thyristors are switched by a PWM signal, as discussed in section 4.4, which is off for two thirds of the switching period (*T*). This has the disadvantage that when a thyristor is switched on, the actual switching on of the thyristor is delayed because of the off-time of the PWM signal. Although the remaining flux of the distribution transformer might be able to support the output voltage for very small loads this is not the case for bigger loads and voltage glitches will be introduced. To suppress these voltage pulses, a resistor and capacitor are connected to the output as seen in Figure 4-10. Where, the capacitor is used to store enough energy to support the output voltage and the resistor is used to limit the current through the capacitor. A 22 Ω resistor (*R*) and a 4.4 µF capacitor (*C*) are used for voltage suppression.

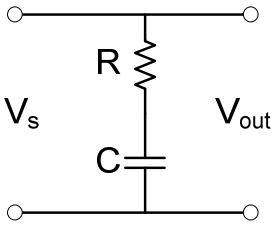

Figure 4-11: Pulse suppression circuit

4.6 Measurements

The measurement circuitry, used for the 3 tap transformer, consists of 12 temperature sensors 2 voltage sensors and 2 current sensors. Of the 12 temperature sensors, 10 are used to monitor the temperatures, at various location of the transformer. As mentioned earlier, the internal temperature measurements were included for model verification in the development process. One temperature sensor is used to measure the temperature of the heat sink on which the thyristors are mounted and the other is used to measure the ambient temperature. The voltage sensors monitor the output voltage of the transformer at the nominal tap and the voltage at the output of the thyristor switches. A 3 V precision reference is used to supply the 1.5 V and 3 V reference voltages which are required by the voltage and current measurement circuitry. 3.3 V is supplied by a LM1117-3.3 voltage regulator.

4.6.1 Temperature measurements

The temperature measurements for the 240 V / 22 kV distribution transformer were done by the circuit shown in Figure 4-13. A 10 kΩ 1% NTC thermistor is attached to the jumper and mounted at the desired location inside the transformer and on the heat sink. As the temperature of the thermistor rises the resistance decreases, thus causing the voltage which is measured by the analogue to digital converter of the processor to drop. The resistance of the thermistor does however not change linearly with temperature and therefore the digital value, of the ADC, is

send to the host where Matlab's "polyfit" function is used to estimate accurately what the temperature is. A polynomial is fitted into the resistance versus voltage curve which is obtained from the datasheets. The coefficients of the polynomial can then be used to calculate the temperature which is correlated to the voltage measured by the ADC, as seen in Figure 4-12.

50 mA fuses together with Zener diodes are used as over voltage protection for temperature sensors located within the transformer. Furthermore earth leakage protection is also present for devices mounted inside or on the transformer

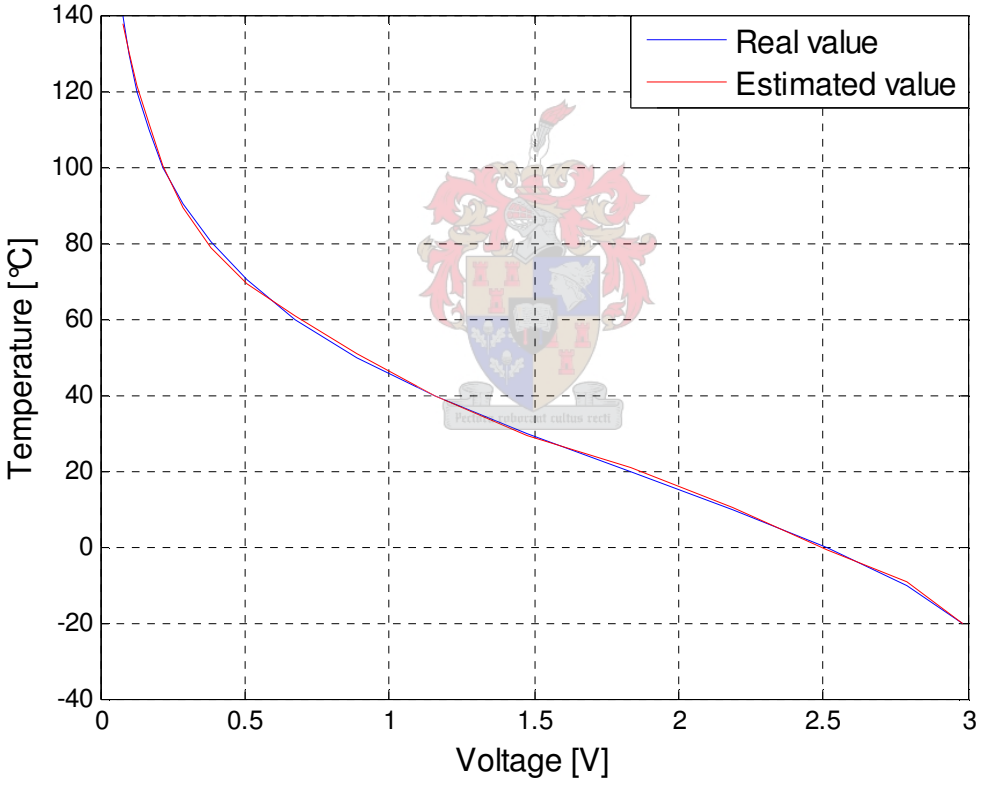

Figure 4-12: Temperature estimation of thyristors, using a seventh order polynomial

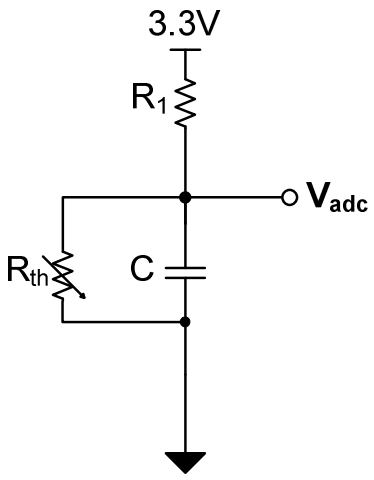

Figure 4-13: Temperature sense circuit used for transformer temperature measurements

For the 6 tap transformer no sensors are installed inside the transformer, as this is not practical for systems used in the field. One linear thermocouple and two thermistors, which use 5 V, are used to measure the ambient temperature and the heat sink temperature. The transformer temperatures are then estimated by software, using the methods discussed in the previous chapter and the measured ambient temperature.

4.6.2 Voltage measurements

Voltage measurements are obtained by using the circuit shown in Figure 4-14. The measurement circuitry is required to measure voltages up to 265 V_{rms}, which represents a over voltage of 15%. Taking into consideration that the input voltage can swing between ±375 V and adding an offset of 1.5 V so that the voltage measurement swings from 0 V to 3 V. Equation 4.9 is used to find the required resistor values. The ADC measurements are then processed by the DSP to calculate the RMS voltages that are measured and the offset is subtracted digitally before the RMS value is calculated on the processor. Two voltage measurements are taken by the controller, namely the nominal tap voltage as well as the output voltage of the system.

$$V_{adc} = \frac{V_{in} \cdot R_1 + V_{REF} \cdot R_2}{R_2 + R_1} \tag{4.9}$$

Where,

V_{adc} is the voltage measured by the ADC

V_{in} is the line voltage of the system

V_{REF} is the 1.5 V reference voltage offset added to V_{in}

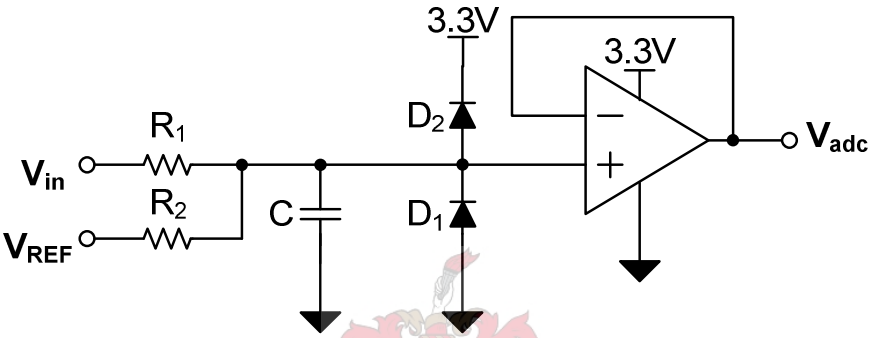

Figure 4-14: Voltage measurement cicuit

As the feedback gain of the operational amplifier is one, the input signal to the operational amplifier is also equal to the output voltage of the operational amplifier. The operational amplifier serves as a buffer to the controller. Clamping diodes are also added to protect against over voltages.

4.6.3 Current measurements

Two current measurement circuits are used, one is used to measure currents when the system is functioning normally (0% to 200% load) and the other is used to measure short circuit currents up to 2500 A. Equation 4.10 and 4.11 are used to determine the values for the different components in the measurement circuit.

$$V_{adc} = \frac{V_1 \cdot R_2 + V_{REF} \cdot R_1}{R_1 + R_2} \tag{4.10}$$

$$V_1 = \frac{I_{rms} \cdot \sqrt{2} \cdot R_b}{CT} \tag{4.11}$$

Where,

V_{adc} is the voltage measured by the ADC

V_1 is the voltage over the burden resistor

V_{REF} is the 3 V reference voltage offset that is added to V_1

I_{rms} is the maximum measured RMS current

CT is the current transformer ratio

The input voltage to the operational amplifier is equal to the output voltage of the operational amplifier, because the feedback gain of the circuit is equal to one. Zener diodes are used to protect the circuit against current surges. The input currents to the current measurement circuits are supplied by CTs. A 150:1 CT and 2500:1 CT are used to measure the normal current and over current respectively. If the output current of the transformer exceeds 150 A, the Zener diodes of the 150 A measurement circuit will start conducting, thus protecting the circuitry against the over current. The 2500 A measurement circuit will however still be functioning, thus allowing the controller to measure the over current for the required period. If the over current situation is not resolved in the required time the taps will be shut off.

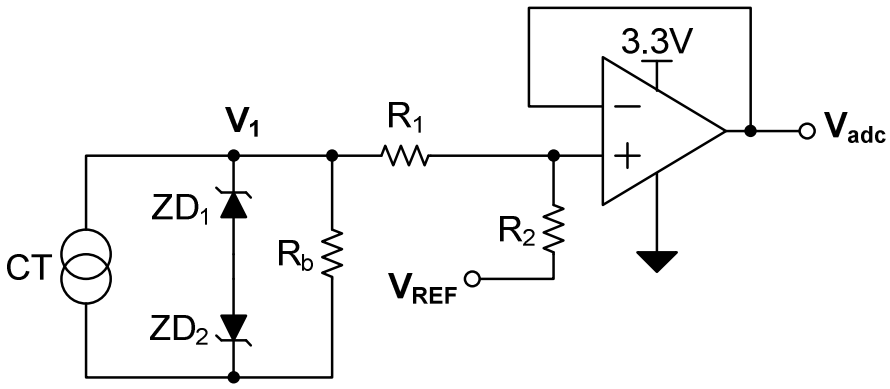

Figure 4-15: Current measurement circuit

4.7 Surge protection

The most common cause of surge voltages are lightning strikes and they can be induced surges on the LV or MV line or direct lightening strikes to the lines. As the transformer is protected against surge voltage on the MV side, only the thyristors that are installed on the LV side have to be protected against voltage and current surges. Two scenarios have to be considered when implementing the surge protection. One situation is when the system is operational and the other is when the system is non-operational (all thyristors are off).

When the system is non-operation it presents a large impedance to surge voltage. To limit these surge voltages, metal-oxide varistors (MOV) are used to clamp the voltage to acceptable levels, as shown in Figure 4-16. The resulting surge current will therefore flow mainly through the MOVs and not through the thyristors. The MOVs that are used are rated for 275 V_{rms} and can handle surge currents up to 40 kA.

When the system is in operational mode it presents a small impedance to surge voltages, which will therefore cause large surge currents to flow through the thyristors that might cause damage. To prevent these currents from flowing through the thyristors, the impedance needs to be increased. This can be done by adding an inductor to the system as seen in Figure 4-16, because the inductor represents a high impedance for short duration pulses. The inductor limits the rate of rise of the surge current during a voltage surge.

It is generally accepted that voltage and current impulses that are applied to evaluate system (against lightning surges) have the shape of the waveform seen in Figure 4-17. The surge waveform is characterised by a certain rise and decay time. Where, the rise time (T_s) and the decay time (T_f), are defined as illustrated in Figure 4-17. Current impulses are normally 8/20 µs or 4/10 µs (T_s/T_f) and voltage impulses are normally 1.2/50 µs.

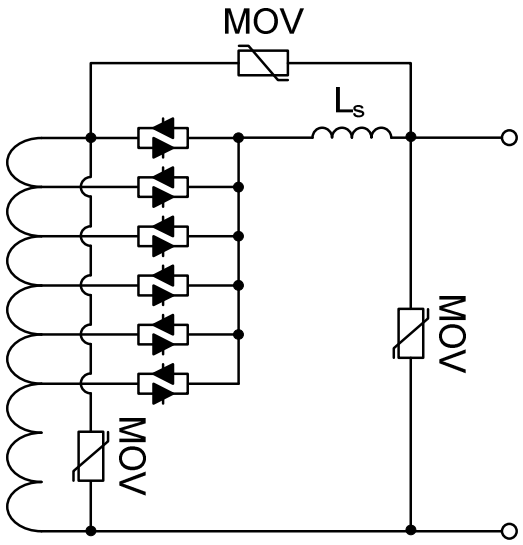

Figure 4-16: Lightning and surge voltage protection

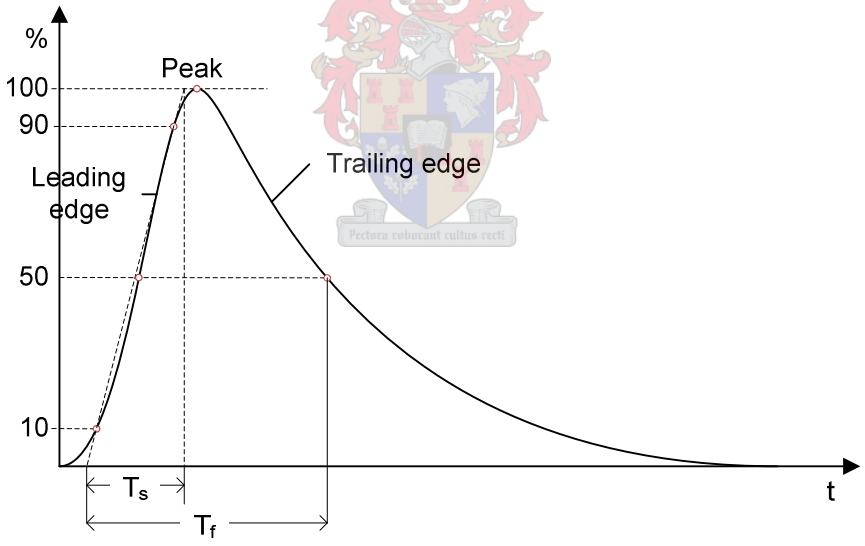

Figure 4-17: Surge impulse waveform

The inductor that is used for limiting the surge current may not saturate and therefore makes use of an air core. To determine the maximum surge current that can be sustained by the thyristors tests were done and can be found in Appendix B. From the tests done on the thyristors it was assumed that a maximum surge

current 10 kA peak is allowed. At a surge current of 10 kA the MOV voltage will be approximately 1050 V. Assuming a 8/20 μs current waveform the required inductance can be calculated using equation 4.13. From the result obtained it was decided to build an inductor with 23 μH which is much bigger than the calculated value.

$$v = L_s \cdot \frac{di}{dt} \tag{4.12}$$

$$L_s = v \cdot \frac{T_s}{I_{peak}} = 1050 \cdot \frac{8\times10^{-6}}{10\times10^{3}} = 840 \text{ nH} \tag{4.13}$$

Where,

v is the MOV clamping voltage

I_{peak} is the peak surge current of 10 kA (*di*)

T_s is the current rise time for a 8/20 μs waveform (*dt*)

An inductor having an inductance of 23 μH and a diameter of 8.5 cm with 16 turns was thus built and installed in the system. A conductor having a cross sectional area of 58.5 mm^2 was used. This yields a current density of 2.4 A/mm^2 when the system is running at twice the rated load current.

4.8 Temperature protection

Temperature protection is implemented to protect the thyristors and the transformer from overheating. The estimation of the transformer temperature is implemented in software by making use of the estimation techniques and the ambient temperature measurement as discussed in chapter 3. To monitor the temperature of the thyristors, two thermistors are used.

By using the model shown in Figure 4-8 the temperature of the heat sink directly below the thyristor can be calculated as shown in equation 4.15 below.

$$\theta_s = \theta_a + (q \times R_{sa}) = 50 + (145 \times 0.35) = 100\,°C \quad (4.14)$$

Where,

θ_s is the heat sink temperature directly below the thyristor

θ_a is the maximum expected ambient temperature

q is power dissipation of the thyristor module at 200% load

R_{sa} is the thermal resistance of the chosen heat sink

As it is not possible to measure the exact temperature of the heat sink underneath the thyristor, a value of 85 °C is used as the maximum heat sink temperature. Two thermistors are used to monitor the temperature, where the bigger of the two readings is used as the heat sink temperature. When the heat sink temperature exceeds 85 °C, the output voltage is stepped down to decrease the output current assuming the load has constant impedance. If the heat sink temperature exceeds 88 °C the taps are switched off for 1 minute.

The transformer temperature protection is implemented similarly to the thyristor temperature protection. When the transformer hotspot is estimated to be 98 °C the output voltage is stepped down to decrease the output current. The value of 98 °C is used as this is the value at which the insulation paper inside the transformer is damaged. When the transformer hotspot temperature reaches 105 °C the taps are switched off and are kept off for 5 min as this more or less the winding time constant of the transformer.

4.9 Software Development

4.9.1 Introduction

The embedded software runs on a TMS320F2812 DSP from TI and is implemented using CCS. CCS is ideal for implementing real-time applications as it makes use of the DSP/BIOS kernel. Design ready code which is common to many applications is also available for DSP-based products from TI. The DSP/BIOS

kernel was therefore used to implement the controller software. Although it is a bit time consuming to get acquainted with DSP/BIOS kernel and to adjust the code for DSP/BIOS operation, it quickly becomes clear that DSP/BIOS significantly simplifies the implementation of real-time systems. A short overview of the functioning of the DSP/BIOS kernel is given below. Furthermore the basic structure of the software is given in section 4.10.

4.9.2 DSP/BIOS

DSP/BIOS firmware provides the following basic capabilities:

- Real-time monitoring and control for program execution and programming of variables in real-time
- Real-time scheduling of multi-threaded systems and communication

The modules in Table 4-4 are provided by DSP/BIOS firmware to accomplish the tasks mentioned above. These modules can be configured in the Configuration Tool which is provided. The Configuration Tool allows the user to setup the system configuration, the real-time monitoring and control, the real-time scheduling and communication, through its visual editor. It therefore saves the user the time of having to set up the header and linker command files. Common header and linker command files for DSP peripherals are also supplied by TI. This simplifies the program development significantly as the user only has to setup the peripherals and add his applications software to get started.

Modules for system configuration	
GBL	Global setting manager
MEM	Memory manager
Modules for real-time monitoring and control	
LOG	Message log manager
STS	Statistic accumulator manager
TRC	Trace manager
Modules for real-time scheduling	
HWI	Hardware Interrupt Manager

SWI	Software Interrupt Manager
IDL	Idle function and processing loop manager
CLK	System clock manager
PRD	Periodic function manager
Modules for real-time communication	
PIP	Data pipe manager
HST	Host input/output manager
RTDX	Real-time data exchange manager

Table 4-4 DSB/Bios configuration modules

4.9.3 Thread scheduling

DSP/BIOS execution threads are independent paths of execution which execute different DSP instructions. An execution thread can be an ISR, a sub routine or a function call. This allows developers to structure threads and apply priorities to the different threads. Multi-threaded applications can therefore run on one processor, by allowing higher priority threads to pre-empt lower priority threads. This has the advantage that hard-time threads are executed on time and soft-time threads are executed when the CPU has spare time. DSP/BIOS has four distinct classes of execution threads namely Hardware Interrupts, Software Interrupts, Synchronized Tasks and Background functions. Hardware Interrupts are the highest priority threads and are triggered by an external event. The Peripheral Interrupt Expansion module enables the processor to respond to 96 different types of hardware interrupts. The Configuration Tool's HWI manager is used to map the ISR to the interrupt. HWI dispatcher of the HWI manager allows the user to mask interrupts in the Configuration Tool.

Software interrupts are similar to hardware interrupts but are, as the name suggests, instantiated in software. Software interrupts, like hardware interrupts, run to completion and are also pre-emptive. They can only be pre-empted by other higher priority software interrupts and hardware interrupts. Software interrupts are instantiated by the SWI_post command.

Unlike SWIs and HWIs, synchronized tasks are capable of suspension and pre-emption whereas HWIs and SWIs can not be suspended. This means, if a task has been posted it can be suspended before it has finished executing, while HWIs and SWIs run to completion. Tasks run on a lower priority than software interrupt but on a higher priority than background idle functions. Tasks can therefore be pre-empted by HWIs, SWIs and higher priority tasks. TSK module is used to manage and schedule synchronized tasks.

4.10 Software Structure

The controller software makes use of HWIs, SWIs and background idle loops and is discussed with the help of Figure 4-18. Timer 2 initiates a HWI when 50 µs have past. This interrupt then sets the ADC to start its conversion. When the ADC has finished converting an ADC interrupt is initiated, which accumulates the measured values for one 50 Hz cycle and calculates the RMS voltage. It is also used to switch between taps. Less time critical SWIs are posted from within the ADC HWI to determine the correct tap setting and to calculate the estimated temperature of the transformer. When the processor has spare time the background idle loops are executed.

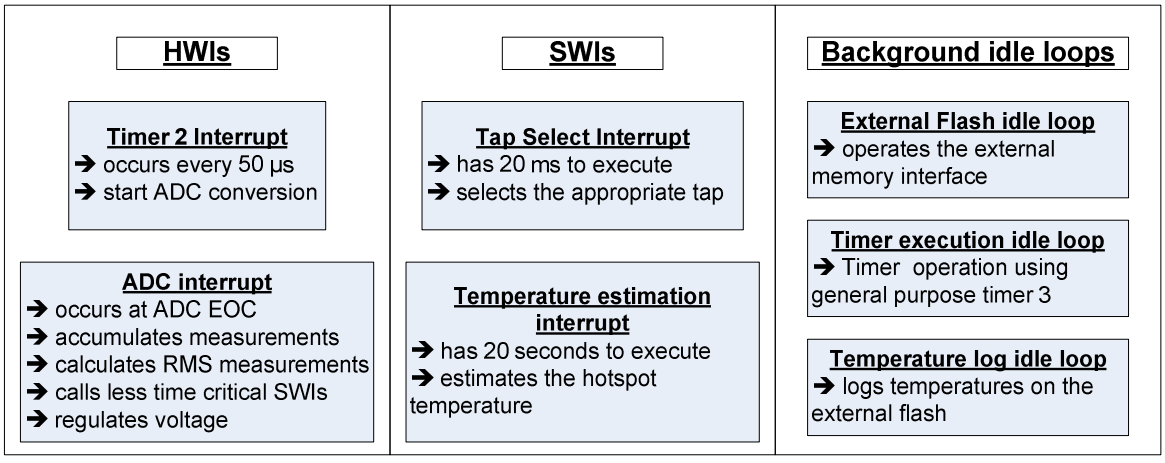

Figure 4-18: Basic software components of controller

4.10.1 Main procedure

The main procedure does not contain a while loop that runs forever as this program was implemented using DSP/BIOS and runs in a background idle loop when the processor is not busy. Furthermore the main loop is used to initialize variables and set up the CPU and the peripherals. Only the peripherals which are used in this application were enabled. After the system peripherals, variables and the transformer temperatures are initialised the hardware interrupts are enabled.

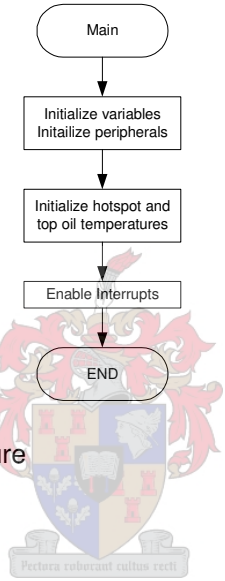

Figure 4-19: Flowchart for main procedure

4.10.2 Transformer estimated temperature initialisation

Before the Interrupts are enabled, the hotspot and the top oil temperature are estimated, so that the initial values used for the temperature estimation are set. This is done so that if the system is shut off, due to an error on the medium voltage side of the transformer, the initial values used are not set to ambient temperature but rather to the estimated value, i.e. the true top oil and hotspot temperature of the transformer. The initial hotspot and top oil temperatures will only be equal to the ambient temperature if the system was off for a long time (±12 hours). The procedure used to determine the top oil and hotspot temperature makes use of the IEC exponential method to estimate the new values after the system was off for a certain time. To be able to recall the top oil and hotspot temperatures, when the system was shut off, the estimated temperatures together

with the time are stored on the external flash every 20 seconds. When the system is then switched on again these values are read from the flash and used to predict the top oil and hotspot temperatures. The top oil, hot spot, ambient temperature and the time are saved on the flash. As it is not possible to know the ambient temperature when the system is off, the ambient temperature for the time the system was off is calculated as the average temperature when the system was shut off and the current temperature.

4.10.3 Hardware Interrupts

The system makes use of two hardware interrupts. Timer 2 of Event Manager A is used to generate a timer period interrupt which is used to start the ADC conversion cycle. This is done by setting the Start of Conversion (SOC) pin high in the first ADC Control register. An End of Conversion (EOC) interrupt is then generated when the ADC has finished converting the specified number of conversions. Table 4-5 gives a summary of the hardware interrupts that are used.

Peripheral	PIE Priority	Hardware Interrupt
ADC	INT1.6	EOC (ADCINT)
EVA (Timer 2)	INT3.1	Period (T2PINT)

Table 4-5: Hardware interrupts

4.10.3.1 Timer 2 period ISR

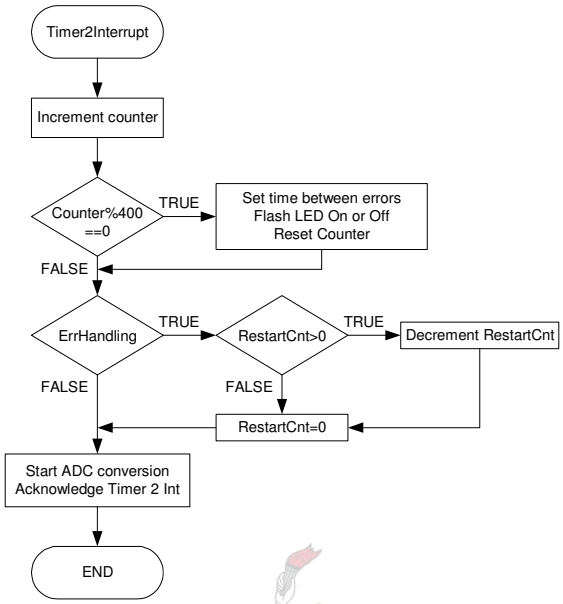

Figure 4-20: Interrupt service routine flowchart for Timer 2 period interrupt

The flow diagram discussing the functionality of the timer 2 interrupt service routine is given is Figure 4-20. Timer 2 is set to post an interrupt every 50 μs. A counter is incremented every time the ISR is called and is used for controlling the flashing time of the system run LED. The counter is also used to determine the time that has passed between errors. If an error has occurred and the taps of the system are off, the restart counter is set to a required value and decremented until the required time has passed. This is used to keep the taps off, for long enough, for errors to be cleared. At the end of the ISR the interrupt is acknowledged and the ADC conversion is started.

4.10.3.2 ADC end of conversion ISR

The ADC interrupt that is triggered after the last conversion of the ADC is finished, is illustrated by the flow diagram in Figure 4-21. If no errors have occurred and the system has been stable for the required time the system LED stops flashing and

is put on. If the system is running and the input voltage is stable, the required tap is selected. After the taps are selected the ADC measurements are read from the result registers and the measurements are processed in the appropriate procedures. The system is then checked for errors by the error handling procedure. The ADC ISR then checks whether a tap change is needed. If a tap change is needed, the system waits until the input voltage is at a peak before it switches to the required tap.

The procedures that process the voltage, current and temperature measurements are called directly from the ADC interrupt service routine. They therefore have the same priority as the interrupt. The error handling procedure is also called directly from the interrupt service routine and thus also runs to completion. Some software interrupts are however instantiated in these procedures and can therefore be pre-empted by the ADC or Timer hardware interrupts.

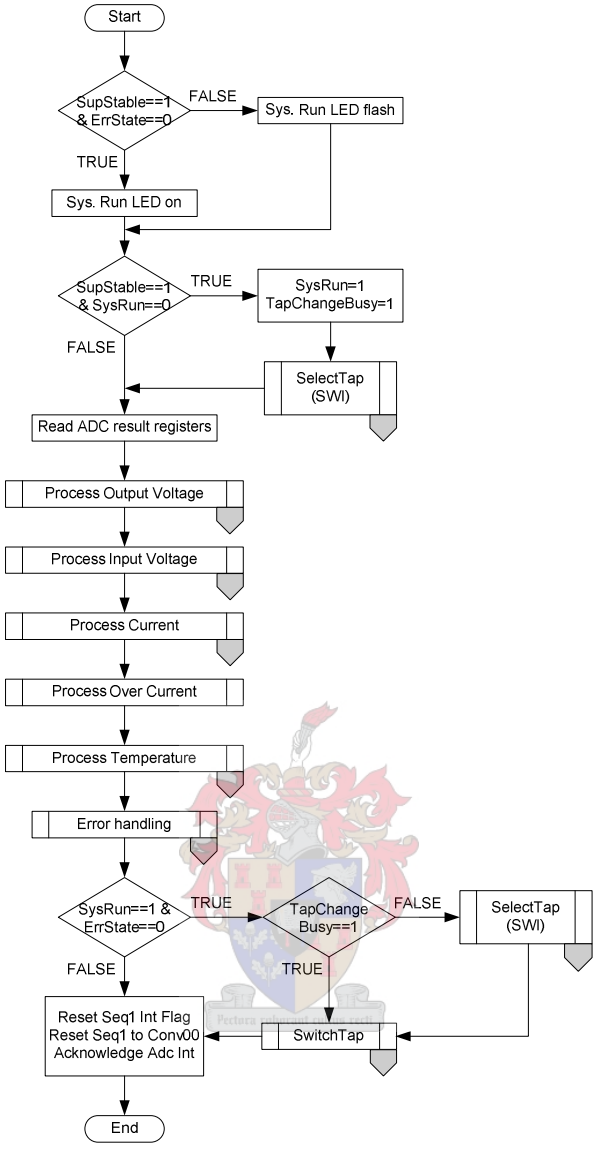

Figure 4-21: Interrupt Service Routine flowchart for ADC interrupt

4.10.4 Software Interrupts

A brief description of the software interrupts and their priorities is given in Table 4-6. The priorities of the software interrupts are determined by the time requirements of the procedures that have to be executed. The tap selection interrupt has a higher priority than the temperature estimation procedure because the transformer temperatures are only estimated every 20 seconds. The

temperature estimation procedure is therefore the least time critical procedure of the two.

Software Interrupt	Priority	Description
SWI_TSL	2	Determines correct tap setting
SWI_Temp	1	Calculates the estimated transformer temperatures by using the measured ambient temperature and output current

Table 4-6: Software interrupts

4.10.4.1 Temperature estimation SWI

The hotspot temperature estimation is done by using the differential IEC method described in Chapter 3. First the measured current is divided by the rated current to obtain the current ratio, K. It is then determined whether the system is put on for the first time. If the system is put on for the first time, the top oil temperature and hotspot temperature is equal to the ambient temperature. If this is not the case the temperatures are set to the values estimated by the temperature initialisation procedure that is executed at the restart. Temperature estimation is performed every 20 seconds, which is sufficient considering that the fastest time constant in the system is 4 minutes. The procedure also sets the state flag of temperature log state machine to write and sets the newly calculated values and the present time to be written to the external flash. This is done, so that when the system is shut off, the temperatures at shut off and the time of shut off are available for the system to calculate the estimated transformer temperatures when the system restarts. A flow diagram of the temperature estimation procedure is given in Figure 4-22.

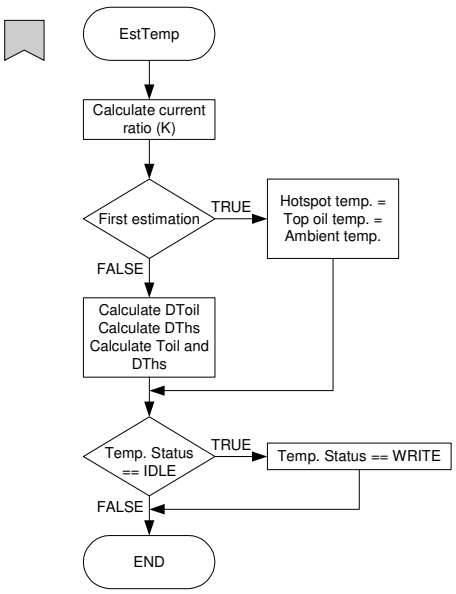

Figure 4-22: Hotspot temperature estimation software interrupt

4.10.4.2 Tap selection SWI

The tap selection is executed by using the software interrupt illustrated in the flow diagram in Figure 4-23. Tap selection is done by evaluating the output voltage, estimated hotspot temperature and the measured heat sink temperature. A tap change due to output voltage is determined by checking if the output voltage is in the required range for a certain tap. If a tap change due to the voltage is required, the required tap is selected. If the heat sink or hotspot temperature is above a certain level the temperature limit mode is set. In this case the tap change due to temperature is determined by selecting a tap so that the temperature of the heat sink or the hotspot decreases. By assuming that the load impedance of the system is constant, the output voltage is decreased to decrease the load current and thereby decreasing the temperature of the heat sink and the hotspot of the transformer. Hysteresis is also introduced for the voltage and the temperature tap selection to prevent the system from alternating between two taps. More detail about the tap position and tap overlap, for the voltage regulation, is given in Appendix C.

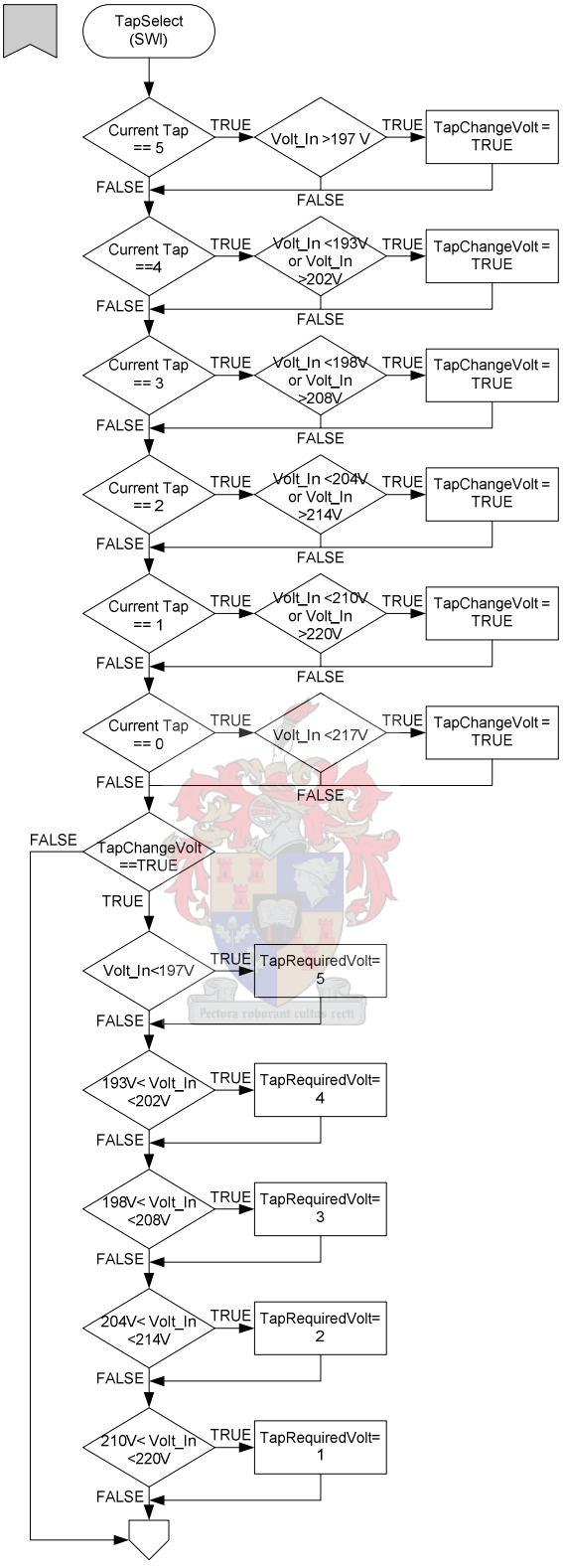
TapSelect (SWI)
Current Tap == 5
TRUE
Volt_In >197 V
TRUE
TapChangeVolt = TRUE
FALSE
FALSE
Current Tap ==4
TRUE
Volt_In <193V or Volt_In >202V
TRUE
TapChangeVolt = TRUE
FALSE
FALSE
Current Tap == 3
TRUE
Volt_In <198V or Volt_In >208V
TRUE
TapChangeVolt = TRUE
FALSE
FALSE
Current Tap == 2
TRUE
Volt_In <204V or Volt_In >214V
TRUE
TapChangeVolt = TRUE
FALSE
FALSE
Current Tap == 1
TRUE
Volt_In <210V or Volt_In >220V
TRUE
TapChangeVolt = TRUE
FALSE
FALSE
Current Tap == 0
TRUE
Volt_In <217V
TRUE
TapChangeVolt = TRUE
FALSE
FALSE
FALSE
TapChangeVolt ==TRUE
TRUE
Volt_In<197V
TRUE
TapRequiredVolt= 5
FALSE
193V< Volt_In <202V
TRUE
TapRequiredVolt= 4
FALSE
198V< Volt_In <208V
TRUE
TapRequiredVolt= 3
FALSE
204V< Volt_In <214V
TRUE
TapRequiredVolt= 2
FALSE
210V< Volt_In <220V
TRUE
TapRequiredVolt= 1
FALSE

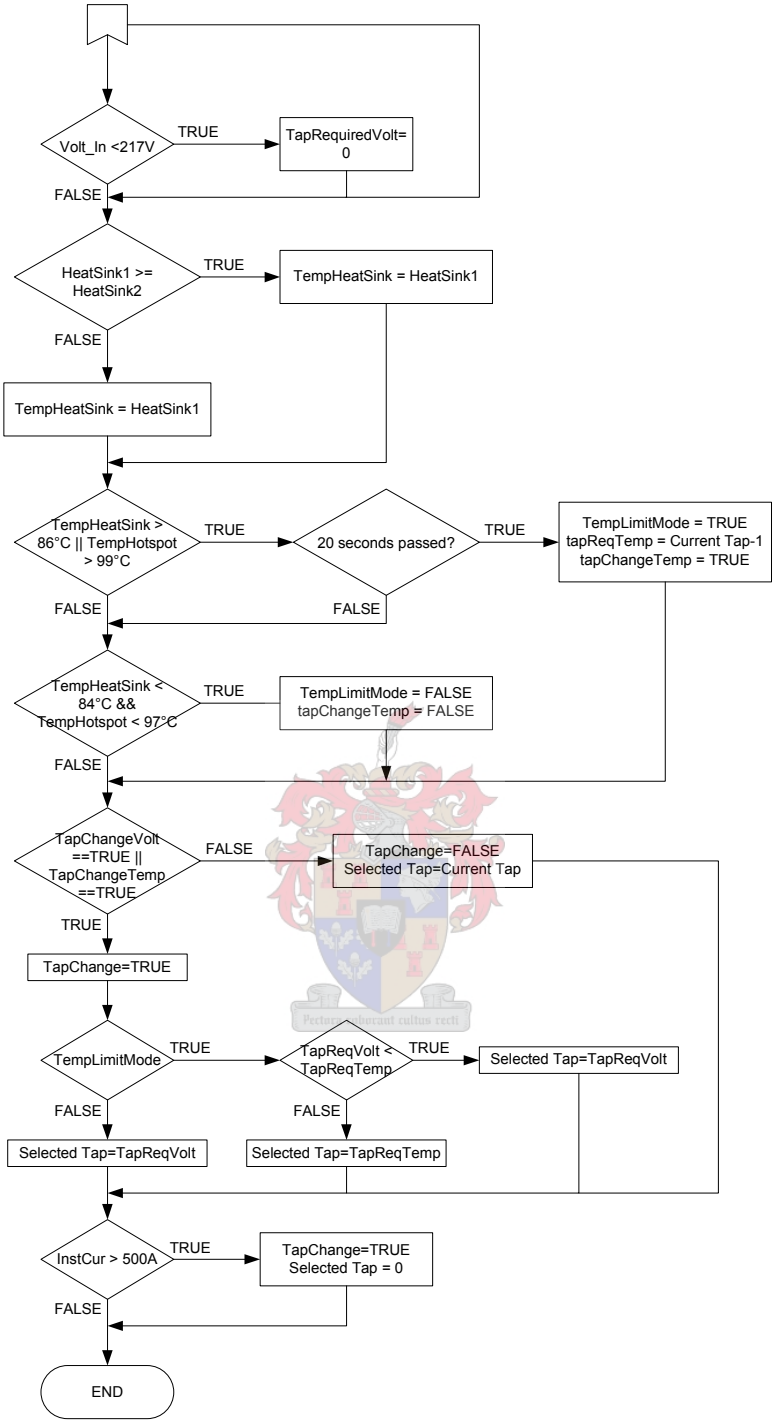

Figure 4-23: Software interrupt, tap selection

If the system is in temperature limit mode, the lowest tap setting will be selected, thereby decreasing the output voltage and the output current. If the output current

peak exceeds 500 A the nominal tap will be selected as it is the only tap that can handle currents of this magnitude for the required time.

4.10.5 Process Measurements

The process measurement procedures are called from the ADC interrupt. They are used to calculate the RMS input voltage, output voltage and output current. The procedures use the same methods to calculate the true RMS voltages and current. Measurements are accumulated for one cycle of the 50 Hz voltages and currents. There are two current accumulate procedures, one is used to measure the current from the 150:1 CT and the other is used to measure the current from the 2500:1 CT. The 2500:1 CT is used to measure overload and short circuit currents until the system switches off or the error is cleared. Both methods are identical and calculate the average RMS current for 1 second, 3 seconds and 20 seconds. These averages are used for over current protection and coordination with circuit breakers that are used in the services connection boxes (refer to Figure 4-5). The flow diagrams for the input voltage, output voltage and output currents is given in Figure 4-24, Figure 4-25 and Figure 4-26.

Pectora roborant cultus recti

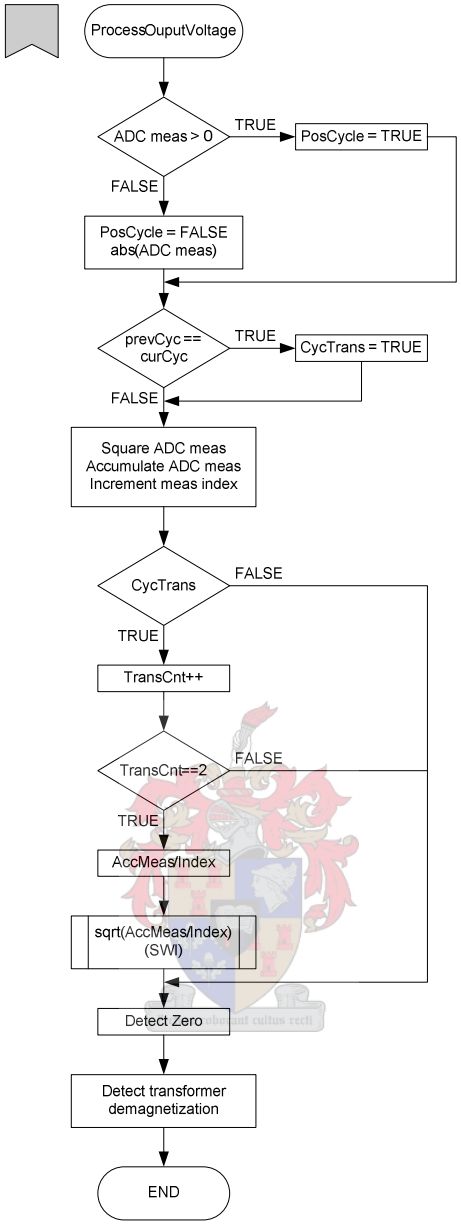

Figure 4-24: Procedure for calculating RMS output voltage, zero detect and transformer demagnetization

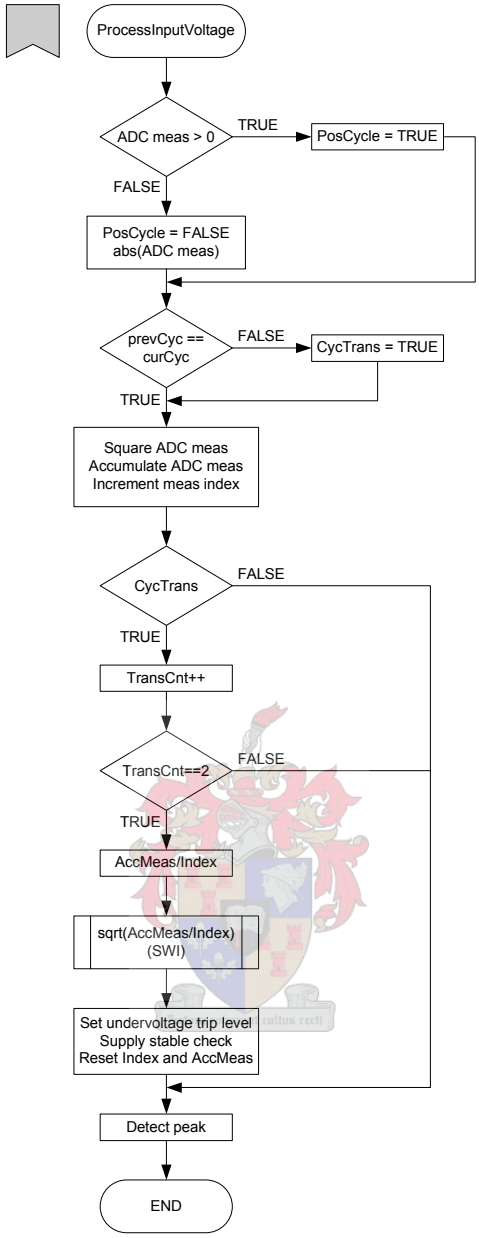

Figure 4-25: Procedure for calculating supply RMS voltage, checking stability of input signal and detecting the peak

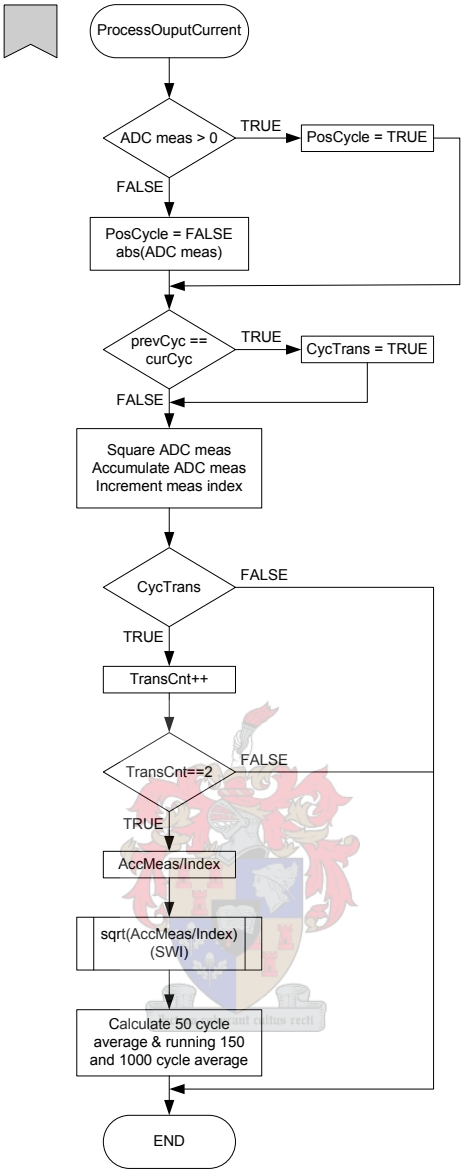

Figure 4-26: Procedure used to calculate RMS output current and running averages of output current for 50, 150 and 1000 cycles

The RMS measurements are calculated as follows:

- ADC measurements is squared
- Squared values are accumulated for one 50 Hz cycle
- Accumulated total of the squared values is divided by the number of samples that were taken (squared average)

- Square root of the squared average is taken to provide the true RMS measurement

4.10.6 Error handling

The error handling procedure that is illustrated in Figure 4-27 is used to ensure that over current, over voltage, under voltage and over temperatures are detected and handled correctly. The type of error that has occurred is made visible to the user by the status LEDs on the communication board. Table 4-7 illustrates the different states represented by the LEDs.

Over current errors are detected for 20 second RMS running averages, 3 second RMS running average, 1 second RMS average, 20 ms RMS measurements and instantaneous peak current. The current limits at which the errors occur are chosen by using Figure 4-7. They are chosen in such a way that the current at which an error occurs, is conducted long enough, to allow the Curve 1 circuit breaker to trip if the error has occurred on the customer side of the system. Voltage errors occur if the nominal tap voltage exceeds 265 V or drops below 115 V. Temperature errors occur when the heat sink temperature or the hotspot temperature exceeds 115 °C. If an error has occurred, the restart counter is set and the taps will be switched off until the counter, which is decremented in the Timer ISR, has expired.

	Over Current	**Over Voltage**	**Under Voltage**	**Over Temperature**	**Normal Operation**
System	Flash	Flash	Flash	Flash	On
Temperature	X	X	X	On	Off
Current	On	X	X	X	Off
Voltage	X	On	Flash	X	Off

Table 4-7: Status LED functionality

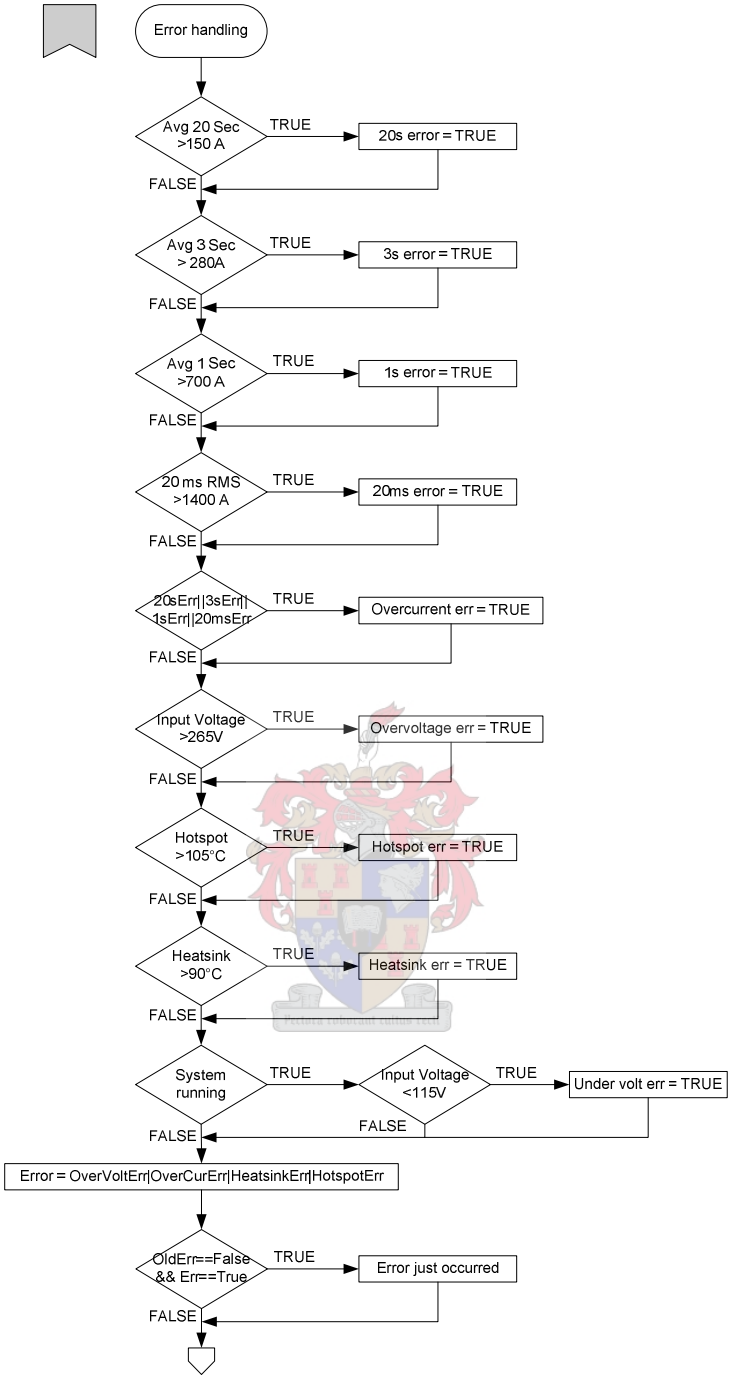
Error handling
Avg 20 Sec >150 A
TRUE
20s error = TRUE
FALSE
Avg 3 Sec > 280A
TRUE
3s error = TRUE
FALSE
Avg 1 Sec >700 A
TRUE
1s error = TRUE
FALSE
20 ms RMS >1400 A
TRUE
20ms error = TRUE
FALSE
20sErr||3sErr|| 1sErr||20msErr
TRUE
Overcurrent err = TRUE
FALSE
Input Voltage >265V
TRUE
Overvoltage err = TRUE
FALSE
Hotspot >105°C
TRUE
Hotspot err = TRUE
FALSE
Heatsink >90°C
TRUE
Heatsink err = TRUE
FALSE
System running
TRUE
Input Voltage <115V
TRUE
Under volt err = TRUE
FALSE
FALSE
Error = OverVoltErr|OverCurErr|HeatsinkErr|HotspotErr
OldErr==False && Err==True
TRUE
Error just occurred
FALSE

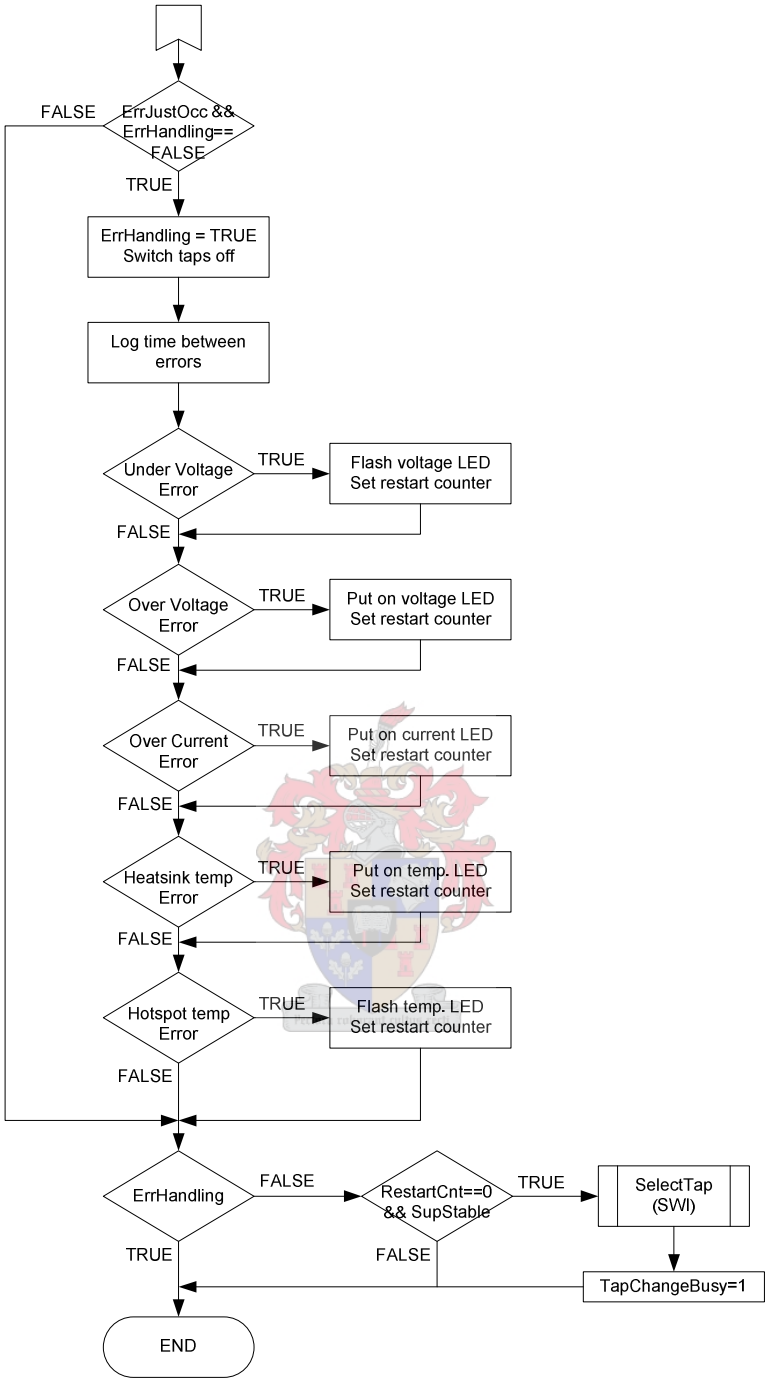

Figure 4-27: Error handling procedure

4.10.7 Background idle loops

Background idle loops are used to implement functions that are the least time critical. They are implemented using the configuration tool and are executed

whenever the processor has spare time. The three background functions are given in Table 4-8 below and are used for external interface, timer execution and temperature logging operation. Short descriptions of the functions, together with the flow diagrams are given below.

Background idle	Description
Flash_exec	External memory interface operation
Timer_exec	Timer operation using general purpose timer 3
Temp_exec	Temperature data logging

Table 4-8: Background idle loops

4.10.7.1 Timer 3 background idle loop

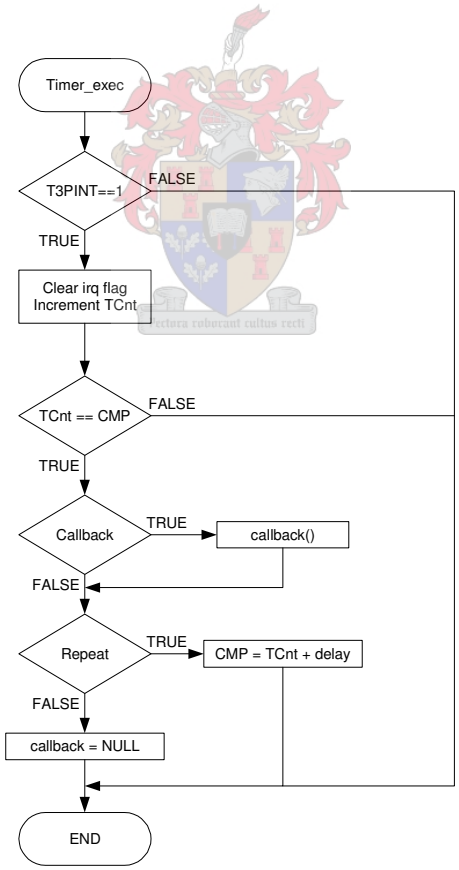

Figure 4-28: Background idle function for timer execution

The background idle function for timer operation using the general purpose timer 3 is illustrated in Figure 4-28. It is used to determine timeouts for flash write operation, sector erase operation and chip erase operations. If a timeout has occurred it sets the execution of the desired callback functions for the different operations.

4.10.7.2 Temperature logging background idle loop

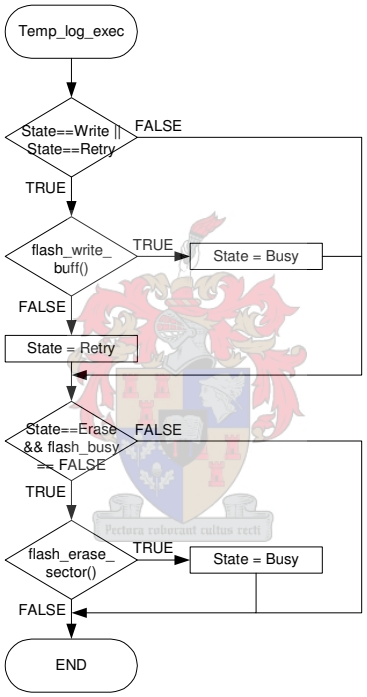

Figure 4-29: Background idle function for temperature logging on external flash

The flow diagram in Figure 4-29 describes the functioning of the background idle loop that is used to write the transformer temperatures to the external flash memory. It is represented by four states namely write, retry, erase and busy. The ready or busy (RY/BY) pin of the flash memory chip is sampled to check whether the flash device is busy and if a write or erase operation was successful. If a write or erase operation was unsuccessful the retry flag is set and the process is repeated until successful. This function is used together with external memory idle

loop to communicate with the external flash. It should be noted that for other logger operations similar idle loops can be added.

4.10.7.3 External memory background idle loop

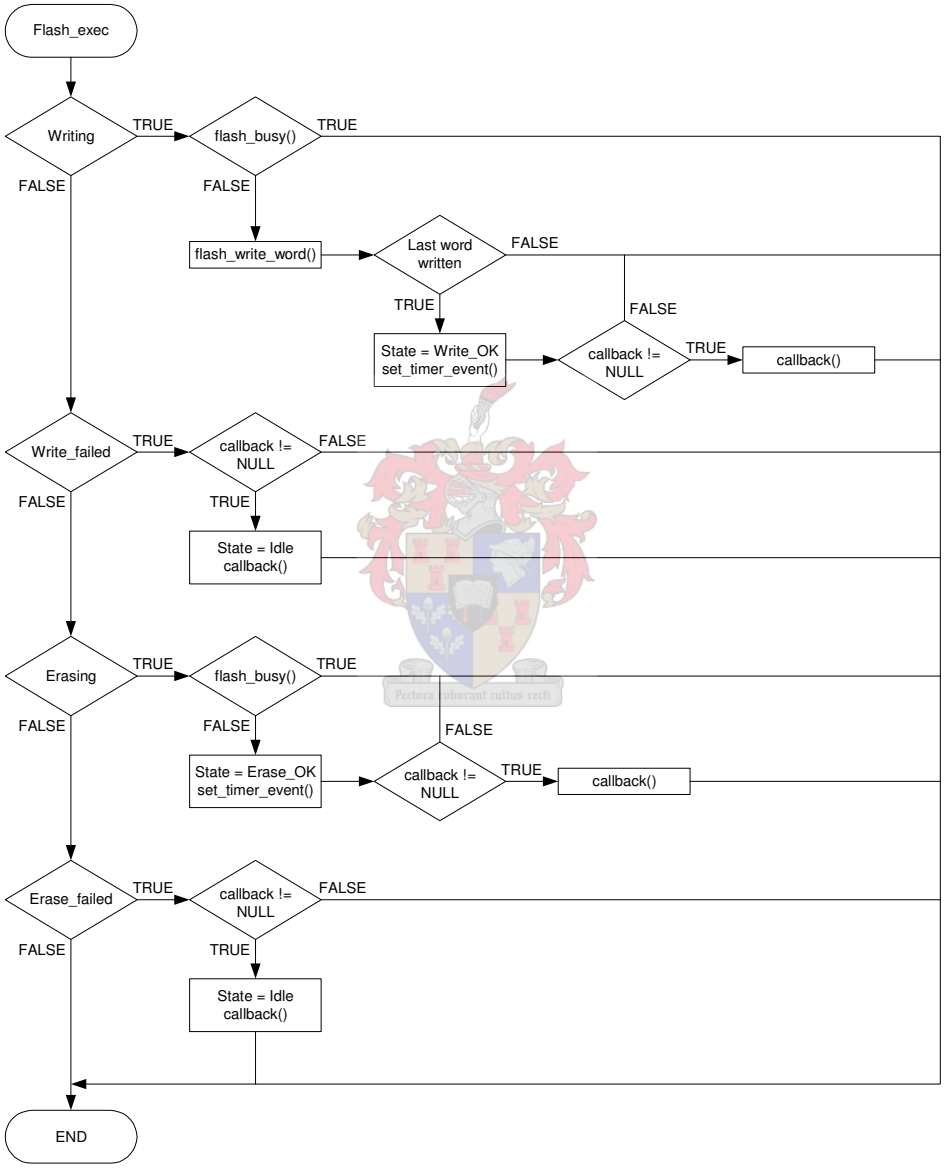

Figure 4-30: Background idle function for external memory interface execution

The external memory background idle loop is used for general operation of the flash memory device. The flow diagram of the background idle function is given in Figure 4-30. It makes use of the following states: Idle, Erase, Erase OK, Erase Failed, Write, Write OK and Write Failed. The RY/BY pin of the flash device is used to verify erase and write operations.

If a write operation is instantiated the loop checks whether the write operation was successful. If the operation was successful it checks whether all the words in the write buffer have been written. When the last word in the buffer has been written it sets Write OK flag and starts a timer event. If no callback function is present the operation is finished and it returns but if a callback function is available it is executed. In the event of a write failure the procedure checks if a callback function is present. If a callback function is present it sets the status flag accordingly and executes the callback function. If an erase operation is instantiated a similar procedure is used as for the write operation. If the erase operation was not successful a callback function is called if one is available.

4.11 Summary

To summarise, this chapter discusses the design of the SRAPET. A 3 tap 16 kVA, 22 kV to 240 V, transformer and a 6 tap, 22 kV to 230 V, transformer were used in the development. The 3 tap transformer was used for temperature tests that were used to verify the temperature estimation techniques that were described in chapter 4. The results of the temperature tests will be discussed in the next chapter. Furthermore the design of the individual components of the controller and the selection of certain components is also explained. Secondly the implementation of the software using the CCS real-time kernel from TI and the controller software were discussed.

5. Results

As discussed earlier two 16 kVA transformers were used. A three tap 22 kV to 240 V was used for temperature tests. The system control was implemented on both transformers. The voltage regulation that is discussed in this chapter only discusses the six tap, 22 kV to 230 V, transformer. The taps boost the input voltage from 0% to 15%. No buck windings are present as it is not necessary to limit the voltage in the applications this step voltage regulator is intended for.

Furthermore this chapter looks at the temperature estimation techniques examined in chapter 3. It looks at the temperature measurements obtained by the thermistors that were placed inside the transformer as discussed in the previous chapter. The measurements are compared to the values given as examples in the IEC. The hotspot temperature is also estimated and compared to the measured temperature of the oil between the HV and the LV windings. It should be noted that it is not possible to measure the true hotspot temperature in this particular case as it would have required them to be inserted when the transformer was built and that was unfortunately not possible and thus thermistors were used to measure where possible.

Pectora roborant cultus recti

5.1 Tests setup

The electrical test setup that is used for temperature rise tests and voltage regulation tests on the 16 kVA transformer is shown in Figure 5-1 below. A, 240 V to 22 kV, three tap transformer is used to step up the voltage to 22 kV and supply the test transformer with 22 kV. The six tap and three tap transformers that were used in the project were both connected to the step-up transformer. The variac is used to adjust the input voltage as required and is connected to the step-up transformers nominal tap. A 160 A fuse is also inserted to limit the current. Earth leakage protection is implemented and protects the temperature sensors as well as the controller. The AC source supplies 230 V, has a 400 A, circuit breaker and

is used to provide earth leakage protection to the controller and it's peripheral boards.

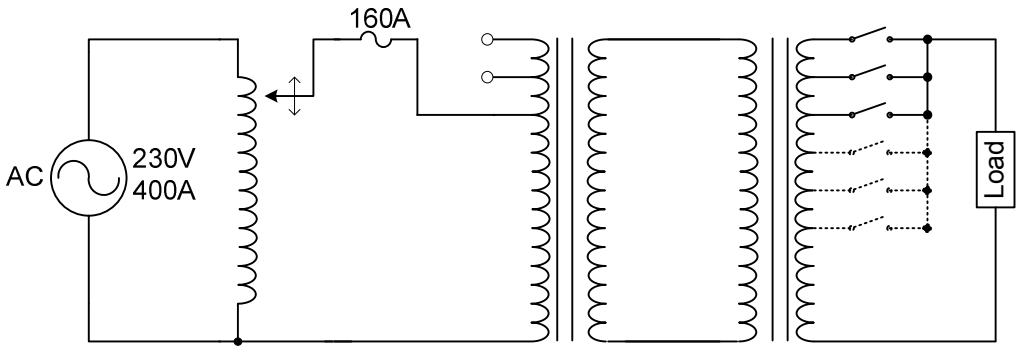

Figure 5-1: Electrical setup

5.2 Voltage regulation

Figure 5-3 and Figure 5-4 show the voltage regulation for a gradually decreasing and increasing input voltage. It can be seen that the output voltage stays constant until the input voltage decreases below 15% of the output voltage. The output voltage then decreases proportionally with the input voltage until it drops below 115 V. When the voltage drops lower than 115 V, the taps are switched off.

The percentage voltage regulation (*VR*) for the system is given in equation 5.1. Where, voltage regulation is defined as the change in output voltage from no-load (V_{RNL}) to full load (V_{RFL}). The voltage regulation can be further improved by adjusting the values at which the taps are switched. For the voltage regulation given above, a voltage drop of 3% is allowed at the output. Thus the output voltage range is given as +15% and -3% for a input voltage of ±15%.

$$VR = \frac{V_{RNL} - V_{RFL}}{V_{RFL}} \times 100 = \frac{230 - 223}{223} \times 100 = 3.14\% \qquad (5.1)$$

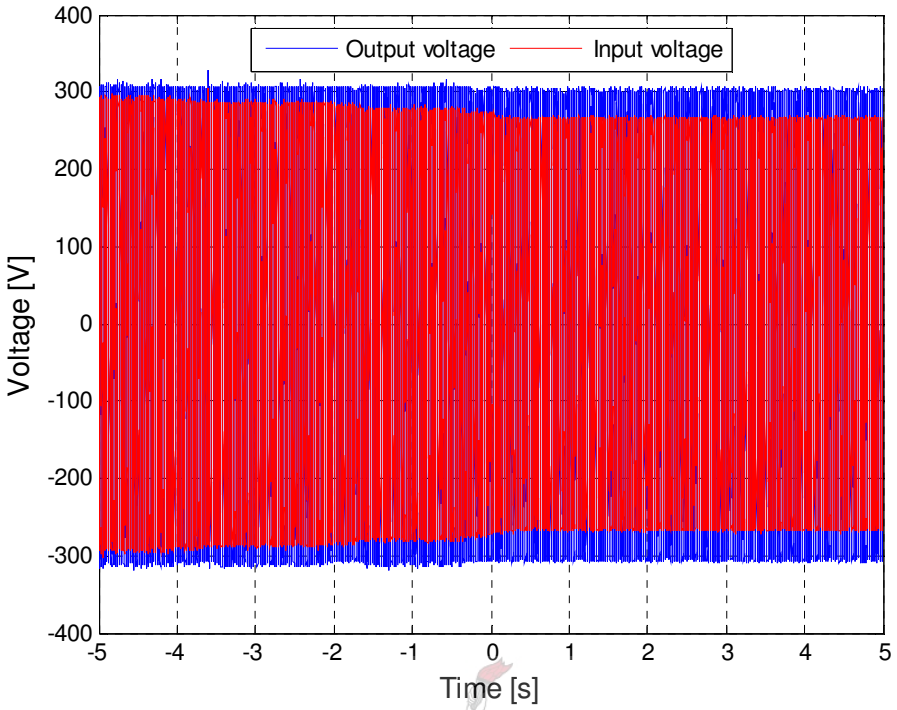

Figure 5-2: Voltage regulation for a gradually decreasing input voltage

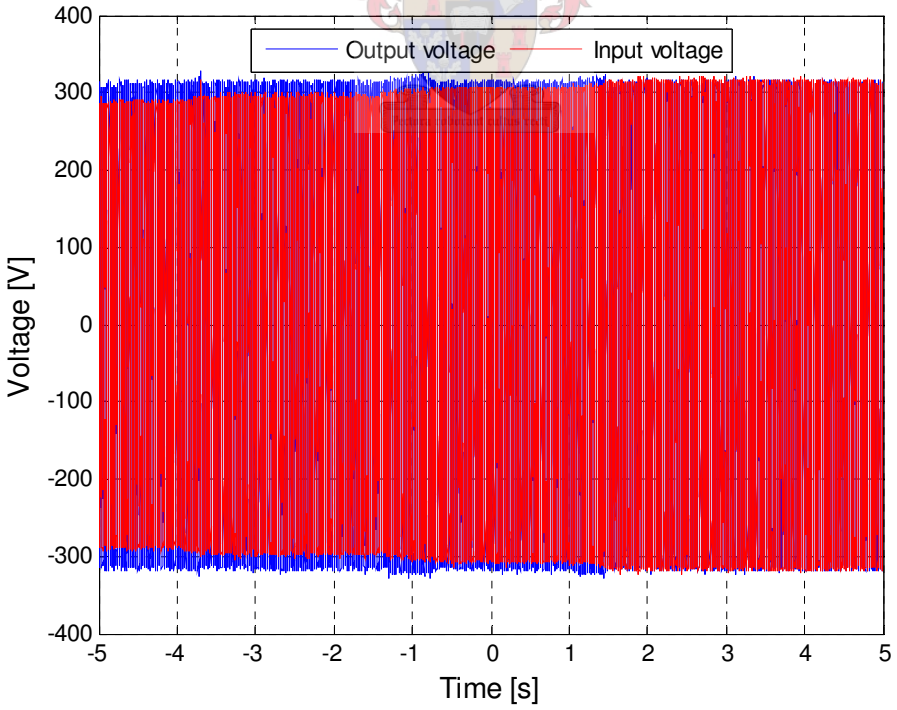

Figure 5-3: Voltage regulation for a gradually increasing input voltage

5.2.1 Response time

The response time of the system refers to the time it takes to react to a change in input voltage and can be discussed with the help of Figure 5-4. Taps are selected after measuring the input voltage of the system for one cycle. The response time is therefore determined by the time it takes to measure the voltage (RMS measurement) as well as the switching time of the semiconductor devices. In this particular case thyristors are used, which have the disadvantage that they are switched off when the current through them becomes zero. To measure the RMS value, the ADC measurements are accumulated for one cycle and the RMS value is then calculated. The quickest possible response time of the system is therefore 20 ms.

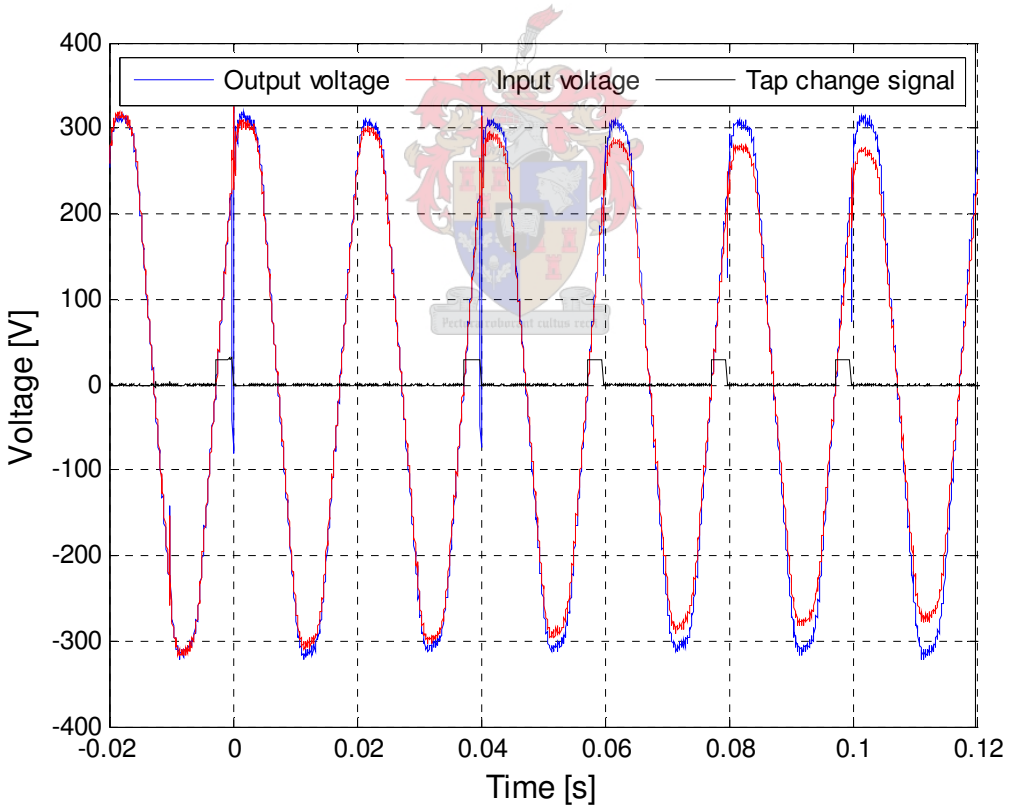

Figure 5-4: Response time

From Figure 5-4 it can be seen that for the system can react within one cycle of the input voltage. A rising edge of the black signal represents the switching of a thyristor module. It can also be seen that the taps are always switched on at a zero crossing of the input voltage. It should also be noted that the input voltage refers to the voltage of the system at the nominal tap of the transformer.

5.2.2 Resistive load

The output voltage and the output current of a 16 kVA resistive load is given in Figure 5-5. Because the load is mainly resistive, the voltage at the point of commutation (i.e. when the current crosses through zero) is close to zero. The switching of the tap does however not take place exactly at the zero crossing of the output voltage, because there is some inductance and the PWM signal that is used to switch the thyristors is off for 66.7% of the time. This is done to prevent saturation of the pulse transformers. The decaying flux of the transformer can however not support the output voltage enough to keep it constant. One method for decreases these glitches in output voltage would be to synchronise the zero crossing, of the output voltage, with the rising edge of the PWM signal. It would however only solve the problem for purely resistive loads as an inductive or capacitive load would introduce a phase shift between the voltage and the current. The thyristors only commutate when the current crosses zero and glitches would therefore still be introduced in the output voltage. This problem is however solved by using the pulse suppression circuit discussed in chapter 4. The pulse suppression circuit stores enough energy for the output voltage to stay constant in the short period both thyristors are off. The maximum delay caused by the off-time of the PWM signal when switching the thyristor, for a 20 kHz signal, is *33.3 µs* as seen in equation 5.2.

$$T_{off} = \frac{1}{f_{PWM}} \times \frac{2}{3} = 50 \times 10^{-6} \times \frac{2}{3} = 33.3 \ \mu s \tag{5.2}$$

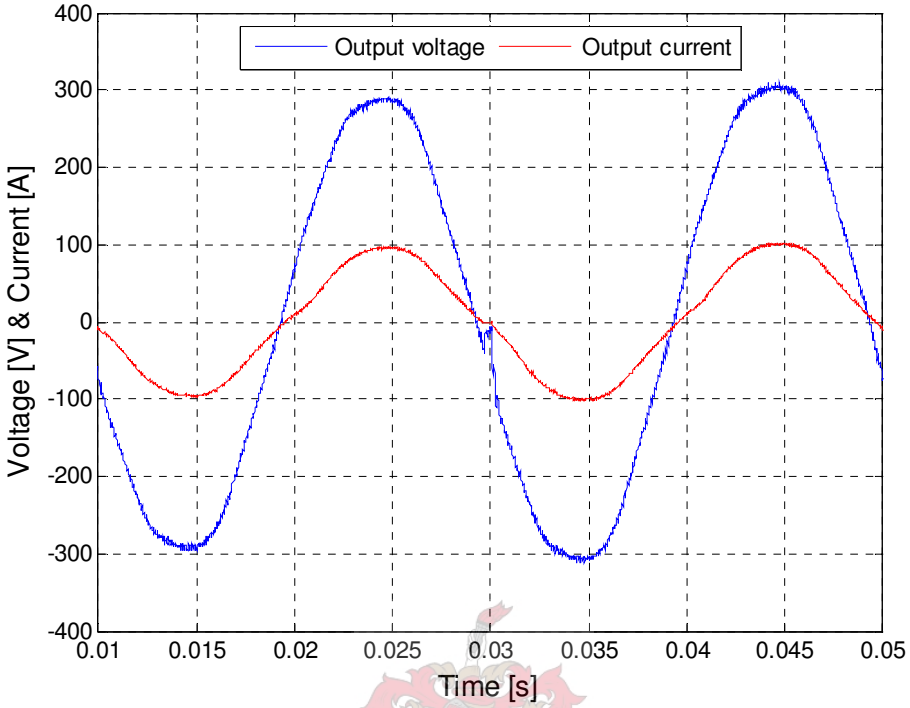

Figure 5-5: Tap switching with 16 kVA resistive load

5.2.3 Inductive load

The stepping up and down of the transformer voltage, with a resistive inductive load is demonstrated in Figure 5-6 and Figure 5-7 below. The power factor (*pf*) of the load is approximately 0.7. The system was switched between the nominal tap and tap 1 of the transformer. From the figures, the effect of the inductance on the voltage glitches is clearly visible and it can be seen that the glitches are large in this particular case. In the case of a purely resistive load it can be seen that the glitches only occur when conduction switches from one thyristor module to another. This can be seen when comparing the output voltage of Figure 5-5 and Figure 5-6. It should also be noted that no peak current is drawn at switch over, which indicates that the tap that is switched off does indeed switch off before the other tap switches on.

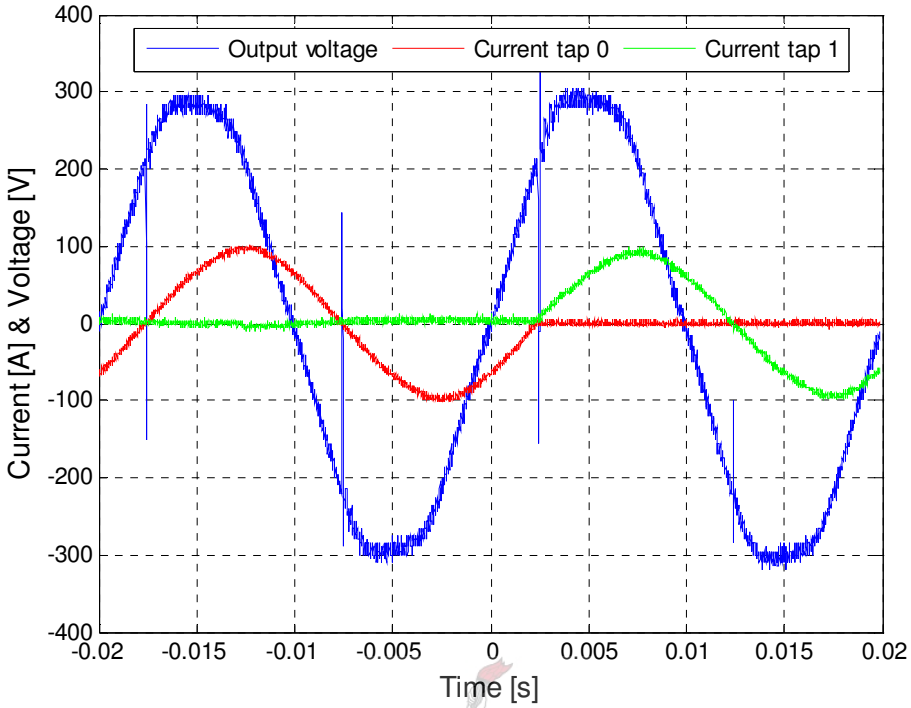

Figure 5-6: Stepping up the voltage with a 16 kVA resistive inductive load

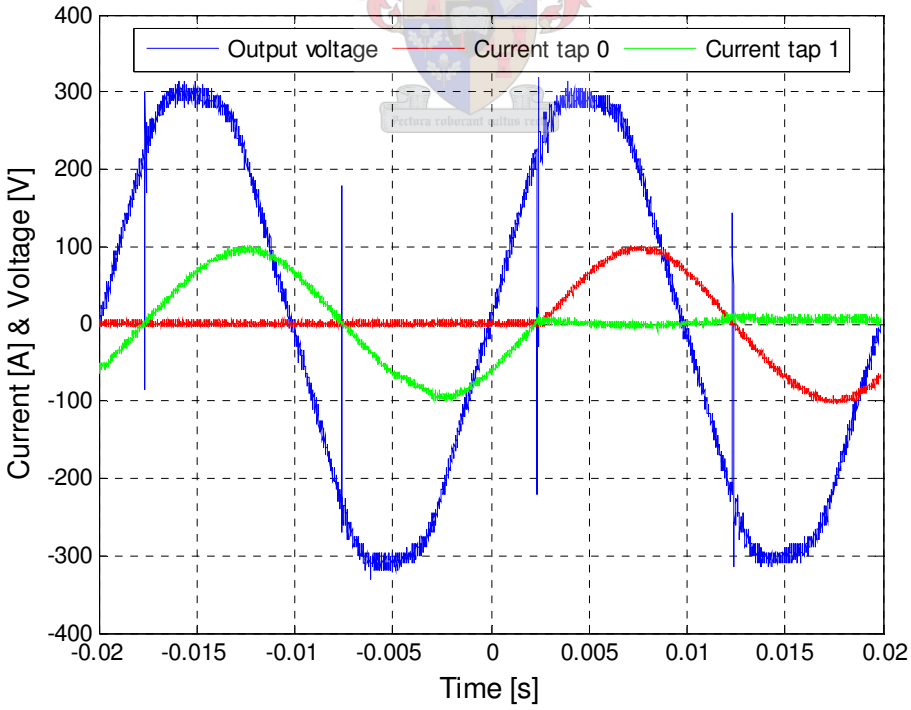

Figure 5-7: Stepping down the voltage with a resistive inductive load

Figure 5-8 shows the output voltage before and after the pulse suppression circuit was added. A 4.4 μF, 400 V, capacitor and a 22 Ω current limiting resistor were used in this case. From the figure it can be seen that the capacitor significantly reduces the glitches. The output voltages, shown in the figure below, were measured for an inductive resistive load. For a purely resistive load they would be considerably smaller, as the voltage would be close to zero when the thyristors commutate.

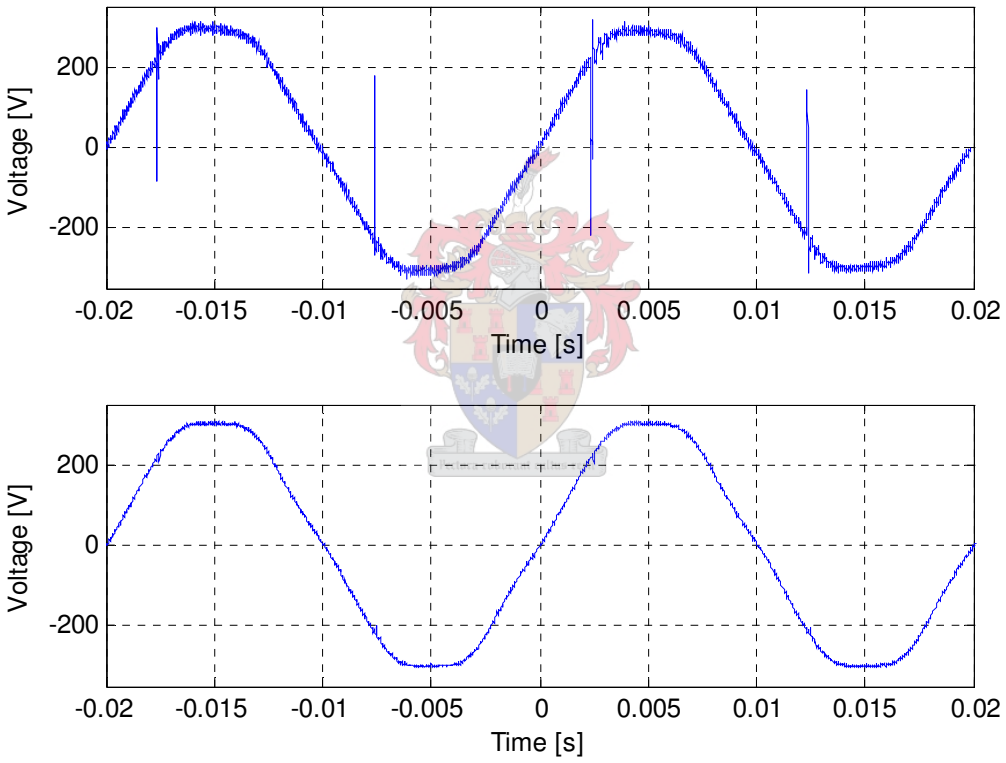

Figure 5-8: Output voltage with pulse suppression

5.3 Temperature estimation

5.3.1 Temperature sensor placement

Temperature sensors on the inside of the transformer tank are positioned as shown in Figure 5-9. Bottom oil measurements are performed by sensors #1, #2, #5, #6 and #9. They are positioned about 5 cm from the bottom of the tank, except for #9 which is about 10 cm from the bottom. Sensors #3, #4, #7 and #8 are positioned between the high voltage and the low voltage windings, as done in [30], whereas sensor #10 is placed between the 2 coils and #11 is placed just above the windings. Sensors #12, #13, #14, #15 and #16 are placed in the top oil, about 5cm below the surface of the oil [1] [29]. A sensor was also placed at the bottom of the transformer, on the outside to determine if it is possible to establish a relationship between the top oil temperature and the temperature of the tank, by measuring the temperature of the bottom plate of the transformer casing.

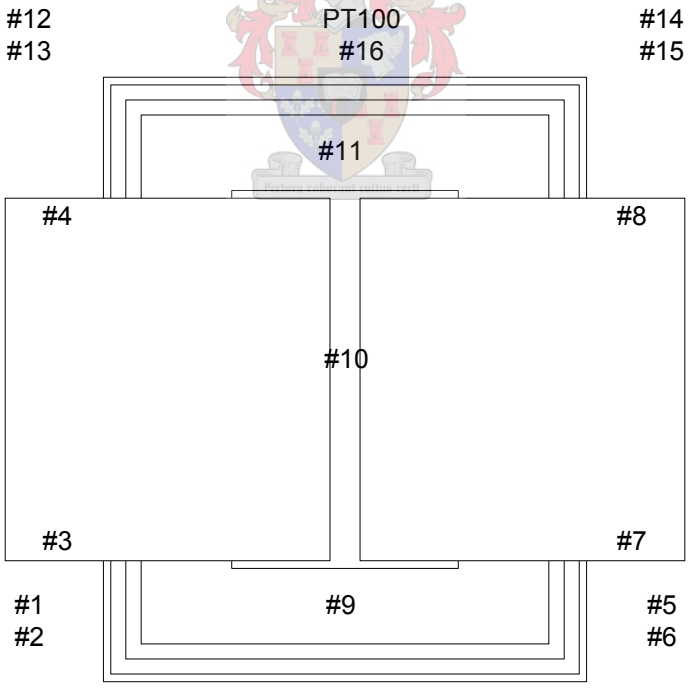

Figure 5-9: Temperature sensor placement

5.3.2 Top oil temperature and top oil time constant

To determine the rated top oil temperature gradient and the top oil time constant, the transformer was operated at 100% load. By using the method described in Annex B.2 of the loading guide for oil-immersed power transformers [23], the ultimate top oil temperature gradient and oil time constant were calculated as 44.4 ℃ and 2.935 hours respectively. The load to no-load loss ratio (*R*) used for the temperature estimation is taken as 4.2 as this was the value measured by short-circuit and open-circuit tests. Figure 5-10 shows the measured top oil temperature gradient, bottom oil temperature gradient and the estimated top oil temperature.

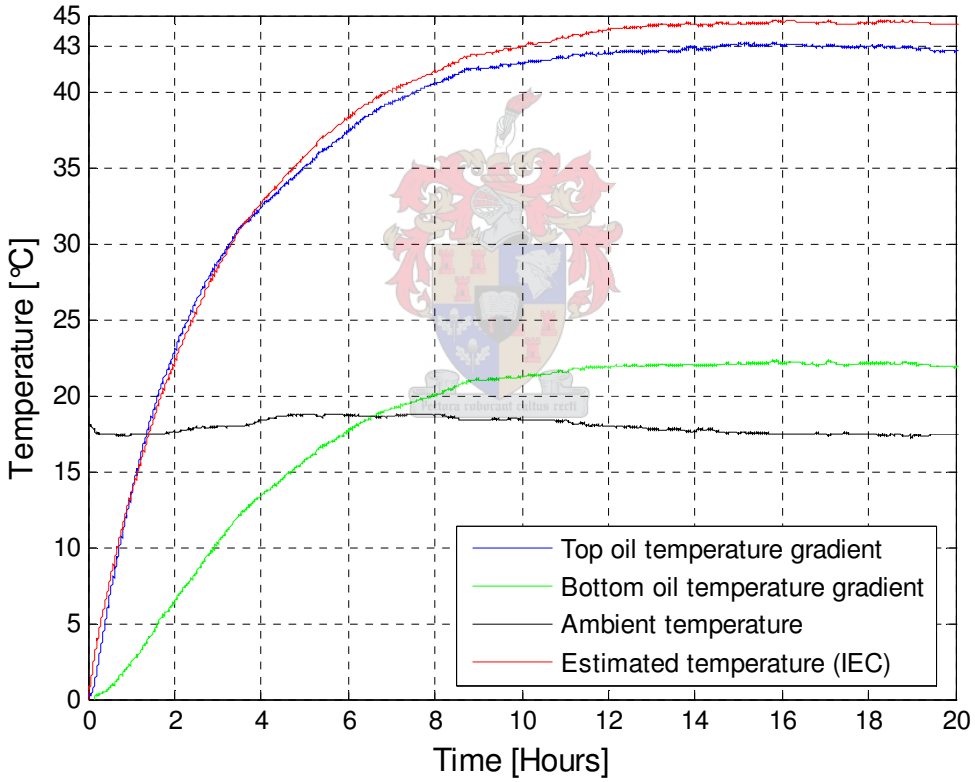

Figure 5-10: Measured top oil time constant and top oil gradient at rated load (100%)

From the measurements shown in Figure 5-10 the average oil temperature at rated load was calculated by adding the top oil temperature to the bottom oil temperature and dividing by two. The values given in the examples of the IEC

standards [23] [24], however differ slightly. The measured top oil time constant (2 hrs 56 min), correlates well with the time constant of 3 hours given in the IEC standards. The top oil gradient at rated load is given as 55 ℃ but was measured to be 44.4 ℃ which is considerably lower than expected.

Figure 5-11 shows the measured top oil temperature gradient for a 125% load and the estimated temperature for the values obtained from the temperature rise test at rated load. Equation 5.3 and 5.4 are used to calculate the ultimate top oil gradient and time constant as proposed by the IEEE and the IEC method.

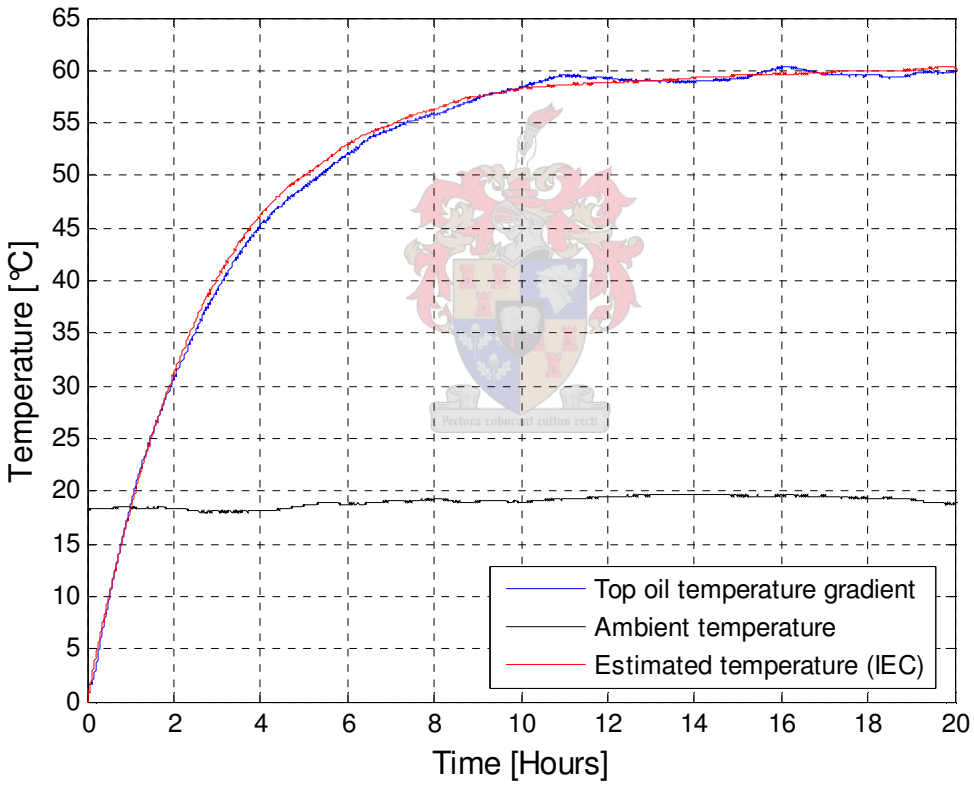

Figure 5-11: Measured top oil time constant and top oil gradient for 125% load

$$\Delta\theta_{TO,U} = \Delta\theta_{TO,R}\left(\frac{K^2 \cdot R+1}{R+1}\right)^{x} = 44.4 \cdot \left(\frac{1.25^2 \cdot 4.2+1}{4.2+1}\right)^{0.8} = 59.9\ ^{\circ}\mathrm{C} \qquad (5.3)$$

$$\tau_{oil} = \tau_{oil,R} \frac{\Delta\theta_{oil,U} / \Delta\theta_{oil,R} - \Delta\theta_{oil,I} / \Delta\theta_{oil,R}}{(\Delta\theta_{oil,U} / \Delta\theta_{oil,R})^{1/x} - (\Delta\theta_{oil,I} / \Delta\theta_{oil,R})^{1/x}} = 2\,\text{hrs}\ \ 43\,\text{min} \qquad (5.4)$$

From Figure 5-11 it can be seen that the calculated top oil gradient and the time constant are estimated accurately. The true temperature is followed quite closely by the estimated temperature.

Figure 5-12 shows the measured top oil temperature gradient for 70% load and the estimated temperature for the values obtained from the temperature rise test at rated load. Equation 5.3 and 5.4 are again used to calculate the top oil gradient and the time constant. The equations are rewritten below with the appropriate values.

$$\Delta\theta_{TO,U} = \Delta\theta_{TO,R}\left(\frac{K^2 \cdot R + 1}{R + 1}\right)^{x} = 44.4 \cdot \left(\frac{0.70^2 \cdot 4.2 + 1}{4.2 + 1}\right)^{0.8} = 29.0\ ^{\circ}\text{C}$$

$$\tau_{oil} = \tau_{oil,R} \frac{\Delta\theta_{oil,U} / \Delta\theta_{oil,R} - \Delta\theta_{oil,I} / \Delta\theta_{oil,R}}{(\Delta\theta_{oil,U} / \Delta\theta_{oil,R})^{1/x} - (\Delta\theta_{oil,I} / \Delta\theta_{oil,R})^{1/x}} = 3\,\text{hrs}\ \ 16\,\text{min}$$

Considering the results discussed in Figure 5-10, Figure 5-11 and Figure 5-12 it becomes clear that the estimation techniques are able to estimate the top oil temperatures accurately for different load steps. It also confirms that the equation for adjusting the time constant is accurate.

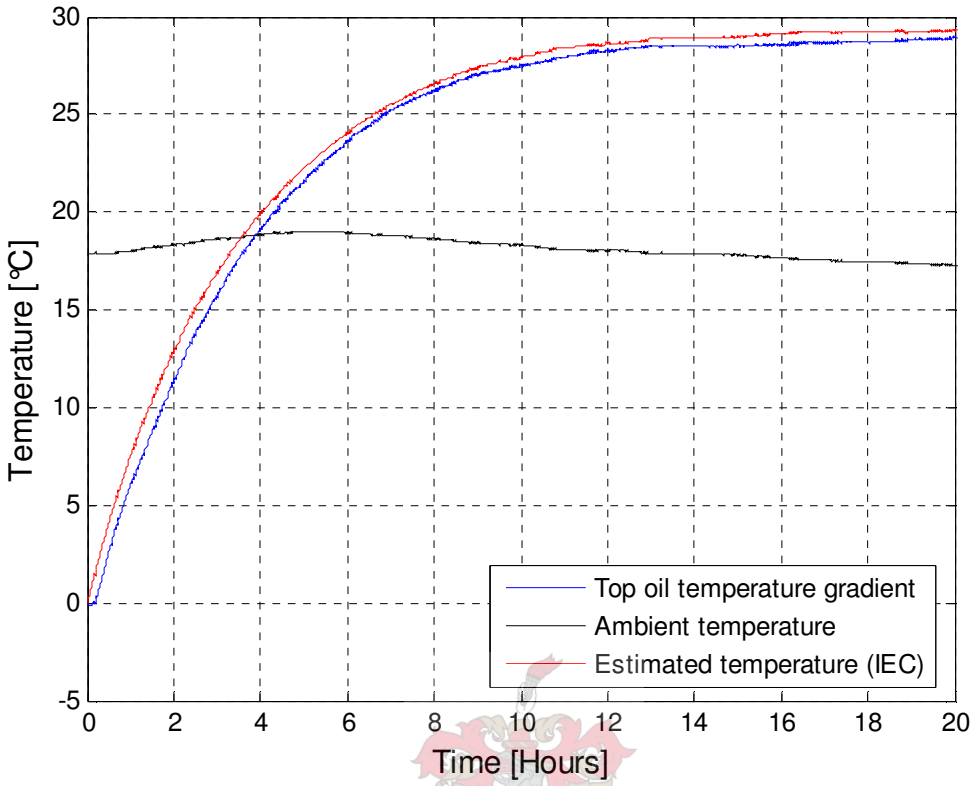

Figure 5-12: Measured top oil time constant and top oil gradient for 70% load

5.3.3 Average winding temperature

To determine the average winding temperature of the transformer the system was run at rated load for 14 hours until the oil temperature stabilised. The system was then shut of and winding resistance measurements were taken at certain time intervals. Equation 5.5 was then used to convert the measured resistance to temperature for copper wires. For aluminium wires 225 is used instead of 235.

$$\theta = \frac{R}{R_c} \cdot (235 + \theta_c) - 235 \qquad (5.5)$$

Where,

θ is the winding temperature

R is the measured resistance

R_c is the resistance measured at temperature θ_c

θ_c is the winding temperature of the winding during R_c measurement

Figure 5-13 shows the measured average winding temperature for rated load together with the exponential curve fitted on the measured data. The temperatures, in the figure, represent the ambient temperature plus the average oil temperature plus the average winding temperature. From the figure it can be seen that the winding time constant is 240 seconds (4 min). The average winding temperature at rated load is measured to be about 84 ℃, meaning that the winding to top oil temperature gradient is 27 ℃ for an ambient temperature of 24 ℃ and . Multiplying the average winding gradient with the proposed hotspot factor of 1.1 yields a hotspot temperature gradient of 30 ℃, which is considerably warmer than the hotspot gradient recommended in the IEC standards (23 ℃).

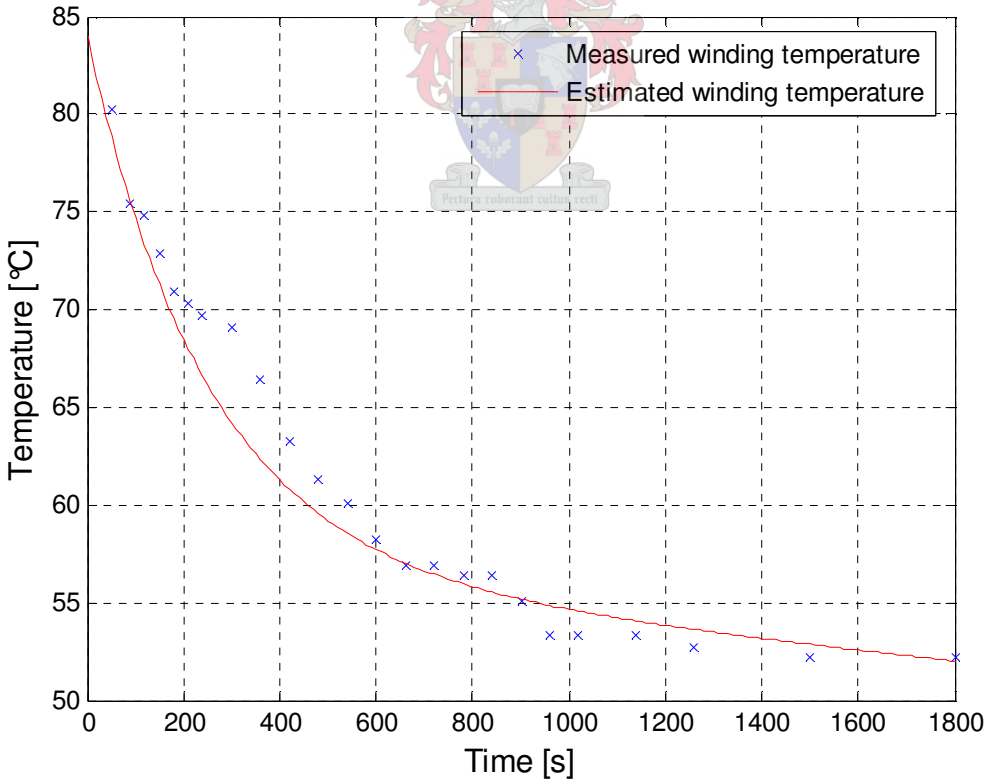

Figure 5-13: Measured winding temperature at rated load

5.3.4 Hotspot and top oil estimation for arbitrarily changing load

Using the top oil to ambient and winding to top oil gradient determined in section 5.3.2 and 5.3.3 further temperature tests were done. The system was tested for arbitrarily changing loads as shown in Figure 5-14 and Figure 5-15. The load was varied between 50%, 100% and 125%. Table 5-1 shows the values that were determined by the temperature tests and are used in the estimation techniques.

Oil time constant ($\tau_{oil,R}$)	3 hours
Winding time constant (τ_w)	4 minutes
Top oil to ambient temperature gradient ($\Delta\theta_{oil,R}$)	44 ℃
Average winding temperature gradient ($\Delta\theta_w$)	17 ℃
Hotspot temperature gradient ($\Delta\theta_{hs,R}$)	30 ℃

Table 5-1: Constants determined by temperature rise tests

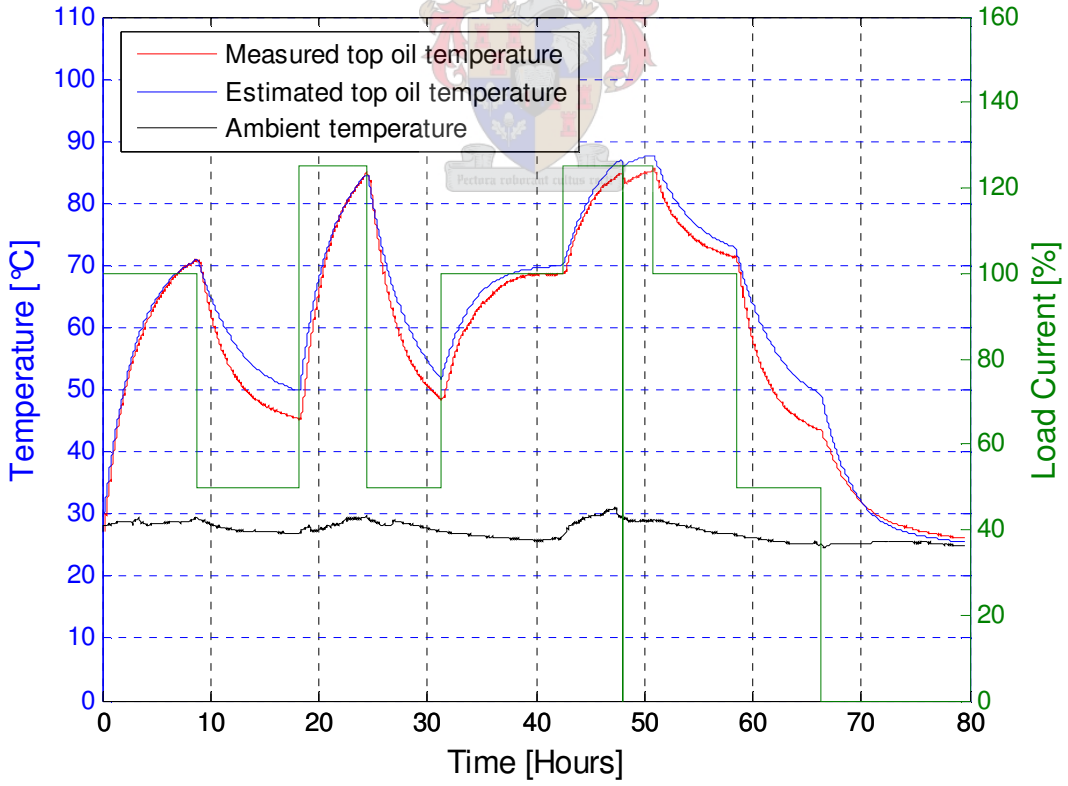

Figure 5-14: Estimation of top oil temperature

Figure 5-14 shows the estimated and measured top oil temperature for the different load steps. The differential IEC method is used to estimate the top oil temperature. The top oil temperature is estimated quite accurately for increasing load steps but seems to make a small error when the load is decreased. The ambient temperature was also measured at each time interval and used in the top oil and hotspot temperature estimation.

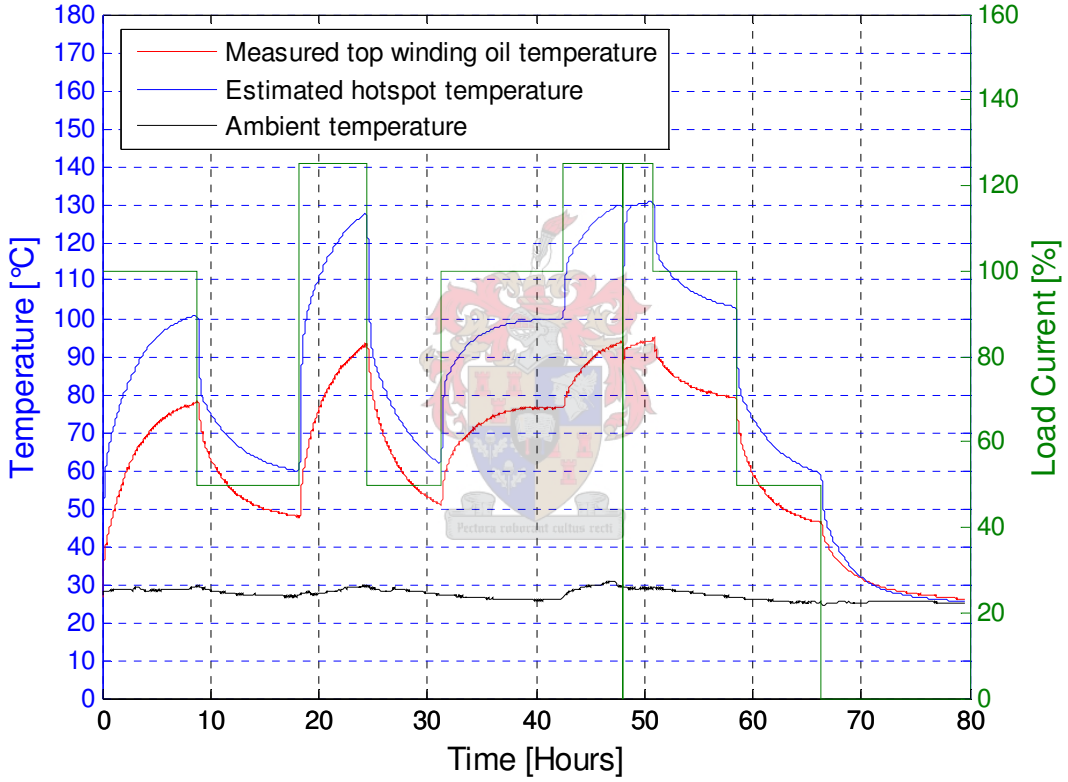

Figure 5-15: Estimated hotspot temperature

Figure 5-15 shows the estimated hotspot temperature of the transformer and the measured temperature of the oil between the windings of the transformer. Because the hotspot temperature could not be measured the oil temperature between the windings, gives the best possible reflection of the hotspot temperature. The recommended values for the for the hotspot over top oil gradient

was taken as 30 °C and the winding time constant as 4 minutes as recommended in the IEC standard. From Figure 5-15 it can be seen that the hotspot temperature is estimated to be considerably hotter than the temperature of the oil between the windings. Although these measurements do not confirm the hotspot temperature estimation the measured values are considerably lower then the estimated values and we can therefore assume that the estimation technique gives a value that should be higher than or close to the true hotspot temperature. Taken into consideration that the IEC standards specify the hotspot temperature to be about 98 °C for non-upgraded paper at rated load the estimation made seem to be accurate. As these results confirm the temperature estimation techniques the differential estimation technique were implemented on the processor and used for temperature protection.

6. Conclusions

This chapter summarises and comments on the work presented in this thesis and gives recommendations for possible future work.

6.1 Summary

In chapter 2, the need for extension of MV lines and the need for dynamic voltage regulation is discussed. Different types of voltage regulation solutions are investigated. After considering the intended purpose of the regulators as well as other factors such as reliability, size, cost and efficiency it was decided to implement a step regulator on a 16 kVA distribution transformer. Similar IGBT were compared and thyristor modules and it was found that thyristors, used as tap switches, provide the most reliable and efficient solution.

Chapter 3 investigates the temperature estimation techniques that can be used to predict the internal temperatures of oil-immersed distribution and power transformers. One method proposed by the IEEE and two methods proposed by the IEC were described. It was decided to implement the differential method, proposed by the IEC, on the processor as it is the method that is best suited for the implementation on a processor and also yields the best results for arbitrarily changing load factors.

The SRAPET was built and makes use of temperature estimation techniques, voltage and current and temperature measurements to implement the control of the system. Voltage measurements are used to select tap settings and thereby regulate the output voltage. The current and temperature measurements are used to implement over current and over temperature protection of the transformer and the thyristors. Furthermore a communication board is also added to the system which can be used to communicate with a host system via an onboard Bluetooth module or a RS232 interface. 2MB of flash memory is also provided and enables

a data logger to be implemented on the same processor in future. Protection of the system against surge current and surge voltages is implemented. Thyristors are used for switching between different taps and were selected to allow the system to run at 200% load and to be able to sustain fault currents without being damaged. An appropriate heat sink was selected for cooling of the thyristors and is fitted with a temperature sensor that protects the thyristors against over temperatures.

The processor that was used is DSP/BIOS compatible and allows the programmer to monitor the implemented software in real-time. It also allows real-time scheduling of procedures that enables more time critical procedures to pre-empt less critical procedures by adjusting their priority levels. This has the advantage that the development time of the control software can be significantly reduced and simplified if the programmer is competent programming with the DSP/BIOS real-time kernel. Although it might initially be more time consuming to make use of the DSP/BIOS kernel it becomes clear that it significantly reduces implementation time when the software developer has learned to operate the DSP/BIOS kernel.

Pectora roborant cultus recti

6.2 Outcomes

- Voltage regulation

The voltage regulation of the system functions well and boosts the output voltage with a maximum of 15%. When the input voltage is decreased and fluctuated, the output voltage stays constant. If the input voltage of the system however exceeds the rated voltage, the output voltage increases as no buck windings are present.

- Response time

For a sag in the input voltage the minimum response time is 20 ms. This is fast compared to the reaction time of some of the voltage regulators discussed in chapter 2. The delay, of one cycle, is caused by the accumulation of ADC

measurements used to calculate the RMS voltage and cannot be increased as the accumulation time is set to one 50 Hz cycle.

- Pulse suppression

For inductive resistive loads, voltage pulses are introduced due to the commutation delay of the thyristors caused by the PWM signal that is used to switch the thyristors and the delay caused by commutation of the thyristors themselves. These voltage pulses can however be successfully suppressed by the use of a capacitor at the output.

- Temperature estimation

The temperature estimation techniques were implemented on the processor. Required constants were determined by temperature tests and used in the estimation techniques. A heat run test was done and the top oil temperature gradient, top oil time constant, average winding temperature and winding time constant were determined. The top oil time constant compares very well to the value given in the IEC standards. The measured value is also found to be the same as the value calculated by using oil quantity and weight of the transformer. Although no method is supplied by the IEC standard to calculate the winding time constant, the value measured by the resistance measurements is indeed the same as the one proposed by the IEC for distribution transformers.

The temperature gradients for the winding and the top oil were also measured and compared. The measured top oil gradient was found to be considerably cooler than the values given in an example in the IEC standards. The average winding rise was also found to be slightly lower in the example than the one that was measured.

As it was not possible to measure the hotspot temperature in the windings, the recommended hotspot factor as given in IEC was used. The hotspot was found to be 98 °C at rated load which corresponds very well with the theory. Another

advantage of the temperature estimation is that the ambient temperature is measured at each time interval and is used for the estimation. If the ambient temperature is for instant very cool, the transformer can be overloaded without causing damage to the system.

It should be noted that the transformer used for the temperature tests was a 16 kVA, 22 kV to 240 V, with 3 taps, whereas the transformer on which the control was implemented was a 16 kVA, 22 kV to 230 V, with 8 taps (only six taps were used for voltage regulation). It should be taken into consideration that the rated voltage is lower, the oil quantity is less and the transformer weight is not the same due to the added windings and bigger tank. Although the top oil time constant can be recalculated it is not known whether the temperatures within the transformer are the same. For the temperature estimation techniques that were implemented on the processor this was however assumed.

- Surge protection

Surge current capabilities of two thyristors were tested. The result of these tests are used to specify the surge capabilities of the system as the transformer is protected against surges and only the thyristors are vulnerable to surges. Further surge protection of the thyristors was therefore added in the form of MOVs and an inductor. A field implementation of the SRAPET will reveal if the given protection functions as required.

- Temperature protection

Temperature estimation and measurements were used to implement temperature protection of the transformer and the thyristors

6.3 Recommendation and future work

- Data logger

A data logger should be added to the system, in future, to gather data and allow monitoring of the load profiles. Provision on the board has been made in the form of onboard Bluetooth modules, flash memory and a RS232 interface. The data logger should be implemented on the current processor. This will mean that few additional costs will be incurred as only a Bluetooth module needs to be added, for the system to function. The acquisition of data will help to detect constantly overloaded transformers and electricity theft. The Bluetooth module has the advantage that the data can be acquired remotely, which is safe and practical.

- Field evaluation

The setup discussed in this report was only tested indoors. To know whether it functions as it should, a field evaluation is required. Problems such as large ambient temperature fluctuations, surge voltages, constant overload conditions and fault currents will be encountered in the field and will further test the operation of the system.

Pectora roborant cultus recti

- Required taps

The transformer that is currently used has 8 taps of which 6 are used. By doing further research it can be determined if all 8 taps should be used or if the number of taps should be reduced or kept the same.

7. References

[1] Meyer B. *Opportunities for in-line transistor-based technologies on MV and LV power distribution networks* Stellenbosch, University of Stellenbosch 2000

[2] Carter-Brown C., Distribution technical bulletin, Eskom Distribution, 02TB-031 2003

[3] Carter-Brown C., Distribution transformer tap management and optimisation, Research Report, Research Division, RES/PR/02/18397 2002

[4] Carter-Brown C., Single-phase distribution transformer tap specification, Research report, Research Division, RES/PR/02/18400 2002

[5] South African Bureau of Standards, *Electricity supply – Quality of supply, Part 2: Voltage characteristics, compatibility levels, limits and assessment methods* NRS 048-2:2003.

[6] South African Bureau of Standards, *Electricity supply – Quality of supply Part 1: Overview of implementation of standards and procedures* NRS 048-1:1996

[7] Dessureau P., Evaluate solid state LTC options for medium power transformers (*EPRI*) 2000

[8] Automatic voltage regulation technologies [online], *published in Power Quality Magazine* [accessed September 2006] Available from: **www.powerdesigners.com/InfoWeb/design_center/articles/AVR/avr.shtm**

[9] Van Schalkwyk C. *Analysis and design of a voltage regulator based on a AC-to-AC converter* Stellenbosch, University of Stellenbosch 2003

[10] Special Transformer Applications [online], Available from: www.allaboutcircuits.com/vol_2/chpt_9/7.html [accessed September 2006]

[11] Constant Voltage Transformers (CVT) or Automatic Voltage Stabilisers (AVS), Advance Electronic Limited, Available from: www.aelgroup.co.uk/pdf/wp_cvtavs.pdf [accessed September 2006]

[12] Autotransformer [online], Available from: http://en.wikipedia.org/wiki/Autotransformer, [accessed September 2006]

[13] Park H.-W., Park S.-J., Park J.-G., Kim C.-U., A novel high-performance voltage regulator for single-phase AC sources, *IEEE transaction on industrial electronics* Vol. 48 (Iss. 3) pp 554-562 2001

[14] Maule D., Voltage dip mitigation, *Power quality application guide 5.3.2*, Copper Development Association 2001

[15] Advance Electronic Limited *Constant Voltage Transformer (CVT) or Automatic Voltage Stabiliser (AVS)?* [online] England, Available from: www.aelgroup.co.uk/pdf/wp_cvtavs.pdf [accessed September 2006]

[16] Integrated Publishing *Magnetic Amplifiers* [online] USA, Available from: http://www.tpub.com/content/neets/14180/css/14180_131.htm [accessed January 2007]

[17] Mueller D., McGranaghan M., Effects of Voltage Sags in Process Industry Applications, *Electrotek Concepts, Inc* [online] Available from: http://www.energymonitoring.com/ [accessed November 2006]

[18] Bauer P., de Haan S.W.H., Electronic tap changer for 10 kV distribution transformer, *EPE'97* Trondheim 1997 pp 3.1010-3.1015

[19] Bauer P., de Haan S.W.H., Protective device for electronic tap changer for distribution transformer, EPE'97 Trondheim 1997 pp 4.282-4.287

[20] Echavarria R., Cotorogea M., Claudio A., Sanchez V., Design and Inplementation of a Fast On-Load Tap Changing Regulator, *CENIDET* Mexico 2000

[21] Alegria E., Khan A., Rajda J., Dewan S. Static Voltage Regulator (SVR) – Ride Through Support For Semiconductor Facilities, *Powersystems World '98 Power Quality Conference*, Santa Clara CA 1998

[22] Beukes J., Serdyn J., du Toit J., Molepo A., EVR as line based compensator, Research report, Research Division RES/RR/04/24248 2004

[23] IEC International Standard, *Loading guide for oil-immersed power transformers* IEC 354: 1991

[24] IEC International Standard, *Loading guide for oil-immersed power transformers* IEC 60076-7: 2005

[25] Susa D. *Dynamic thermal modelling of power transformers* Helsinki, Helsinki University of Technology 2005 (Doctoral dissertation)

[26] Winders J.J. *Power transformers principles and applications* New York, Marcel Dekker 2002

[27] Swift G., Molinski T.S., Lehn W., A fundamental approach to transformer thermal modelling, Part 1, *IEEE transaction on power delivery* Vol. 16, (Iss.2) pp 171-175 2001

[28] Aubin J., Bergeron R., Morin R., Distribution transformer overloading capability under cold-load pickup conditions, *IEEE transaction on power delivery* Vol.7 (Iss.4) pp 1883-1891 1990

[29] IEEE standard test code for liquid-immersed distribution, *Power and regulator transformers* IEEE Std. C57.12.90 – 1999.

[30] Galli A.W., Cox M.D., Temperature rise of small oil-filled distribution transformers supplying non-sinusoidal load currents, *IEEE transaction on power delivery* Vol.11 (Iss.1) pp 283-291 1996

[31] Glover J.D., Sarma M.S. *Power systems analysis and design*, 3rd Edition, Pacific Grove, USA, BROOKS/COLE, 2002

Appendix A – Detailed software description

File description for application specific software

Source files	Description
errorhandling.c	Error-handling and Status LED switching modules
init.c	Peripheral interface initialisation
init_var.c	Global variable initialisation
isr.c	Contains interrupt service routines
main.c	Main procedure
measure.c	Measurements, tap selection and RMS calculation module
rtc.c	Real-time clock module
timer.c	Timer module
xint.c	External memory interface module
Header files	Description
errorhandling.h	Definition of structures and constant for errorhandling.c
init.h	Definition of constant for init.c
isr.h	Definition of constant for isr.c
main.h	Definition of structures and constant for main.c
measure.h	Definition of structures and constant for measure.c
rtc.h	Definition of structures and constant for rtc.c
timer.h	Definition of structures and constant for timer.c
typedef.h	General type definitions
Command file	Description
DSP281x_Headers _BIOS_flash.cmd	DSP281x Peripheral registers linker command file. Modified for running from on-chip flash

Table A- 1: Description of source and header files

File description for design ready code from TI

Source files	Description
DSP281x_CodeStartBranch.asm	Branch for redirecting code execution after boot
DSP281x_GlobalVariableDefs.c	DSP281x Global Variables and Data Section Pragmas

Header files	Description
DSP281x_Adc.h	Device ADC Register Definitions
DSP281x_CpuTimers.h	CPU 32-bit Timers Register Definitions
DSP281x_DevEmu.h	Device Emulation Register Definitions
DSP281x_Device.h	Device Definitions
DSP281x_ECan.h	Device eCAN Register Definitions
DSP281x_Ev.h	Device Event Manager Register Definitions
DSP281x_Gpio.h	General Purpose I/O Definitions
DSP281x_Mcbsp.h	Device McBSP Register Definitions
DSP281x_PieCtrl.h	Device PIE Control Register Definitions
DSP281x_PieVect.h	Devices PIE Vector Table Definitions
DSP281x_Sci.h	Device SCI Register Definitions
DSP281x_Spi.h	DSP281x Device SPI Register Definitions
DSP281x_SysCtrl.h	Device System Control Register Definitions
DSP281x_Xintf.h	DSP281x Device External Interface Register
DSP281x_XIntrupt.h	Device External Interrupt Register Definitions

Table A- 2: Design ready code files from TI

Build environment

The software is configured using Code Composer Studio 3 ('C2000) IDE from Texas Instruments. The project file SRAPET.pjt contains all the relevant files and settings required to build the project. The on-chip flash programmer, supplied by Texas Instruments, is supplied and used to program the software on the DSP flash. Table A- 1 gives software version information that was used.

Code Composer Studio ('C2000)	Version 3.1.19.0
C2800 Code Generation Tools	V4.1.0

Table A- 3: Software version information

Types and numeric systems

Because some types are hardware dependent and differ from types used on a PC, a number of basic types were defined to standardize the structure definitions between the PC and the TMS320F2812. These types were defined in *typedef.h* as shown in Table A- 4 below.

BYTE	Unsigned integer (PC: 8 bit value)
WORD	Unsigned long integer (16 bit unsigned; PC: unsigned short)
DWORD	Unsigned long integer (32 bit unsigned; PC: unsigned integer)
VWORD	Volatile unsigned integer (16 bit volatile unsigned)
BOOL	True = 1, False = 0 (Only for “C” language)

Table A- 4: Type definitions

Procedure descriptions

Error handling (errorhandling.c)

Procedure	Description
void errorhandling(void)	Detects and handles errors
void LED_Switch(Uns _LED, Bool _On)	Switches desired LEDs on or off
void HaltProgram()	Halts program if required

Table A- 5: Procedures in errorhandling.c

Initialise peripherals (init.c)

Procedure	Description
void InitSystem()	Initialises system and peripheral clocks
void InitGpio()	Initialises general purpose I/O pins
void InitADC()	Initialises ADC
void InitEvTimer()	Initialises event manager timers
void InitPieCtrl()	Initialises PIE control
void InitScia()	Initialises asynchronous serial interface
void InitRtc()	Initialises real-time clock module
void InitFlash()	Initialises on-chip flash
void Xint()	Initialises external memory interface

void userInit()	Initialises the .trcdata section before main. Is set in configuration file
void InitTemp()	Calculates initial transformer temperatures

Table A- 6: Procedures in init.c

Initialise variables (init_var.c)

Procedure	Description
void init_var(void)	Detects and handles errors

Table A- 7: Procedure in init_var.c

Interrupt service routines (isr.c)

Procedure	Description
void isr_pieint3_1(void)	Timer 2 period interrupt Sets ADC start of conversion Also used for time keeping
void isr_pieint1_6(void)	ADC end of conversion interrupt Accumulates measurement Highest priority interrupt Synchronises tap switching

Table A- 8: Procedures in isr.c

Main (main.c)

Procedure	Description
void main()	Initialises peripherals and variables

Table A- 9: Procedure in main.c

Measure (measure.c)

Procedure	Description
void Output_Acc()	Accumulates ADC measurements and calculates RMS value for output voltage

void Input_Acc()	Accumulates ADC measurements and calculates RMS value for input voltage
void Current_Acc()	Accumulates ADC measurements and calculates RMS value for current
void OverCur_Acc()	Accumulates ADC measurements and calculates RMS value for over current
void Temp_Acc()	Accumulates ADC measurements and calculates average temperatures
void SWI_Temp()	Calculates the estimated transformer temperatures
void SWI_Tsl()	Selects the desired tap setting by taking temperature, voltage and current into consideration
void TapSwitch(Uns TapNum, Bool On)	Switches desired tap on or off
LgUns Sqrt(LgUns SqrdAvg)	Calculates and returns the square root of a number
void temp_log_exec()	Background idle procedure used for logging temperatures on the external flash memory
void flash_write_temp_callback(Int res)	Callback function for writing temperature data to flash
void flash_erase_temp_callback(Int res)	Callback function for erasing logged temperatures

Table A- 10: Procedures in measure.c

Real-time clock (rtc.c)

Procedure	Description
BYTE bcd_to_bin(BYTE bcd)	Converts binary coded decimal value to binary
BYTE bin_to_bcd(BYTE bin)	Convert a binary value to binary coded decimal

WORD rtc_byte_to_spi3wire(BYTE data)	Converts a byte to a value that can be send via the SPI
WORD rtc_spi3wire_to_byte(BYTE data)	Converts a value received via the SPI to its true value
WORD rtc_write_byte(BYTE data)	Sends a sigle byte to the RTC
void rtc_read_clk()	Reads all 8 RTC registers
void rtc_write_clk()	Writes to RTC in burst mode
time_t rtc_get_time(void)	Gets the time from the RTC and stores in the “ti_time” format
void rtc_set_time(time_t)	Sets the time of the RTC using the rtc_write_clk() procedure

Table A- 11: Procedures in rtc.c

Timer (timer.c)

Procedure	Description
void timer_init(void)	Initialises specific timer module
void timer_cpu_delay_1us(DWORD cnt)	Implements a delay which runs for *cnt* microseconds
void set_timer_event(DWORD idx, WORD delay, type_callback callback, WORD flags)	Sets timer events for different operations
void timer_exec(void)	Background idle procedure used for timer module operation

Table A- 12: Procedures in timer.c

External memory interface (xint.c)

Procedure	Description
void flash_init(void)	Initialise external flash module
void flash_write_open(void)	Opens flash for writing
void flash_write_word(WORD data, DWORD laddr)	Writes a word to address ‘laddr’
void flash_reset(void)	Returns the flash to the read state

int flash_erase_sector(DWORD laddr, type_FlashCallback callback)	Erases flash sector to which 'laddr' points
void flash_read_buf(WORD *dst, WORD cnt, DWORD laddr)	Reads a series of values from flash
int flash_write_buff(WORD *src, WORD cnt, DWORD dst, type_FlashCallback callback)	Writes a series of values to the flash
void flash_write_timeout_callback()	Callback function for a write timeout
void flash_erase_timeout_callback()	Callback function for a erase timeout
void flash_erase_chip_callback(int res)	Callback function for chip erase
void flash_exec(void)	Background idle procedure used for flash module operation
int flash_erase_chip (type_FlashCallback callback)	Erases entire chip

Table A- 13: Procedures in xint.c

Appendix B – Thyristor test report

UNIVERSITY OF THE WITWATERSRAND
Private Bag 3, WITS 2050, South Africa - Telegram "Uniwits" - Telex 4-27125SA - Telephone (011) 717 7111

ELECTRIC POWER RESEARCH GROUP

Electric Power Research Group
School of Electrical and Information Engineering
Private Bag 3
WITS 2050
South Africa

Tel: (011) 717 7237
Fax: (011) 403 1929
email: n.west@ee.wits.ac.za
ref: ThyristorReport.pdf

Combination and current impulse testing of thyristors

Prepared for: Dr. J. Beukes
Stellenbosch University
Prepared by: N. J. West, A. A. Beutel, I. R. Jandrell
Date of report: October 29, 2006

Notes

- This report consists of 4 pages (not including this front cover page) and shall be presented in full at all times.
- The results presented apply only to the units tested, with or without modifications as noted in the report.
- Presentation of test results in this report does not imply approval by the University of the product(s) tested. The results may, however, be used in promotional material as proof of performance by the customer, but only as presented and explicitly stated in this report

1 Introduction

Two thyristor modules were tested with combination and current impulse waveforms. Each thyristor module contained two thyristors. Therefore a total of four thyristors were tested. The test procedure was as follows: A combination waveform (8/20 μs short circuit current, 1.2/80 μs open circuit voltage) was applied starting at 2 kA and ending at 8 kA in steps of 2 kA. If by the end of the test the thyristors were still operational, current impulses (8/20 μs short circuit current) were applied in steps of 2 kA until the thyristor failed. After each impulse the resistance between anode and cathode was measured using a digital multimeter. One impulse was applied at each current level. All impulses appplied had a positive polarity.

2 Test results

All four thyristors survived up to a peak current of 8 kA with the generator in combination mode. After this test, the generator was used in current mode and impulses up to 22 kA were applied to the thyristors.

The two modules were labeled A and B. In each module, a thyristor connected between pins 1 and 2 was called '1' and a thyristor connected between 1 and 3 was called '2'.

Typical open circuit voltage and short circuit current waveforms produced by the generator can be seen in *Fig.* 1 and 2.

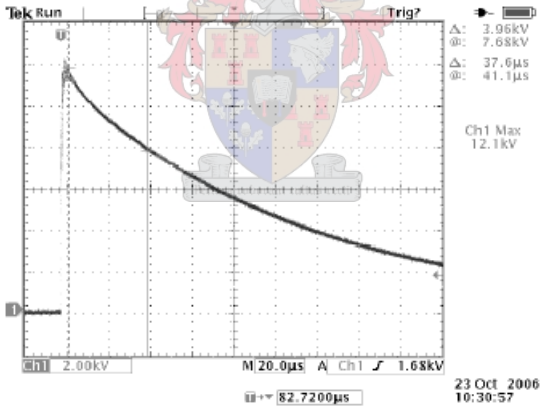

Figure 1: Typical open circuit voltage impulse waveform in combination mode

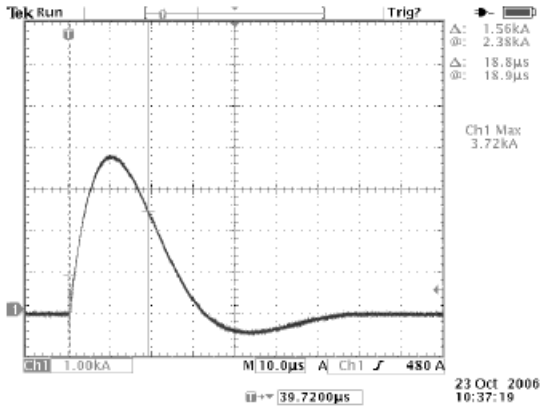

Figure 2: Typical short circuit current impulse waveform

2.1 Thyristor A

Both thyristors of module A failed at a current of 10 kA. Failure was as a short circuit.

Table 1: Test results: Module A1

Impulse Number	Peak Current (kA)	Resistance (Ω)	Status
1	2.16	900 k	PASS
2	3.98	870 k	PASS
3	5.86	880 k	PASS
4	7.80	5.15	PASS
5	10.30	0.80	FAIL

2.2 Thyristor B

Both thyristors of module B failed at a current level of 22 kA. Failure was as a short circuit.

Table 2: Test results: Module A2

Impulse Number	Peak Current (kA)	Resistance (Ω)	Status
1	2.13	1.1 M	PASS
2	4.06	1.1 M	PASS
3	5.92	1.1 M	PASS
4	7.96	1.2 M	PASS
5	9.84	0.45	FAIL

Table 3: Test results: Module B1

Impulse Number	Peak Current (kA)	Resistance (Ω)	Status
1	2.14	900 k	PASS
2	4.12	800 k	PASS
3	5.96	780 k	PASS
4	8.00	857 k	PASS
5	9.84	700 k	PASS
6	12.40	700 k	PASS
7	14.50	700 k	PASS
8	17.00	700 k	PASS
9	18.70	600 k	PASS
10	21.20	0.18	FAIL

Table 4: Test results: Module B2

Impulse Number	Peak Current (kA)	Resistance (Ω)	Status
1	2.12	1.1 M	PASS
2	4.01	998 k	PASS
3	5.92	970 k	PASS
4	8.00	1.0 M	PASS
5	10.30	740 k	PASS
6	12.20	750 k	PASS
7	14.10	680 k	PASS
8	16.50	650 k	PASS
9	18.20	600 k	PASS
11	22.60	0.16	FAIL

3 Conclusion

All four thyristors were tested with 8/20 μs current impulses with peak values up to 22 kA. The thyristors of module A failed at a peak current of 10 kA. Thyristor B1 failed at a peak current of 21.2 kA. Thyristor B2 at a current of 22.6 kA. In all cases, failure was as a short circuit.

Appendix C – SRAPET tap positions

The tap positions and impedances of the 6 tap transformer that is used in this project are given in Table C- 1 below. The transformer has a nominal impedance of 3.5%. The tap positions given in the table refer to the nominal tap voltage as no measurements were taken on the primary side of the transformer.

Tap number	0	1	2	3	4	5
Tap impedance [%]	3.50	3.58	3.67	3.75	3.83	3.92
Tap position [V]	230.0	223.3	217.0	211.0	205.4	200

Table C- 1: Transformer impedances and tap position on nominal tap

Table C- 2, Table C- 3 and Table C- 4 show the output voltages for loads of 0%, 100% and 200%. It also indicates the active area and the amount of overlap that exists between taps. The highlighted numbers in the nominal tap's column indicate that it is off. All nominal tap values are given because the nominal voltage is used as the input voltage that is used for tap selection.

Vsup [%]	Vout					
	Tap0	Tap1	Tap2	Tap3	Tap4	Tap5
100.0	230.0					
99.5	228.9					
99.0	227.7					
98.5	226.6					
98.0	225.4					
97.5	224.3					
97.0	223.1	229.8				
96.5	222.0	228.6				
96.0	220.8	227.4				
95.5	219.7	226.2				
95.0	218.5	225.1				
94.5	217.4	223.9	230.6			
94.0	216.2	222.7	229.4			
93.5	215.1	221.5	228.1			
93.0	213.9		226.9			
92.5	212.8		225.7			
92.0	211.6		224.5			
91.5	210.5		223.3	230.0		
91.0	209.3		222.0	228.7		
90.5	208.2		220.8	227.5		
90.0	207.0			226.2		
89.5	205.9			224.9		

89.0	204.7			223.7	230.4	
88.5	203.6			222.4	229.1	
88.0	202.4			221.2	227.8	
87.5	201.3				226.5	
87.0	200.1				225.2	
86.5	199.0				223.9	230.6
86.0	197.8				222.6	229.3
85.5	196.7				221.3	228.0
85.0	195.5					226.6
84.5	194.4					225.3
84.0	193.2					224.0
83.5	192.1					222.6
83.0	190.9					221.3

Table C- 2: Output voltage for 0% load

Vsup	Vout					
[%]	Tap0	Tap1	Tap2	Tap3	Tap4	Tap5
104.0	230.8					
103.5	229.7					
103.0	228.6					
102.5	227.5					
102.0	226.4					
101.5	225.3					
101.0	224.2	230.7				
100.5	223.1	229.6				
100.0	222.0	228.4				
99.5	220.8	227.3				
99.0	219.7	226.1				
98.5	218.6	225.0				
98.0	217.5	223.8	230.4			
97.5	216.4	222.7	229.2			
97.0	215.3	221.6	228.0			
96.5	214.2		226.8			
96.0	213.1		225.7			
95.5	212.0		224.5			
95.0	210.9		223.3	229.8		
94.5	209.7		222.1	228.6		
94.0	208.6		221.0	227.4		
93.5	207.5			226.2		
93.0	206.4			225.0		
92.5	205.3			223.8	230.3	
92.0	204.2			222.6	229.0	
91.5	203.1			221.3	227.8	
91.0	202.0				226.5	
90.5	200.9				225.3	
90.0	199.8				224.0	230.6
89.5	198.6				222.8	229.3
89.0	197.5				221.6	228.0
88.5	196.4					226.7
88.0	195.3					225.4
87.5	194.2					224.2
87.0	193.1					222.9
86.5	192.0					221.6

Table C- 3: Output voltage for 100% load

Vsup [%]	Vout					
	Tap0	Tap1	Tap2	Tap3	Tap4	Tap5
107.5	229.9					
107.0	228.9					
106.5	227.8					
106.0	226.7					
105.5	225.7					
105.0	224.6					
104.5	223.5	229.8				
104.0	222.5	228.7				
103.5	221.4	227.6				
103.0	220.3	226.5				
102.5	219.2	225.4				
102.0	218.2	224.3				
101.5	217.1	223.2	229.5			
101.0	216.0	222.1	228.4			
100.5	215.0	221.0	227.2			
100.0	213.9		226.1			
99.5	212.8		225.0			
99.0	211.8		223.9	230.2		
98.5	210.7		222.7	229.0		
98.0	209.6		221.6	227.8		
97.5	208.6			226.7		
97.0	207.5			225.5		
96.5	206.4			224.3		
96.0	205.3			223.2	229.5	
95.5	204.3			222.0	228.3	
95.0	203.2			220.9	227.1	
94.5	202.1				225.9	
94.0	201.1				224.7	
93.5	200.0				223.5	229.8
93.0	198.9				222.3	228.5
92.5	197.9				221.1	227.3
92.0	196.8					226.1
91.5	195.7					224.9
91.0	194.6					223.6
90.5	193.6					222.4

Table C- 4: Output voltage for 200% load